

การปรับปรุงการสัมผัสในเอทีอาร์เอฟทีไออาร์สเปกโทรสโกปี



นางสาวณัฐสิมา คีณา

วิทยานิพนธ์นี้เป็นส่วนหนึ่งของการศึกษาตามหลักสูตรปริญญาวิทยาศาสตรมหาบัณฑิต

สาขาวิชาเคมี ภาควิชาเคมี

คณะวิทยาศาสตร์ จุฬาลงกรณ์มหาวิทยาลัย

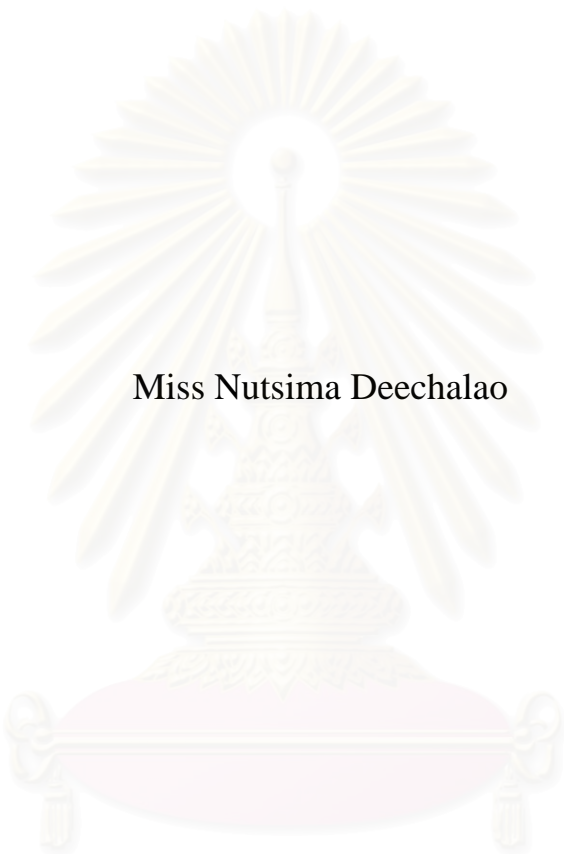
ปีการศึกษา 2544

ISBN 974-17-0347-3

ลิขสิทธิ์ของจุฬาลงกรณ์มหาวิทยาลัย

# IMPROVEMENT OF CONTACT IN ATR FT-IR SPECTROSCOPY

Miss Nutsima Deechalao



สถาบันวิทยบริการ  
จุฬาลงกรณ์มหาวิทยาลัย

A Thesis Submitted in Partial Fulfillment of the Requirements  
for the Degree of Master of Science in Chemistry  
Department of in Chemistry  
Faculty of Science  
Chulalongkorn University  
Academic Year 2001  
ISBN 974-17-0347-3

**Thesis Title** Improvement of Contact in ATR FT-IR Spectroscopy  
**By** Miss Nutsima Deechalao  
**Field of Study** Chemistry  
**Thesis Advisor** Assistant Professor Sanong Ekgasit, Ph.D.

---

Accepted by Faculty of Science, Chulalongkorn University in Partial Fulfillment of the Requirements for the Master's Degree

.....Deputy Dean for Administrative Affairs  
(Associate Professor Pipat Karntiang, Ph.D.) Acting Dean, Faculty of Science

Thesis Committee

.....Chairman  
(Associate Professor Sirirat Kokpol, Ph.D.)

.....Thesis Advisor  
(Assistant Professor Sanong Ekgasit, Ph.D.)

.....Member  
(Associate Professor Supot Hannongbua, Ph.D.)

.....Member  
(Varawut Tangpasuthadol, Ph.D.)

ณัฐสิมา ดีเฉลา : การปรับปรุงการสัมผัสในเทคนิคเอทีอาร์เอฟทีไออาร์สเปกโทรสโกปี  
(IMPROVEMENT OF CONTACT IN ATR FT-IR SPECTROSCOPY)

อาจารย์ที่ปรึกษา : ผศ. ดร. สอนง เอกสิทธิ์, 114 หน้า. ISBN 974-17-0347-3

การสัมผัสที่ีระหว่างสารตัวอย่างและเอทีอาร์ปริซึมมีความสำคัญมากในเอทีอาร์เอฟทีไออาร์สเปกโทรสโกปี ถ้าการสัมผัสไม่ดีจะเกิดช่องอากาศขึ้นระหว่างสารตัวอย่างและเอทีอาร์ปริซึม งานวิจัยนี้ได้ศึกษาอิทธิพลของช่องอากาศที่เกิดขึ้น พบว่าช่องอากาศมีผลกระทบต่อค่าการดูดกลืนแสงของสารตัวอย่าง ช่องอากาศยังมีขนาดใหญ่ขึ้น ทำให้ค่าการดูดกลืนแสงของสารตัวอย่างน้อยลง โดยเฉพาะอย่างยิ่งในกรณีที่สารตัวอย่างมีผิวขรุขระ ค่าการดูดกลืนแสงมีความสัมพันธ์กับความขรุขระของผิวสารตัวอย่าง ยิ่งผิวหน้าของตัวอย่างมีความขรุขระมาก ค่าการดูดกลืนแสงยิ่งน้อยลง การลดลงของค่าการดูดกลืนแสงเกิดขึ้นเนื่องจากช่องอากาศเปลี่ยนลักษณะของสนามไฟฟ้าซึ่งมีผลให้เกิดอันตรกิริยาระหว่างสนามไฟฟ้ากับสารตัวอย่างน้อยลง ในงานวิจัยนี้เทคนิคการเพิ่มค่าการดูดกลืนแสงของสารตัวอย่างของแข็งได้ถูกพัฒนาขึ้น โดยการแทนที่ช่องอากาศด้วยของเหลวซึ่งมีค่าดัชนีหักเหใกล้เคียงกับของสารตัวอย่าง จากการทดลองพบว่าค่าการดูดกลืนแสงของสารตัวอย่างของแข็งเมื่อมีของเหลวเข้าช่วยมีค่าเพิ่มขึ้นอย่างเห็นได้ชัด นอกจากนี้แล้วงานวิจัยนี้ได้มีการเสนอเทคนิคเพื่อคำนวณหาบัลค์สเปกตรัมของสารตัวอย่างของแข็งบัลค์สเปกตรัมของสารตัวอย่างของแข็งได้จากการคำนวณภายใต้สภาวะที่มีการดูดกลืนแสงต่ำ ความเหมาะสมของเทคนิคการเพิ่มค่าการดูดกลืนแสงและเทคนิคการคำนวณบัลค์สเปกตรัมของสารตัวอย่างของแข็งนั้นได้มีการตรวจสอบทั้งทางด้านทฤษฎีและด้านการทดลอง

สถาบันวิทยบริการ  
จุฬาลงกรณ์มหาวิทยาลัย

ภาควิชา.....เคมี  
สาขาวิชา.....เคมี  
ปีการศึกษา..... 2544

ลายมือชื่อนิสิต.....  
ลายมือชื่ออาจารย์ที่ปรึกษา.....  
ลายมือชื่ออาจารย์ที่ปรึกษาร่วม.....

## 4272277723 : MAJOR CHEMISTRY

KEYWORD: ATR FT-IR, OPTICAL CONTACT, EVANESCENT FIELD,  
SPECTRAL ENHANCEMENT, BULK SPECTRUM.

NUTSIMA DECHALAO: IMPROVEMENT OF CONTACT IN ATR FT-IR  
SPECTROSCOPY. THESIS ADVISOR : ASST. PROF. SANONG  
EKGASIT, Ph.D. 114 pp. ISBN 974-17-0347-3.

A good contact between a sample and ATR prism is crucial for attenuated total reflection Fourier transform infrared spectroscopy. If a good contact is not achieved, there is an air gap between the solid sample and the IRE. This research studied the influence of the air gap. The air gap affects the absorbance of the sample. The greater air gap, the smaller the absorbance, especially for solid sample with rough surface. The greater is the roughness, the smaller is the absorbance. In this research, a technique for enhancing absorbance of the solid sample is developed. By replacing the air gap with a liquid of similar refractive index to that of the sample, absorbance of the solid sample in liquid assisted-system contact is significantly improved. Moreover, a technique for calculating the bulk spectrum of the solid sample from observed spectra is proposed. The accurate bulk spectrum can be obtained under small absorption condition. Applicability of these techniques has been theoretically and experimentally verified.

สถาบันวิทยบริการ  
จุฬาลงกรณ์มหาวิทยาลัย

Department.....Chemistry..... Student's signature.....  
Field of study.....Chemistry..... Advisor's signature.....  
Academic year.....2001..... Co-advisor's signature.....

## ACKNOWLEDGEMENTS

I would like to thank Associate Professor Dr. Sirirat Kokpol, Associate Professor Dr. Supot Hannongbua, and Dr. Varawut Tangpasuthadol for their substantial advice as thesis committee.

I also thank all members of Spectroscopy Research Group and acknowledge computers and other academic facility supplies from The Austrian-Thai Center (ATC) and instrumental support from Bruker Analytical and Medical Instrument South East Asia.

Finally, I would like to thank my thesis advisor, Assistant Professor Dr. Sanong Ekgasit, who made useful recommendations, suggestion, encouragement, and understanding of my studies.



สถาบันวิทยบริการ  
จุฬาลงกรณ์มหาวิทยาลัย

# CONTENTS

	Page
ABSTRACT IN THAI.....	iv
ABSTRACT IN ENGLISH.....	v
ACKNOWLEDGEMENTS.....	vi
LIST OF FIGURES.....	ix
LIST OF ABBREVIATIONS.....	xxiv
LIST OF SYMBOLS.....	xxiv
CHAPTER I INTRODUCTION.....	1
1.1. Optical Contact and ATR FT-IR Spectroscopy .....	1
1.2 The Objective of This research .....	4
1.2. The Scope of This research.....	4
CHAPTER II THEORETICAL BACKGROUND.....	5
2.1. ATR FT-IR Spectroscopy.....	5
2.2. ATR Spectral intensity .....	8
2.3. Problem with contact between Sample and IRE .....	12
2.4. A Solution for Contact Problem in ATR Technique.....	13
2.5. Calculation for Bulk spectrum of Solid Sample.....	14
CHAPTER III EXPERIMENT.....	17
3.1. Spectral Simulation.....	17
3.1.1. The Influence of an Air Gap .....	17
3.1.2. A Technique for Intensity Enhancement .....	18
3.1.3. Calculation of Bulk ATR Spectrum.....	18

	Page
3.2. ATR Spectral Acquisition.....	19
3.2.1. Materials .....	19
3.2.2. Experimental	
Procedure.....	20
3.2.2.1 The Influence of an Air Gap.....	20
3.2.2.2 Absorbance Enhancement.....	20
3.2.2.2.1 Influence of Organic Liquid.....	20
3.2.2.2.2 Influence of Surface Roughness.....	22
3.2.2.3 Bulk ATR Spectra from observed spectra.....	23
 CHAPTER IV RESULTS AND DISCUSSION.....	 24
4.1 Spectral Simulation.....	24
4.1.1 The Influence of an Air Gap.....	26
4.1.2 A Technique for Intensity Enhancement .....	27
4.1.3 Calculation of Bulk ATR Spectrum.....	29
4.2. ATR Spectral Acquisition.....	31
4.2.1 The Influence of an Air Gap.....	31
4.2.2 Absorbance Enhancement.....	37
4.2.2.1 Influence of Organic Liquid.....	37
4.2.2.2 Influence of Surface Roughness.....	47
4.2.3 Bulk ATR Spectra from observed spectra.....	57
 CHAPTER V CONCLUSIONS.....	 85
REFERENCES.....	87
APPENDICES.....	90
CURRICULUM VITAE.....	114



## LIST OF FIGURES

Figure		Page
1.1	ATR spectra of a hard and rigid solid sample with different thickness of an air gap. The thickness of the air gap is altered by pressing the sample against the IRE.....	3
2.1	ATR configuration.....	6
2.2	Evanescent wave at the boundary between IRE and sample .....	7
2.3	Depth dependent MSEvF at various angles of incidences. The simulation parameters are $\nu = 1000 \text{ cm}^{-1}$ , $n_0 = 4.0$ , $n_1 = 1.5$ , $k_1 = 0$ , $\theta = 30^\circ, 35^\circ, 40^\circ, 45^\circ, 50^\circ, 55^\circ, 60^\circ$ .....	11
2.4	Depth dependent MSEvF at various angles of frequencies. The simulation parameter are $n_0 = 4.0$ , $n_1 = 1.5$ , $k_1 = 0$ , $\nu = 500, 1000, 1500, 3000 \text{ cm}^{-1}$ .....	11
2.5	The decay characteristic of the MSEvF at various air gap thickness (solid lines) and those under optical contact (broken lines). The simulation parameters are $n_0 = 4.0$ , $\theta = 45^\circ$ , $\nu = 1000 \text{ cm}^{-1}$ , $n_{air} = 1.0$ , $n_f = 1.5$ , and the air gap thickness of 0.0, 0.1, 0.2, 0.3, 0.5, and $1.0 \mu\text{m}$ .....	13
2.6	A schematic illustration of a three-phase system of isotropic media.....	14
4.1	Complex refractive index spectrum of medium 1 in mid-infrared region (A) and absorption index spectrum (B).....	24
4.2	Simulated ATR spectrum of medium 1 under optical contact. The simulation parameters are $n_0 = 4.0$ , $n_1 = 1.5$ , and $\theta = 45^\circ$ .....	25
4.3	Complex refractive index spectrum of medium 2 in mid-infrared region (A) and absorption index spectrum (B).....	25
4.4	Simulated ATR spectrum of medium 2 under optical contact. The simulation parameters are $n_0 = 4.0$ , $n_1 = 1.5$ , and $\theta = 45^\circ$ .....	25

Figure	Page
4.5 ATR spectra of medium 2 at various thickness of the air gap: 0.00 (A), 0.005 (B), 0.05 (C) and 0.5 $\mu\text{m}$ (D). The simulation parameters are the same as those of Figure 4.4.....	26
4.6 Simulated ATR spectra of medium 2 (solid line) at various thickness of medium 1: 0.005 (A), 0.05 (B), and 0.5 (C). The dotted lines show spectra of the system at the corresponding thickness of air gap.....	28
4.7 Calculated bulk ATR spectrum of medium 2 (C) acquired by subtracting out bulk ATR spectrum of medium 1 (B) from three-phase spectrum of Ge IRE/medium1/medium2 (A) with the thickness of medium 1 of 0.005 $\mu\text{m}$ . The dotted line is simulated bulk ATR spectrum of medium 2.....	29
4.8 Calculated bulk ATR spectrum of medium 2 (C) acquired by subtracting out bulk ATR spectrum of medium 1 (B) from three-phase spectrum of Ge IRE/medium1/medium2 (A) with the thickness of medium 1 of 0.05 $\mu\text{m}$ . The dotted line is simulated bulk ATR spectrum of medium 2.....	30
4.9 Calculated bulk ATR spectrum of medium 2 (C) acquired by subtracting out bulk ATR spectrum of medium 1 (B) from three-phase spectrum of Ge IRE/medium1/medium2 (A) with the thickness of medium 1 of 0.5 $\mu\text{m}$ . The dotted line is simulated bulk ATR spectrum of medium 2 .....	30
4.10 ATR spectra of PVC at various applied pressures acquired via multiple reflection IRE accessory with 45° ZnSe IRE.....	32
4.11 ATR spectra of PC at various applied pressures acquired via multiple reflection IRE accessory with 45° ZnSe IRE.....	32

Figure	Page
4.12 ATR spectra of PVC acquired by multiple reflection accessory (A) and single reflection accessory (B) with 45° ZnSe IRE.....	34
4.13 ATR spectra of PC acquired by multiple reflection accessory (A) and single reflection accessory (B) with 45° ZnSe IRE.....	35
4.14 ATR spectra of PVC at various applied pressures in single reflection acquired via 45° ZnSe IRE in single reflection system.....	35
4.15 ATR spectra of PC at various applied pressures in single reflection acquired via 45° ZnSe IRE in single reflection system.....	36
4.16 ATR spectrum of <i>i</i> -propanol acquired in multiple reflection ATR accessory with 45° ZnSe IRE.....	37
4.17 ATR spectrum of mineral oil acquired in multiple reflection ATR accessory with 45° ZnSe IRE.....	37
4.18 ATR spectra of three-phase system of ZnSe/ <i>i</i> -propanol/PVC acquired by multiple reflection ATR accessory using 45° ZnSe IRE; spectrum of PVC on ZnSe IRE under an applied pressure (A), spectrum of PVC with thin <i>i</i> -propanol film (B), and spectrum of PVC with a thinner <i>i</i> -propanol film (C).....	38
4.19 ATR spectra of three-phase system of ZnSe/mineral oil/PVC acquired by multiple reflection ATR accessory using 45° ZnSe IRE; spectrum of PVC on ZnSe IRE under an applied pressure (A), spectrum of PVC with thin mineral oil film (B), and spectrum of PVC with a thinner mineral oil film(C).....	39
4.20 ATR spectra of three-phase system of ZnSe/ <i>i</i> -propanol/PC acquired by multiple reflection ATR accessory using 45° ZnSe IRE; spectrum of PC on ZnSe IRE under an applied pressure (A), spectrum of PC with thin <i>i</i> -propanol film (B), and spectrum of PC with a thinner <i>i</i> -propanol film(C).....	40

Figure	Page
4.21 ATR spectra of PC in a three-phase system (ZnSe/ <i>i</i> -propanol/PC) by acquired by single reflection accessory with 45° ZnSe IRE. Spectrum of PVC on ZnSe IRE under an applied pressure (A), spectrum of PVC with thin <i>i</i> -propanol film (B), and spectrum of PC with thinner <i>i</i> -propanol film (C).....	43
4.22 ATR spectrum of <i>i</i> -propanol acquired in single reflection ATR accessory with 45° ZnSe IRE.....	42
4.23 ATR spectrum of mineral oil acquired in single reflection ATR accessory with 45° ZnSe IRE.....	42
4.24 ATR spectra of three-phase system of ZnSe/ <i>i</i> -propanol/PVC acquired by single reflection ATR accessory using 45° ZnSe IRE; spectrum of PVC on ZnSe IRE under an applied pressure (A), spectrum of PVC with thin <i>i</i> -propanol film (B), and spectrum of PVC with a thinner <i>i</i> -propanol film (C).....	43
4.25 ATR spectra of three-phase system of ZnSe/mineral oil/PVC acquired by single reflection ATR accessory using 45° ZnSe IRE; spectrum of PVC on ZnSe IRE under an applied pressure (A), spectrum of PVC with thin mineral oil film (B), and spectrum of PVC with a thinner mineral oil film (C).....	44
4.26 ATR spectra of three-phase system of ZnSe/ <i>i</i> -propanol/PC acquired by single reflection ATR accessory using 45° ZnSe IRE; spectrum of PC on ZnSe IRE under an applied pressure (A), spectrum of PC with thin <i>i</i> -propanol film (B), and spectrum of PC with a thinner <i>i</i> -propanol film (C).....	45

Figure	Page
4.27 ATR spectra of three-phase system of ZnSe/mineral oil/PC acquired by single reflection ATR accessory using 45° ZnSe IRE; spectrum of PC on ZnSe IRE under an applied pressure (A), spectrum of PC with thin mineral oil film (B), and spectrum of PC with a thinner mineral oil film (C).....	46
4.28 ATR spectra of PC at various surface roughness under an applied pressure acquired by multiple reflection ATR accessory using 45° ZnSe IRE; Spectrum of flat PC (A), spectrum of PC rough 1200 (B), spectrum of PC rough 400 (C) and spectrum of PC rough 100 (D).....	47
4.29 ATR spectra of three-phase system of ZnSe/ <i>i</i> -propanol/PC rough 1200 acquired by multiple reflection ATR accessory using 45° ZnSe IRE; spectrum of PC rough 1200 on ZnSe IRE under an applied pressure (A), spectrum of PC rough 1200 with thin <i>i</i> -propanol film (B), and spectrum of PC rough 1200 with thinner <i>i</i> -propanol film (C).....	48
4.30 ATR spectra of three-phase system of ZnSe/ <i>i</i> -propanol/PC rough 400 acquired by multiple reflection ATR accessory using 45° ZnSe IRE; spectrum of PC rough 400 on ZnSe IRE under an applied pressure (A), spectrum of PC rough 400 with thin <i>i</i> -propanol film (B), and spectrum of PC rough 400 with thinner <i>i</i> -propanol film (C).....	49
4.31 ATR spectra of three-phase system of ZnSe/ <i>i</i> -propanol/PC rough 100 acquired by multiple reflection ATR accessory using 45° ZnSe IRE; spectrum of PC rough 100 on ZnSe IRE under an applied pressure (A), spectrum of PC rough 1200 with thin <i>i</i> -propanol film (B), and spectrum of PC rough 1200 with thinner <i>i</i> -propanol film (C).....	49

Figure	Page
4.32 ATR spectra of three-phase system of ZnSe/mineral oil/PC rough 1200 acquired by multiple reflection ATR accessory using 45° ZnSe IRE; spectrum of PC rough 1200 on ZnSe IRE under an applied pressure (A), spectrum of PC rough 1200 with thin mineral oil film (B), and spectrum of PC rough 1200 with thinner <i>i</i> -propanol film (C)..	50
4.33 ATR spectra of three-phase system of ZnSe/mineral oil/PC rough 400 acquired by multiple reflection ATR accessory using 45° ZnSe IRE; spectrum of PC rough 400 on ZnSe IRE under an applied pressure (A), spectrum of PC rough 400 with thin mineral oil film (B), and spectrum of PC rough 400 with thinner <i>i</i> -propanol film (C).....	50
4.34 ATR spectra of three-phase system of ZnSe/mineral oil/PC rough 100 acquired by multiple reflection ATR accessory using 45° ZnSe IRE; spectrum of PC rough 100 on ZnSe IRE under an applied pressure (A), spectrum of PC rough 1200 with thin mineral oil film (B), and spectrum of PC rough 1200 with thinner <i>i</i> -propanol film (C). The insets are added for clarity.....	51
4.35 ATR spectra of PC with various surface roughness under applied pressure acquired by single reflection system accessory using 45° ZnSe IRE. ATR spectra of flat PC (A), ATR spectra of PC rough 1200 (B), ATR spectra of PC rough 400 (C), and ATR spectra of PC rough 100 (D) .....	52
4.36 ATR spectra of a three-phase system of ZnSe/ <i>i</i> -propanol/PC rough 1200 acquired by single reflection ATR accessory using 45° ZnSe IRE; spectrum of PVC under an applied pressure (A), spectrum of PC rough 1200 with thin <i>i</i> -propanol film (B), and spectrum of PC rough 1200 with thinner <i>i</i> -propanol film (C).....	53



Figure	Page
4.37 ATR spectra of a three-phase system of ZnSe/ <i>i</i> -propanol/PC rough 400 acquired by single reflection ATR accessory using 45° ZnSe IRE; spectrum of PVC under an applied pressure (A), spectrum of PC rough 400 with thin <i>i</i> -propanol film (B), and spectrum of PC rough 400 with thinner <i>i</i> -propanol film (C).....	54
4.38 ATR spectra of a three-phase system of ZnSe/ <i>i</i> -propanol/PC rough 100 acquired by single reflection ATR accessory using 45° ZnSe IRE; spectrum of PVC under an applied pressure (A), spectrum of PC rough 100 with thin <i>i</i> -propanol film (B), and spectrum of PC rough 100 with thinner <i>i</i> -propanol film (C).....	54
4.39 ATR spectra of a three-phase system of ZnSe/mineral oil/PC rough 1200 acquired by single reflection ATR accessory using 45° ZnSe IRE; spectrum of PVC under an applied pressure (A), spectrum of PC rough 1200 with thin mineral oil film (B), and spectrum of PC rough 1200 with thinner mineral oil film (C).....	55
4.40 ATR spectra of a three-phase system of ZnSe/mineral oil/PC rough 400 acquired by single reflection ATR accessory using 45° ZnSe IRE; spectrum of PVC under an applied pressure (A), spectrum of PC rough 400 with thin mineral oil film (B), and spectrum of PC rough 400 with thinner mineral oil film (C).....	56
4.41 ATR spectra of a three-phase system of ZnSe/mineral oil/PC rough 100 acquired by single reflection ATR accessory using 45° ZnSe IRE; spectrum of PVC under an applied pressure (A), spectrum of PC rough 100 with thin mineral oil film (B), and spectrum of PC rough 100 with thinner mineral oil film (C).....	56

Figure	Page	
4.42	Calculated bulk ATR spectrum of PVC acquired by multiple reflection ATR accessory (C) obtained by subtracting bulk ATR spectrum of <i>i</i> -propanol (B) from a three-phase system spectrum of ZnSe/ <i>i</i> -propanol/PVC (A) with 0.034 $\mu\text{m}$ thickness of <i>i</i> -propanol. The dotted line is spectrum of PVC under applied pressure.....	57
4.43	Calculated bulk ATR spectrum of PVC acquired by multiple reflection ATR accessory (C) obtained by subtracting bulk ATR spectrum of <i>i</i> -propanol (B) from a three-phase system spectrum of ZnSe/ <i>i</i> -propanol/PVC (A) with 0.017 $\mu\text{m}$ thickness of <i>i</i> -propanol. The dotted line is spectrum of PVC under applied pressure.....	58
4.44	Comparison between the calculated bulk ATR spectrum of PVC shown in Figure 4.42 (solid line) and Figure 4.43 (dotted line).....	58
4.45	Calculated bulk ATR spectrum of PVC acquired by multiple reflection ATR accessory (C) obtained by subtracting bulk ATR spectrum of mineral oil (B) from a three-phase system spectrum of ZnSe/mineral oil/PVC (A) with 0.210 $\mu\text{m}$ thickness of mineral oil. The dotted line is spectrum of PVC under applied pressure.....	59
4.46	Calculated bulk ATR spectrum of PVC acquired by multiple reflection ATR accessory (C) obtained by subtracting bulk ATR spectrum of mineral oil (B) from a three-phase system spectrum of ZnSe/mineral oil/PVC (A) with 0.150 $\mu\text{m}$ thickness of mineral oil. The dotted line is spectrum of PVC under applied pressure.....	59
4.47	Comparison between the calculated bulk ATR spectrum of PVC shown in Figure 4.45 (solid line) and Figure 4.46 (dotted line).....	60



Figure	Page	
4.48	Calculated ATR bulk spectrum of PC acquired by multiple reflection accessory with (C) obtained by subtracting ATR bulk spectrum of <i>i</i> -propanol (B) from ATR three-phase system spectrum of ZnSe/ <i>i</i> -propanol/PC (A) with 0.047 $\mu\text{m}$ thickness of <i>i</i> -propanol. The dotted line is spectrum of PC under applied pressure.....	61
4.49	Calculated ATR bulk spectrum of PC acquired by multiple reflection accessory with (C) obtained by subtracting ATR bulk spectrum of <i>i</i> -propanol (B) from ATR three-phase system spectrum of ZnSe/ <i>i</i> -propanol/PC (A) with 0.013 $\mu\text{m}$ thickness of <i>i</i> -propanol. The dotted line is spectrum of PC under applied pressure.....	61
4.50	Comparison between the calculated bulk ATR spectrum of PC shown in Figure 4.48 (solid line) and Figure 4.49 (dotted line).....	62
4.51	Calculated ATR bulk spectrum of PC acquired by multiple reflection accessory with (C) obtained by subtracting ATR bulk spectrum of mineral oil (B) from ATR three-phase system spectrum of ZnSe/mineral oil/PC (A) with 0.330 $\mu\text{m}$ thickness of mineral oil. The dotted line is spectrum of PC under applied pressure.....	62
4.52	Calculated ATR bulk spectrum of PC acquired by multiple reflection accessory with (C) obtained by subtracting ATR bulk spectrum of mineral oil (B) from ATR three-phase system spectrum of ZnSe/mineral oil/PC (A) with 0.230 $\mu\text{m}$ thickness of mineral oil. The dotted line is spectrum of PC under applied pressure. ....	63
4.53	Comparison between the calculated bulk ATR spectrum of PC shown in Figure 4.51 (solid line) and Figure 4525 (dotted line).....	63

Figure	Page	
4.54	Calculated bulk ATR spectrum of PC rough 1200 acquired by multiple reflection ATR accessory (C) obtained by subtracting bulk ATR spectrum of <i>i</i> -propanol (B) from a three-phase system spectrum of ZnSe/ <i>i</i> -propanol/PC rough 1200 (A) with 0.052 $\mu\text{m}$ thickness of <i>i</i> -propanol. The dotted line is spectrum of PC rough 1200 under applied pressure. ....	64
4.55	Calculated bulk ATR spectrum of PC rough 400 acquired by multiple reflection ATR accessory (C) obtained by subtracting bulk ATR spectrum of <i>i</i> -propanol (B) from a three-phase system spectrum of ZnSe/ <i>i</i> -propanol/PC rough 400 (A) with 0.038 $\mu\text{m}$ thickness of <i>i</i> -propanol. The dotted line is spectrum of PC rough 400 under applied pressure.....	65
4.56	Calculated bulk ATR spectrum of PC rough 100 acquired by multiple reflection ATR accessory (C) obtained by subtracting bulk ATR spectrum of <i>i</i> -propanol (B) from a three-phase system spectrum of ZnSe/ <i>i</i> -propanol/PC rough 100 (A) with 0.061 $\mu\text{m}$ thickness of <i>i</i> -propanol. The dotted line is spectrum of PC rough 100 under applied pressure.....	65
4.57	Calculated bulk ATR spectrum of PVC acquired by single reflection ATR accessory (C) obtained by subtracting bulk ATR spectrum of <i>i</i> -propanol (B) from a three-phase system spectrum of ZnSe/ <i>i</i> -propanol/PVC (A) with 0.008 $\mu\text{m}$ thickness of <i>i</i> -propanol. The dotted line is spectrum of PVC under applied pressure.....	67

Figure	Page	
4.58	Calculated bulk ATR spectrum of PVC acquired by single reflection ATR accessory (C) obtained by subtracting bulk ATR spectrum of <i>i</i> -propanol (B) from a three-phase system spectrum of ZnSe/ <i>i</i> -propanol/PVC (A) with 0.007 $\mu\text{m}$ thickness of <i>i</i> -propanol. The dotted line is spectrum of PVC under applied pressure.....	67
4.59	Comparison between the calculated bulk spectrum of PVC shown in Figure 4.57 (solid line) and Figure 4.58 (dotted line).....	68
4.60	Calculated bulk ATR spectrum of PVC acquired by single reflection ATR accessory (C) obtained by subtracting bulk ATR spectrum of mineral oil (B) from a three-phase system spectrum of ZnSe/mineral oil/PVC (A) with 0.043 $\mu\text{m}$ thickness of mineral oil. The dotted line is spectrum of PVC under applied pressure.....	69
4.61	Calculated bulk ATR spectrum of PVC acquired by single reflection ATR accessory (C) obtained by subtracting bulk ATR spectrum of mineral oil (B) from a three-phase system spectrum of ZnSe/mineral oil/PVC (A) with 0.012 $\mu\text{m}$ thickness of mineral oil. The dotted line is spectrum of PVC under applied pressure.....	69
4.62	Comparison between the calculated bulk spectrum of PVC shown in Figure 4.60 (solid line) and Figure 4.61 (dotted line).....	70
4.63	Calculated bulk ATR spectrum of PC acquired by single reflection ATR accessory (C) obtained by subtracting bulk ATR spectrum of <i>i</i> -propanol (B) from a three-phase system spectrum of ZnSe/ <i>i</i> -propanol/PC (A) with 0.220 $\mu\text{m}$ thickness of <i>i</i> -propanol. The dotted line is spectrum of PC under applied pressure.....	70

Figure	Page	
4.64	Calculated bulk ATR spectrum of PC acquired by single reflection ATR accessory (C) obtained by subtracting bulk ATR spectrum of <i>i</i> -propanol (B) from a three-phase system spectrum of ZnSe/ <i>i</i> -propanol/PC (A) with 0.120 $\mu\text{m}$ thickness of <i>i</i> -propanol. The dotted line is spectrum of PC under applied pressure.....	71
4.65	Comparison between the calculated bulk spectrum of PC shown in Figure 4.63 (solid line) and Figure 4.64 (dotted line).....	71
4.66	Calculated bulk ATR spectrum of PC acquired by single reflection ATR accessory (C) obtained by subtracting bulk ATR spectrum of mineral oil (B) from a three-phase system spectrum of ZnSe/mineral oil/PC (A) with 0.088 $\mu\text{m}$ thickness of mineral oil. The dotted line is spectrum of PC under applied pressure.....	72
4.67	Calculated bulk ATR spectrum of PC acquired by single reflection ATR accessory (C) obtained by subtracting bulk ATR spectrum of mineral oil (B) from a three-phase system spectrum of ZnSe/mineral oil/PC (A) with 0.051 $\mu\text{m}$ thickness of <i>i</i> -propanol. The dotted line is spectrum of PC under applied pressure.....	72
4.68	Comparison between the calculated bulk spectrum of PC shown in Figure 4.66 (solid line) and Figure 4.67 (dotted line).....	73
4.69	ATR spectra of PVC acquired by single reflection ATR accessory using ZnSe IRE (A) and Ge IRE (B) with 45° angle of incidence.....	74
4.70	ATR spectra of PC acquired by single reflection ATR accessory using ZnSe IRE (A) and Ge IRE (B) with 45° angle of incidence.....	74

Figure	Page	
4.71	Calculated bulk ATR spectrum of PVC acquired by single reflection ATR accessory (C) obtained by subtracting bulk ATR spectrum of mineral oil (B) from a three-phase system spectrum of Ge/ mineral oil /PVC (A) with 0.013 $\mu\text{m}$ thickness of mineral oil. The dotted line is spectrum of PVC under applied pressure.....	75
4.72	Calculated bulk ATR spectrum of PVC acquired by single reflection ATR accessory (C) obtained by subtracting bulk ATR spectrum of mineral oil (B) from a three-phase system spectrum of Ge/ mineral oil /PVC (A) with 0.007 $\mu\text{m}$ thickness of mineral oil. The dotted line is spectrum of PVC under applied pressure.....	75
4.73	Comparison between the calculated bulk spectrum of PVC shown in Figure 4.71 (solid line) and Figure 4.72 (dotted line).....	76
4.74	Calculated bulk ATR spectrum of PC acquired by single reflection ATR accessory (C) obtained by subtracting bulk ATR spectrum of mineral oil (B) from a three-phase system spectrum of Ge/ mineral oil /PC (A) with 0.037 $\mu\text{m}$ thickness of mineral oil. The dotted line is spectrum of PC under applied pressure. ....	77
4.75	Calculated bulk ATR spectrum of PC acquired by single reflection ATR accessory (C) obtained by subtracting bulk ATR spectrum of mineral oil (B) from a three-phase system spectrum of Ge/ mineral oil /PC (A) with 0.027 $\mu\text{m}$ thickness of mineral oil. The dotted line is spectrum of PC under applied pressure. ....	77
4.76	Comparison between the calculated bulk spectrum of PC shown in Figure 4.74 (solid line) and Figure 4.75 (dotted line).....	78

Figure	Page	
4.77	Calculated bulk ATR spectrum of PC rough 1200 acquired by single reflection ATR accessory (C) obtained by subtracting bulk ATR spectrum of mineral oil (B) from a three-phase system spectrum of Ge/ mineral oil /PC rough 1200 (A) with 0.119 $\mu\text{m}$ thickness of mineral oil. The dotted line is spectrum of PC rough 1200 under applied pressure.....	79
4.78	Calculated bulk ATR spectrum of PC rough 1200 acquired by single reflection ATR accessory (C) obtained by subtracting bulk ATR spectrum of mineral oil (B) from a three-phase system spectrum of Ge/ mineral oil /PC rough 1200 (A) with 0.058 $\mu\text{m}$ thickness of mineral oil. The dotted line is spectrum of PC rough 1200 under applied pressure.....	80
4.79	Comparison between the calculated bulk spectrum of PC rough 1200 shown in Figure 4.77 (solid line) and Figure 4.78 (dotted line).....	80
4.80	Calculated bulk ATR spectrum of PC rough 400 acquired by single reflection ATR accessory (C) obtained by subtracting bulk ATR spectrum of mineral oil (B) from a three-phase system spectrum of Ge/ mineral oil /PC rough 400 (A) with 0.134 $\mu\text{m}$ thickness of mineral oil. The dotted line is spectrum of PC rough 400 under applied pressure.....	81
4.81	Calculated bulk ATR spectrum of PC rough 400 acquired by single reflection ATR accessory (C) obtained by subtracting bulk ATR spectrum of mineral oil (B) from a three-phase system spectrum of Ge/ mineral oil /PC rough 400 (A) with 0.092 $\mu\text{m}$ thickness of mineral oil. The dotted line is spectrum of PC rough 400 under applied pressure.....	81



Figure	Page
4.82 Comparison between the calculated bulk spectrum of PC rough 400 shown in Figure 4.80 (solid line) and Figure 4.81 (dotted line).....	82
4.83 Calculated bulk ATR spectrum of PC rough 100 acquired by single reflection ATR accessory (C) obtained by subtracting bulk ATR spectrum of mineral oil (B) from a three-phase system spectrum of Ge/ mineral oil /PC rough 100 (A) with 0.154 $\mu\text{m}$ thickness of mineral oil. The dotted line is spectrum of PC rough 100 under applied pressure.....	82
4.84 Calculated bulk ATR spectrum of PC rough 100 acquired by single reflection ATR accessory (C) obtained by subtracting bulk ATR spectrum of mineral oil (B) from a three-phase system spectrum of Ge/ mineral oil /PC rough 100 (A) with 0.106 $\mu\text{m}$ thickness of mineral oil. The dotted line is spectrum of PC rough 100 under applied pressure. ....	83
4.85 Comparison between the calculated bulk spectrum of PC rough 100 shown in Figure 4.83 (solid line) and Figure 4.84 (dotted line).....	83

## LIST OF ABBREVIATIONS

ATR	: attenuated total reflection
$d_p$	: penetration depth
FT-IR	: Fourier transform infrared
Ge	: germanium
IRE	: internal reflection element
MATR	: multiple attenuated total reflection
MSEF	: mean square electric field
MSEvF	: mean square evanescent field
PC	: polycarbonate
PVC	: polyvinyl chloride
ZnSe	: zinc selenide

## LIST OF SYMBOLS

$\mu$	: micro
-------	---------

สถาบันวิทยบริการ  
จุฬาลงกรณ์มหาวิทยาลัย



# CHAPTER I

## INTRODUCTION

### 1.1 Optical Contact and ATR FT-IR Spectroscopy

Infrared spectroscopy is a particularly useful analytical technique because of its enormous versatility. In general infrared spectrum can be obtained, nondestructively. To collect an infrared spectrum various sampling technique can be employed such as transmission, reflection, reflection absorption and attenuated total reflection techniques. The choice for sampling technique depends strongly on the nature of the sample and the required information. For surface characterization, attenuated total reflection Fourier transform infrared (ATR FT-IR) spectroscopy is one of the most widely used technique in infrared spectroscopy. The phenomenon of total internal reflection in visible region was reported by Issac Newton.<sup>1</sup> The phenomenon remains unexplored until the early 1960s. It became a sampling technique for infrared spectroscopy with the pioneer efforts of Harrick and Fahrenfort.<sup>2, 3</sup> At the present, ATR FT-IR technique has been used in a wide variety of applications including qualitative analysis,<sup>4, 5</sup> quantitative analysis,<sup>6, 7</sup> diffusion studies,<sup>8, 9</sup> surface characterization,<sup>10, 11</sup> depth profiling,<sup>12</sup> and environmental application.<sup>13, 14</sup>

In contrast to transmission technique, ATR technique is well known as a surface characterization technique. The transmission technique has certain limitation related to the lack of surface sensitivity. As a result, certain applications such as degradation studied, surface reaction and modification cannot be investigated by he transmission technique. For surface characterization, it is essential that the information coming from the bulk of material must be distinguishable from that of the surface or interface. For transmission measurement, an average information is observed from bulk and surface of the sample. Due to the nature of the sample, the contribution of the surface information to the total absorption is small compared to that of the bulk. The surface region has a thickness of few nanometers or

sub-micrometers while that of the bulk is in the order of tens of micrometers. ATR accessories employ an internal reflection element (IRE) with a high refractive index on which the sample is placed. The difference in refractive indices between the IRE and the sample causes the infrared energy to be internally reflected. At each reflection, the electric component of the beam penetrates into the sample by a short distance from the IRE/sample interface. Typically the reflected radiation penetrates the sample to a depth of only a few micrometers.

As a result, only the surface information is observed in ATR technique. The electric field is strongest at the IRE/sample interface and exponentially decays to zero as a function of depth within the interface region. According to the decay characteristic of the electric field, the contact between the sample and the IRE plays a major role on the spectral quality obtained from an ATR experiment. From physical characteristic of sample, liquid sample always wet the surface of IRE. As a result, a perfect contact (i.e., optical contact) between liquid sample and the IRE is always achieved. The solid sample, on the other hand, rarely has a good contact with the IRE especially the sample with rough surface. Although the solid sample with mirror-flat surface is employed, the optical contact between the sample and the IRE is difficult to obtain due to dust and local irregularity of the surface. When the system does not achieve an optical contact, there is always an air gap between the sample and the IRE. The spectral intensity is decreased since the region of the near the surface of the IRE, where the electric field is strongest, is occupied by an air gap. The larger is the air gap, the smaller is the observed spectral intensity. If an air gap is large enough, the spectrum cannot be observed.

จุฬาลงกรณ์มหาวิทยาลัย

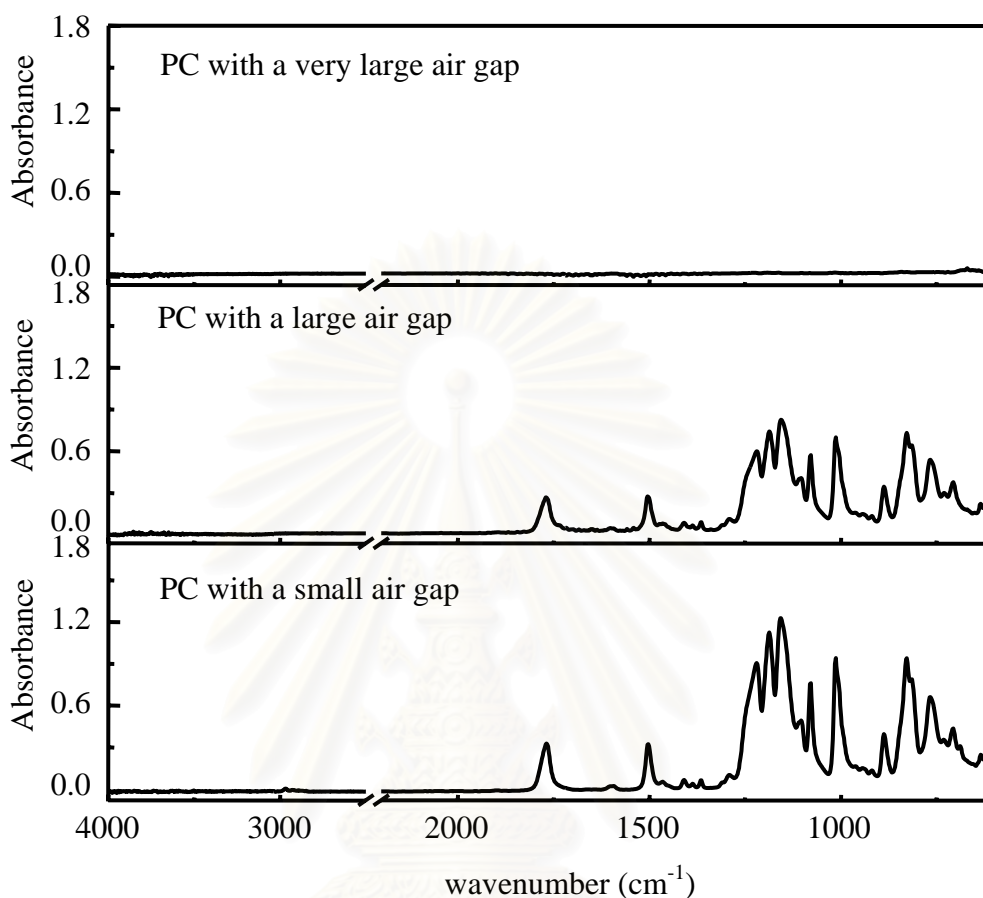


Figure 1.1 ATR spectra of a hard and rigid solid sample with different thickness of an air gap. The thickness of the air gap is altered by pressing the sample against the IRE.

An optical contact is important for quantitative analysis since quantitative characteristics of the sample can be drawn only when the optical contact is achieved. Equations expressing the relationship between ATR absorbance and material characteristic are defined based on the optical contact.

In a general practice, applying pressure to a solid sample against the IRE is the technique for improving the contact between the sample and the IRE. This technique is not always applicable since the excessive force may damage the IRE and/or cause a rapid deterioration of the IRE especially when a soft IRE is employed. Although the pressure is applied, a good contact between the IRE and the sample is

not normally achieved especially with a hard and rigid solid sample. Solution casting and hot pressing have been employed for achieving an optical contact.<sup>15, 16</sup> However, these techniques cannot be employed with pre-made film. Moreover, the solution casting or hot pressing process required long preparation time and the preparation procedures may affect the morphology of the sample. Using an ATR cell with a pressurized gas is another technique for maintaining a good contact.<sup>9, 17</sup> However, the pressurized gas may interfere with the sample and cause spectra to change. Moreover, contact improving by pressurized gas is rather complicated and requires skilled personal.

## **1.2 The Objective of This Research**

The objective of this research is to develop a new technique for enhancing ATR absorbance and to determine a bulk ATR spectrum of a solid sample which optical contact is difficult to achieve.

## **1.3 The Scope of This Research**

1. Improve the contact between the IRE and the solid sample by using the organic liquid.
2. Develop a technique for calculating bulk ATR spectra of the solid sample where optical contact is difficult to achieve.

สถาบันวิทยบริการ  
จุฬาลงกรณ์มหาวิทยาลัย

## CHAPTER II

### THEORETICAL BACKGROUND

#### 2.1 ATR FT-IR Theory

When light travels in a medium with high refractive index (i.e., denser medium) impinge at the interface of a medium with lower refractive index (i.e., rarer medium) at an angle greater than the critical angle, total reflection occurs. The critical angle can be calculated from the refractive indices of the denser medium and the rarer medium by the following expression:<sup>18</sup>

$$\theta_c = \sin^{-1}(n_1 / n_0) \quad (2.1)$$

where  $n_0$  and  $n_1$  are the refractive indices of the denser medium and that of the rarer medium, respectively.

Under non-absorbing condition (i.e., the rarer medium is transparent or absorption index of the medium,  $k_1$ , equal zero), the incident light is totally reflected at the interface. Since no light travels across the interface and there is no reflection loss due to absorption, this phenomenon is defined as total reflection phenomenon. When the rarer medium is absorbing (i.e., its absorption index is greater than zero), there is a reflection loss due to absorption. Reflectance of the beam leaving IRE/sample interface is less than unity. This phenomenon is defined as attenuated total reflection (ATR) phenomenon.

In an ATR configuration, the denser medium (i.e., an internal reflection element, IRE) is in contact with an optically rarer medium (i.e., a sample) as shown in Figure 2.1. The IRE is infrared transparent and has a refractive index  $n_0$ .

The sample is infrared absorbing and has a complex refractive index at frequency  $\nu$  ( $\text{cm}^{-1}$ ) of:<sup>18</sup>

$$\hat{n}_1 = n_1 + ik_1 \quad (2.2)$$

where  $i$  is equal  $\sqrt{-1}$ ,  $n_1$  and  $k_1$  are refractive index and absorption index, respectively. The absorption index is directly related to the absorption coefficient,  $\alpha$ , by the expression:<sup>18</sup>

$$\alpha(\nu) = 4\pi\nu k_1(\nu) \quad (2.3)$$

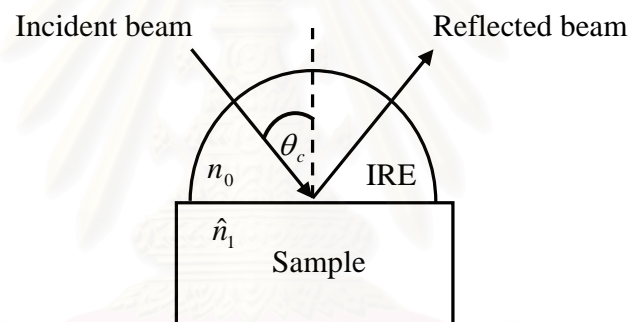


Figure 2.1 show an ATR configuration.

Under the ATR condition, although there is no light travels across the IRE/sample interface. There exist a strong electric field at the interface. The field is known as the evanescent field. The field is strongest at the sample surface. It exponentially decays to zero within a few micrometers from surface of the sample. The field interacts with the sample and causes a reflection loss in the reflected beam.

The rapid decay of the evanescent field is the unique characteristic that makes ATR technique a surface characterization technique. The decay characteristic of the evanescent field can be expressed in terms of the distance from IRE/sample interface by the following expression:<sup>1</sup>



$$E_z = E_0 e^{-2z/d_p} \quad (2.4)$$

where  $E_0$  and  $E_z$  are the evanescent fields at the IRE/sample interface and at depth  $z$  in the sample, respectively, and  $d_p$  is penetration depth. The penetration depth is defined by the distance from the IRE/sample interface where the evanescent field decays to  $1/e$  at its strength at the interface. The penetration depth is given in terms of experimental condition and material characteristics by:<sup>1</sup>

$$d_p = \frac{1}{2\pi\nu n_0 (\sin^2 \theta - (n_1/n_0)^2)^{1/2}} \quad (2.5)$$

where  $\nu$  ( $\text{cm}^{-1}$ ) is the frequency of the IR radiation and  $\theta$  is the angle of incidence. The evanescent field characteristic at the boundary between IRE and sample is shown in Figure 2.2.<sup>1</sup>

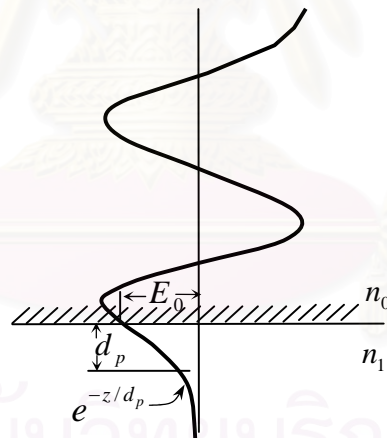


Figure 2.2 Evanescent wave at the boundary between IRE and sample.

According to equation 2.5, there are several important parameters that affect the observed spectrum and spectral qualities. One of them is the index matching. At a fixed angle of incidence, the penetration depth is larger for better index matching (i.e.,  $n_1$  is similar to  $n_0$ ). The refractive indices of standard IRE span from 2.4 to 4.0. When an organic material (refractive index of 1.5) is placed in contact with a ZnSe IRE (refractive index of 2.4), the ratio of the refractive indices is  $(n_1/n_0) = 0.625$ .

In contrary, when an organic material is in contact with a germanium IRE (refractive index of 4.0), the ratio of the refractive indices becomes 0.375. According to equation 2.5, the penetration depth with ZnSe as the IRE is greater than that with Ge. The expression also indicates that the penetration depth depend largely on the frequency of the incident beam. As the frequency of the infrared light increases the penetration depth decreases. However in FT-IR practice, it is often convenient to express frequency in terms of wavenumber, the penetration depth decreases when wavenumber increases. This also leads to a decrease of relative band intensities in the ATR spectrum with increasing wavenumber when compared to a transmission spectrum of the sample. Furthermore, changing the angle of incident changes the penetration depth. If the angle of incident is increased, the penetration depth will be decreased and the spectral intensity will be decreased. The greater penetration depth implies a greater distance from surface of the sample where chemical information can be observed by ATR technique.

## 2.2 ATR Spectral Intensity

In ATR experiment, the magnitudes of the interaction between light and the sample can be expressed in terms of absorbance. The absorbance depends on both the material properties (e.g., refractive index of the IRE and complex refractive index of the sample) and the experimental parameters (e.g., angle of incidence and polarization of the incident beam). The relationship between absorbed and reflected intensity in an ATR spectrum is given by:<sup>19</sup>

$$A_l(\theta, \nu) = 1 - R_l(\theta, \nu) \quad (2.6)$$

where  $A(\theta, \nu)$  and  $R(\theta, \nu)$  are absorptance and reflectance, respectively and  $l$  indicates the polarization of the incident beam. The polarization direction is given with respect to the plane of incidence. The plane of incidence is defined as the plane that contains both incident and reflected beam. For  $p$ -polarization, the electric component of the electromagnetic wave is parallel to the plane of incidence while the magnetic



component is perpendicular to the plane of incidence. Whereas, the electric component of the electromagnetic wave with  $s$ -polarization is perpendicular to the plane of incidence while the magnetic component is parallel to the plane of incidence. In general, absorptance in ATR can be expressed in terms of experimental parameters and material characteristic by the following expression:<sup>19</sup>

$$A_l(\theta, \nu) = \frac{4\pi\nu}{n_0 \cos\theta} \int_0^\infty n_1(\nu) k_1(\nu) \langle E_{z_l}^2(\theta, \nu) \rangle dz \quad (2.7)$$

where  $\langle E_{z_l}^2(\theta, \nu) \rangle$  is the mean square electric field (MSEF) at depth  $z$ .

Under a small absorption condition, the decay behavior of the MSEF is the same as that of the mean square evanescent field (MSEvF). Therefore, the MSEF can be estimated from the MSEvF by:<sup>19</sup>

$$\begin{aligned} \langle E_{z_l}^2(\theta, \nu) \rangle &= \frac{1 + R_l(\theta, \nu)}{2} \langle E_{z_l}^2(\theta, \nu) \rangle_{k=0} \\ \langle E_{z_l}^2(\theta, \nu) \rangle &= \frac{1 + R_l(\theta, \nu)}{2} \langle E_{0l}^2(\theta, \nu) \rangle_{k=0} e^{-2z/d_p} \end{aligned} \quad (2.8)$$

where  $\langle E_{0l}^2(\theta, \nu) \rangle_{k=0}$  and  $\langle E_{z_l}^2(\theta, \nu) \rangle_{k=0}$  are the MSEvF at the interface between the IRE and the sample and at depth  $z$ , respectively.

From equations 2.7 and 2.8, absorptance of an isotropic medium is given in term the MSEvF by:<sup>19</sup>

$$A_l(\theta, \nu) = \frac{4\pi\nu}{n_0 \cos\theta} \int_0^\infty n_1(\nu) k_1(\nu) \frac{1 + R_l(\theta, \nu)}{2} \langle E_{z_l}^2(\theta, \nu) \rangle_{k=0} dz$$

$$2 \frac{1 - R_i(\theta, \nu)}{1 + R_i(\theta, \nu)} = \frac{4\pi\nu}{n_0 \cos\theta} \int_0^\infty n_1(\nu) k_1(\nu) \langle E_{z'}^2(\theta, \nu) \rangle_{k=0} dz$$

$$-\ln R_i(\theta, \nu) \cong \frac{4\pi\nu}{n_0 \cos\theta} \int_0^\infty n_1(\nu) k_1(\nu) \langle E_{z'}^2(\theta, \nu) \rangle_{k=0} dz \quad (2.9)$$

In general, the ATR spectral intensity that obtains from a spectrometer is in absorbance unit. The spectral intensity in absorbance unit is defined in terms of the reflectance by:<sup>19</sup>

$$A_i(\theta, \nu) = -\log[(R_i, \theta, \nu)] \quad (2.10)$$

According to equations 2.9 and 2.10, an ATR spectral intensity in absorbance unit is given in term of experimental conditions and material characteristics by:<sup>19</sup>

$$A_i(\theta, \nu) \cong \frac{4\pi\nu}{\ln(10) n_0 \cos\theta} \int_0^\infty n_1(\nu) k_1(\nu) \langle E_{z'}^2(\theta, \nu) \rangle_{k=0} dz \quad (2.11)$$

The above expression indicates that the MSEvF is one of the important factors that affect the ATR spectral intensity. The MSEvF depends on both the angle of incidence and frequency of the incident beam as shown in Figures 2.3 and 2.4, respectively.<sup>20</sup>

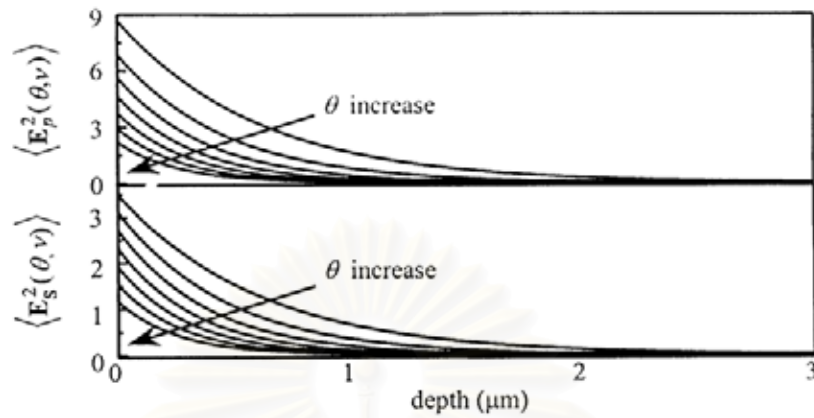


Figure 2.3 Depth dependent MSEvF at various angles of incidences. The simulation parameters are  $\nu = 1000 \text{ cm}^{-1}$ ,  $n_0 = 4.0$ ,  $n_1 = 1.5$ ,  $k_I = 0$ ,  $\theta = 30^\circ, 35^\circ, 40^\circ, 45^\circ, 50^\circ, 55^\circ, 60^\circ$ .

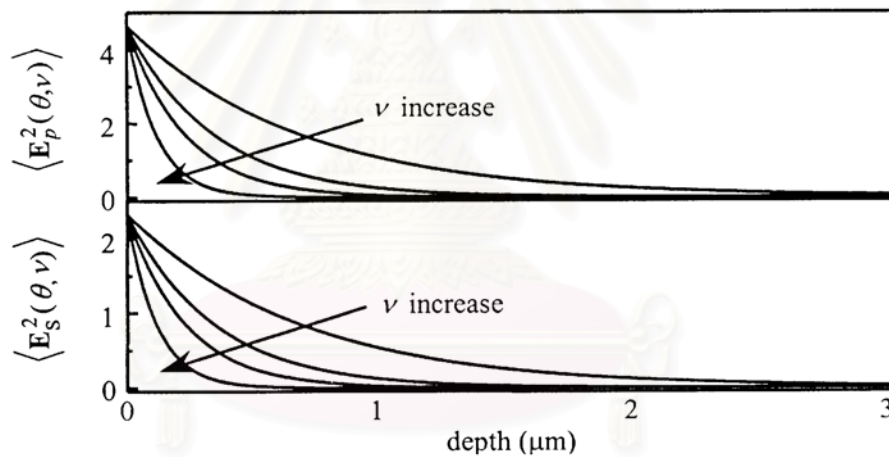


Figure 2.4 Depth dependent MSEvF at various frequencies. The simulation parameters are  $n_0 = 4.0$ ,  $n_1 = 1.5$ ,  $k_I = 0$ ,  $\theta = 30^\circ, 35^\circ, 40^\circ, 45^\circ, 50^\circ, 55^\circ, 60^\circ$ ,  $\nu = 500, 1000, 1500, 3000 \text{ cm}^{-1}$ .

As the angle of incidence increases, the MSEF at the surface (i. e.,  $z = 0$ ) becomes smaller. The greater the angle of incidence, the faster the field decays. Figure 2.4 indicates that if the refractive indices at two different frequencies are the same, the MSEF at the surface are the same but their decay characteristics are different. The greater the frequency, the faster the field decays. Since the evanescent wave decays rapidly with the distance from the surface, it is important to have a good contact between IRE and sample.

### 2.3 Problem in Optical Contact Between Sample and IRE

As mentioned previously, an optical contact between the IRE and a sample is required in the ATR measurement. Liquid samples always have optical contact with the IRE. Solid sample, on the other hand, does not have a good contact with IRE. There is always an air gap between the sample and IRE. When there is an air gap in the system, the spectral intensity is severely deteriorated. Since the refractive index of an air gap is 1.0 while that of the organic sample is approximately 1.5, the strength and decays characteristic of the MSEvF in the system with an air gap is altered by the refractive index mismatch. The unusual decay behavior of the MSEvF with *p*-polarization and *s*-polarization are shown in Figure 2.5. The Figure indicates that the MSEvF with *p*-polarization is altered by the air gap compared to that of the *s*-polarization. Since a part of the strong electric field is occupied by the air gap, which does not involve in any absorption, absorbance of the sample in ATR spectra is decreased. The magnitude of reduction depends largely on the thickness of the air gap. The greater is the air gap, the smaller is the absorbance. In a worse case, spectrum of the sample cannot be observed since the MSEvF decay to zero within the thickness of the air gap. Moreover, the relationship between the absorbance and material characteristics in a system with an air gap does not follow the expression given in Equation 2.11. As a result, the quantitative characteristic of the sample cannot be drawn from such a spectrum.

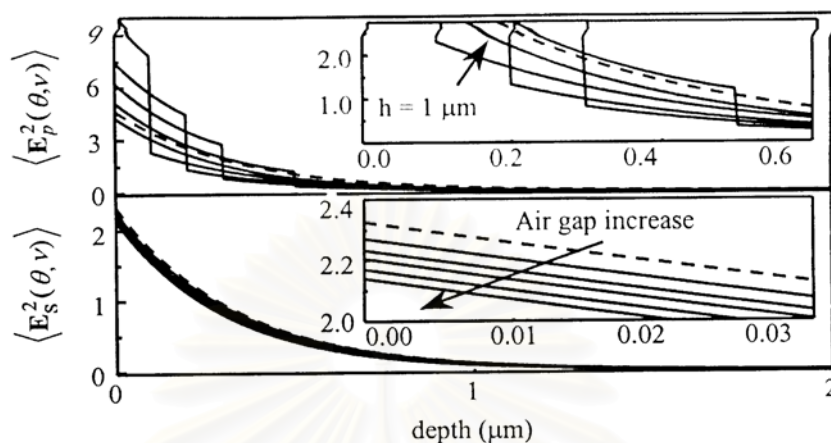


Figure 2.5 The decay characteristic of the MSEvF at various air gap thickness (solid lines) and those under optical contact (broken lines). The simulation parameters are  $n_o = 4.0$ ,  $\theta = 45^\circ$ ,  $\nu = 1000 \text{ cm}^{-1}$ ,  $n_{air} = 1.0$ ,  $n_p = 1.5$ , and the air gap thickness of 0.0, 0.1, 0.2, 0.3, 0.5, and 1.0  $\mu\text{m}$ .

## 2.4 A Solution for Contact Problem in ATR Technique

When the contact between the solid sample and the IRE is not perfect. It is important to use pressure or force to press the sample against the IRE. However, the magnitude of pressure that can be applied to achieve optical contact is limited. If the sample is harder than the IRE, the applied pressure will lead to rapid deterioration of the IRE. In addition, the excessive force may damage morphology of the sample. Liquid always has optical contact with the IRE. An air gap is then replaced by liquid with similar refractive index as that of the solid sample. As a result, the strength and decay characteristics of the MSEvF in this system are similar to those with the optical contact.<sup>20</sup> In case where the solid sample is an organic compound, an organic liquid can be employed as the intermediate layer between the IRE and the solid sample. When the contact problem is solved by organic liquid, the obtained ATR spectrum becomes a spectrum of a three-phase system. This system consists of the IRE, medium 1 (organic liquid) and medium 2 (the solid sample). Medium 1 has a thickness of  $h$ , while medium 2 has an infinite thickness, as illustrated in Figure 2.6.

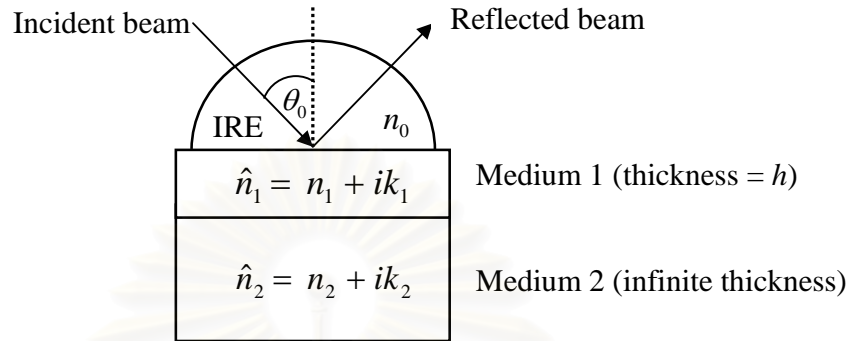


Figure 2.6 A schematic illustration of a three-phase system of isotropic media.

The obtained spectrum consists of both the absorption of the solid sample and that of the organic liquid. The bulk spectrum of the solid sample can be obtained by subtracting the bulk organic liquid from a three-phase spectrum.

## 2.5 Calculation for Bulk spectrum of Solid sample

In a three-phase system, the IRE is assumed to be homogenous, isotropic and transparent with a refractive index  $n_0$ . Medium 1 and medium 2 are homogenous, isotropic, and absorbing with complex refractive index  $\hat{n}_1$  and  $\hat{n}_2$ , respectively.

The obtained spectral intensity in a three-phase system is a result of the interaction between the MSEvF and both absorbing media. Therefore, the absorbance of the three-phase can be expressed as the summation of the absorbance of each medium as:<sup>21</sup>

$$A_l(\theta, \nu) = \frac{4\pi\nu}{n_0 \cos\theta} \left[ \int_0^h n_1(\nu)k_1(\nu) \langle E_{z'}^2(\theta, \nu) \rangle dz + \int_h^\infty n_2(\nu)k_2(\nu) \langle E_{z'}^2(\theta, \nu) \rangle dz \right] \quad (2.12)$$

Under a small absorption approximation, The MSEF can be estimated from the MSEvF as shown previously in equation 2.8. By substituting equation 2.8 into equation 2.10 and using the approximation:<sup>21</sup>

$$\frac{R_l - 1}{R_l + 1} \cong \frac{\ln R_l}{2}$$

The following expression can be obtained.<sup>21</sup>

$$\ln R_l = -\frac{2\pi\nu d_p \langle E_{0l}^2(\theta, \nu) \rangle_{k=0}}{n_0(\nu) \cos \theta} \left\{ \left(1 - e^{-2h/d_p}\right) n_1(\nu) k_y(\nu) + e^{-2h/d_p} n_2(\nu) k_2(\nu) \right\} \quad (2.13)$$

Moreover, in the case where refractive indices of media 1 and 2 are similar, the reflectance can be expressed in a simple form as:<sup>21</sup>

$$\ln R_l = (1 - e^{-4\pi h \nu \sqrt{\sigma}}) \ln R_{01l} + e^{-4\pi h \nu \sqrt{\sigma}} \ln R_{02l} \quad (2.14)$$

where  $\sigma = n_0^2 \sin^2 \theta_0 - n_1^2$ . As a result, the reflectance of a three-phase system can be expressed as:<sup>21</sup>

$$\ln R_l = \left(1 - e^{-2h/d_p}\right) \ln R_{01l} + e^{-2h/d_p} \ln R_{02l} \quad (2.15)$$

where  $R_{01l}$  and  $R_{02l}$  are bulk ATR reflectance of medium 1 and 2, respectively. According to equation 2.10, the ATR spectral intensity in absorbance units of a three-phase system can be simplified to:<sup>21</sup>

$$A_l = \left(1 - e^{-2h/d_p}\right) A_{01l} + e^{-2h/d_p} A_{02l} \quad (2.16)$$



where  $A_l$  is the absorbance of a three-phase system,  $A_{01l}$  and  $A_{02l}$  are the absorbance of the bulk materials. According to equation 2.16, when the absorbance of a three-phase system and that of the bulk organic liquid are obtained, the absorbance of the bulk solid sample can be calculated.



สถาบันวิทยบริการ  
จุฬาลงกรณ์มหาวิทยาลัย



## CHAPTER III

### EXPERIMENT

#### 3.1 Spectral Simulation

All programs for spectral simulation were written in MATLAB program (Maths Works Inc.). The process of simulation consists of two steps. First, the refractive index spectrum and absorption index spectrum were generated via a Lorentz model with the refractive index at an infinite frequency of 1.5. The medium 1, which represents an organic liquid, has two absorption bands at 2000 and 3500  $\text{cm}^{-1}$  with an equally maximum absorption index of 0.05 and full width at half-height of 20 (Appendix A). The medium 2, which represents a solid sample, has four absorption bands at 900, 1500, 2500 and 3000  $\text{cm}^{-1}$  with an equally maximum absorption index of 0.05 and full width at half-height of 30 (Appendix B). The obtained spectra in the first step were stored in ASCII files format and used as an input data for further simulation of ATR spectra. The detail descriptions for all employed equations and all parameters were given elsewhere.<sup>22, 23</sup> The ATR spectra of the medium 1 and the medium 2 were simulated at a 45° angle of incidence with non-polarization and with a refractive index of the IRE of 4.0 (Appendix C).

The simulated spectra were employed to verify the limitation of the technique for improving the optical contact and the technique for calculating the bulk spectra of solid sample in ATR measurement.

##### 3.1.1 The Influence of an Air Gap

The complex refractive index spectrum and the absorption spectrum of an air gap were generated with the refractive index at an infinite frequency of 1.0 and with an equally maximum absorption index of 0. The ATR spectra of medium 2

with 0.005, 0.05 and 0.5  $\mu\text{m}$  air gap were simulated using the MATLAB program given in Appendix D.

### 3.1.2 A Technique for Intensity Enhancement

The simulated spectra of medium 1 and medium 2 obtained from section 3.1 were employed as media for a three-phase system spectral simulation. The ATR spectra of the three-phase system were simulated at various thickness of medium 1 (0.005, 0.05 and 0.5  $\mu\text{m}$ ),  $45^\circ$  angle of incidence with non-polarization and a refractive index of IRE of 4.0 (Appendix E).

### 3.1.3 Calculation of Bulk ATR Spectrum

According to equation 2.16, the bulk spectrum of the solid sample can be calculated from the spectrum of a three-phase system and bulk spectrum of liquid by the following expression:

$$A_s = \frac{A_{3p} - (1 - e^{-2h/dp})A_f}{e^{-2h/dp}} \quad (3.1)$$

Where  $A_s$  is the calculated bulk ATR spectrum of the solid sample,  $A_{3p}$  is the ATR spectrum of the three-phase system,  $A_f$  is the bulk ATR spectrum of the liquid film,  $h$  is the thickness of the liquid film and  $d_p$  is the penetration depth.

The absorbance of the bulk medium 1 was obtained from section 3.1, while the absorbance of a three-phase system and the thickness of medium 1 were obtained from section 3.1.2. The detail of the calculation was described in Appendix F.

## 3.2 ATR Spectral Acquisition

All spectra were collected at a resolution of  $4\text{ cm}^{-1}$  with 16 scans co-addition using Bruker Vector 33 FT-IR spectrometer equipped with a DTGS detector. The multiple attenuated total reflection (MATR) accessory with  $45^\circ$  Zinc selenide (ZnSe) IRE (Spectra Tech, U.S.A.) and the variable angle reflection accessory (the Seagull™, Harrick Scientific, U.S.A) with a hemispherical ZnSe and Germanium (Ge) IRE were employed for all ATR spectral acquisitions. Three types of samples were used for the goodness-of-contact investigation: a soft and rubbery solid sample, a hard and rigid solid sample with flat surface and a hard and rigid solid sample with rough surface. Two types of organic liquid were used for the suitability-of-liquid investigation: a low viscosity organic liquid and a high viscosity organic liquid.

### 3.2.1 Materials

#### a) Multiple Reflection System

1. Polyvinylchloride (PVC) ( $10 \times 50 \times 3\text{ mm}$ )
2. Flat-surfaced Polycarbonate (PC) ( $10 \times 50 \times 1\text{ mm}$ )
3. Rough-surfaced PC ( $10 \times 50 \times 1\text{ mm}$ )
4. *i*-Propanol
5. Mineral oil

#### b) Single Reflection System

1. PVC ( $6 \times 6 \times 1\text{ mm}$ )
2. Flat-surfaced PC ( $6 \times 6 \times 1\text{ mm}$ )
3. Rough-surfaced PC ( $6 \times 6 \times 1\text{ mm}$ )
4. *i*-Propanol
5. Mineral oil

### **3.2.2 Experimental Procedure**

#### **3.2.2.1 The Influence of an Air Gap**

##### **a) Multiple Reflection System**

1. PVC was placed against ZnSe IRE without the applied pressure, the spectrum of PVC was then collected using MATR accessory.
2. PVC in 1 was pressed by pressure clamp, the spectrum of PVC was then collected. The applied pressure was increased and ATR spectra of PVC were collected until no more significant increment of absorbance was observed.
3. The same procedures as described in 1 and 2 were repeated using PC as a sample instead of PVC.

##### **b) Single Reflection System**

1. PVC was placed against ZnSe IRE without the applied pressure, the spectrum of PVC was then collected using the variable angle reflection accessory.
2. The pressure was applied to the PVC sample in 1, the spectrum of PVC was then collected. The applied pressure was increased and ATR spectra of PVC were collected until no more significant increment of absorbance was observed.
3. The same procedures as described in 1 and 2 were repeated using PC as a sample instead of PVC and the spectra of PC at various the applied pressures were acquired.

#### **3.2.2.2 Absorbance Enhancement**

##### **3.2.2.2.1 Influence of Organic Liquid**

###### **a) Multiple Reflection System**

1. PVC was placed against ZnSe IRE. The pressure is then applied onto the sample at the same level as that described in 3.2.2.1. ATR spectrum of PVC was then collected via MATR accessory.
2. PVC was removed from ZnSe IRE, then the IRE was cleaned and dried.

3. *i*-Propanol was spread over ZnSe IRE and ATR spectrum of *i*-propanol was collected.

4. *i*-Propanol was spread as a thin liquid film over ZnSe IRE. A piece of PVC was placed on *i*-propanol. Pressure was applied onto the sample in order to squeeze the excess amount of *i*-propanol and to vary the thickness of *i*-propanol film, the three-phase system spectra of ZnSe/*i*-propanol/PVC were taken simultaneously as the applied pressure was increased.

5. PVC and *i*-propanol were removed from ZnSe IRE. ZnSe IRE was cleaned and dried.

6. Mineral oil was employed as a liquid film in stead of *i*-propanol. The three-phase system spectra of ZnSe/mineral oil/PVC at various thickness of mineral oil were collected.

The same procedures as described in 1 to 6 were repeated using PC as a solid sample instead of PVC. ATR spectrum of PC, the three-phase system spectra of ZnSe/*i*-propanol/PC and the three-phase system spectra of ZnSe/mineral oil/PC were acquired.

#### **b) Single Reflection System**

1. PVC was placed against ZnSe IRE. The pressure is then applied onto the sample at the same level as that described in 3.2.2.1. ATR spectrum of PVC was then collected via the variable angle reflection accessory.

2. PVC was removed from ZnSe IRE, then the IRE was cleaned and dried.

3. *i*-Propanol was spread over ZnSe IRE and ATR spectrum of *i*-propanol was collected.

4. *i*-Propanol was spread as a thin liquid film over ZnSe IRE. A piece of PVC was placed on *i*-propanol. Pressure was applied onto the sample in order to squeeze the excess amount of *i*-propanol and to vary the thickness of *i*-propanol film, the three-phase system spectra of ZnSe/*i*-propanol/PVC were taken simultaneously as the applied pressure was increased.

5. PVC and *i*-propanol were removed from ZnSe IRE. ZnSe IRE was cleaned and dried.

6. Mineral oil was employed as a liquid film instead of *i*-propanol. The three-phase system spectra of ZnSe/mineral oil/PVC at various thickness of mineral oil were collected.

The same procedures as described in 1 to 5 were repeated using PC as a solid sample instead of PVC. ATR spectrum of PC, the three-phase system spectra of ZnSe/*i*-propanol/PC and the three-phase system spectra of ZnSe/mineral oil/PC were acquired.

### 3.2.2.2.2 Influence of Surface Roughness

#### a) Multiple Reflection System

PC with the rough surface was created by sandpaper. The degrees of roughness were varied by various numbers of sandpaper; number 1200, 400 and 100. The PC samples were then called PC rough 1200, PC rough 400 and PC rough 100, respectively. The greater the number of the sandpaper, the smaller roughness.

The experimental procedures were the same as described in topic influence of organic liquid. ATR spectra of PC rough 1200, ATR spectra of PC rough 400, ATR spectra of PC rough 100, the three-phase system spectra of ZnSe/ *i*-propanol/PC rough 1200, ZnSe/mineral oil/PC rough 1200, the three-phase system spectra of ZnSe/*i*-propanol/PC rough 400, ZnSe/mineral oil/PC rough 400, ZnSe/ *i*-propanol/PC rough 100 and ZnSe/mineral oil/PC rough 100 were collected via MATR accessory.

#### b) Single Reflection System

The experimental procedures were the same as described in multiple reflection system, except the variable angle reflection accessory was employed instead of the MATR accessory.



### 3.2.2.3 Bulk ATR Spectra from observed spectra

1. The three-phase system spectra, which obtained from section 3.2.2.2 were employed for calculating the thickness of organic liquid using equation 2.16 (Appendix G).

2. The obtained thickness of organic liquid, the bulk spectrum of organic liquid and the three-phase system spectra in section 3.2.2.2 were employed as input data for calculating the bulk spectrum of solid sample. The program of calculating the bulk spectrum of solid sample in this section was the same as that in 3.1.3 (Appendix H).



สถาบันวิทยบริการ  
จุฬาลงกรณ์มหาวิทยาลัย

## CHAPTER IV

### RESULTS AND DISCUSSION

#### 4.1 Spectral Simulation

The proposed technique for calculating bulk ATR spectra from the observed spectra will be first verified by spectral simulation using optical theory. From the optical theory, if the complex refractive index (i.e., refractive index and absorption index) of a material is known, its spectrum under various experimental conditions can be calculated. The complex refractive index spectrum of medium 1 (i.e., the liquid medium) in the mid-infrared region is shown in Figure 4.1 while a simulated ATR spectrum of medium 1 shown in Figure 4.2. The complex refractive index spectrum of medium 2 (i.e., the solid substrate) is shown in Figure 4.3 while its simulated ATR spectrum is shown in Figure 4.4.

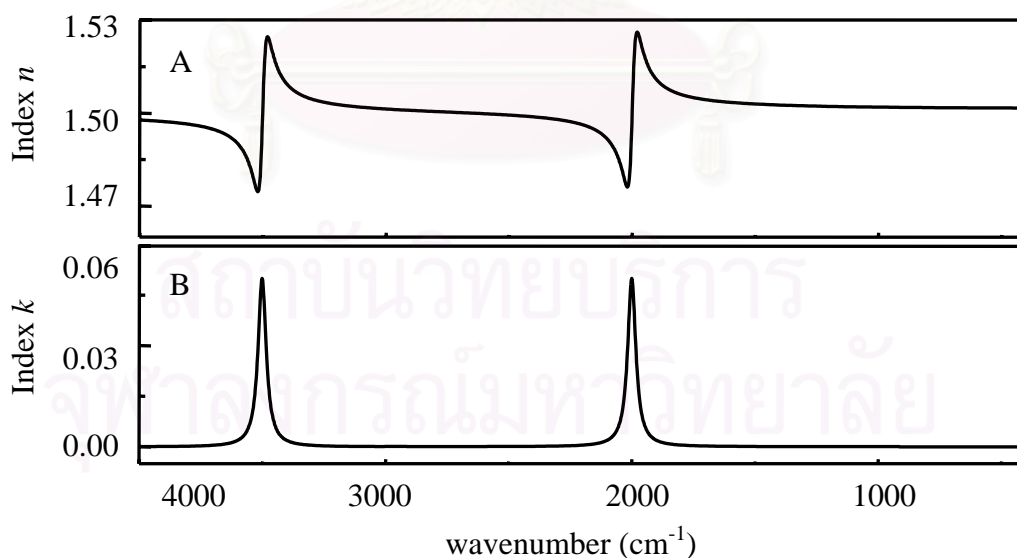


Figure 4.1 Complex refractive index spectrum of medium 1 in mid-infrared region (A) and absorption index spectrum (B).

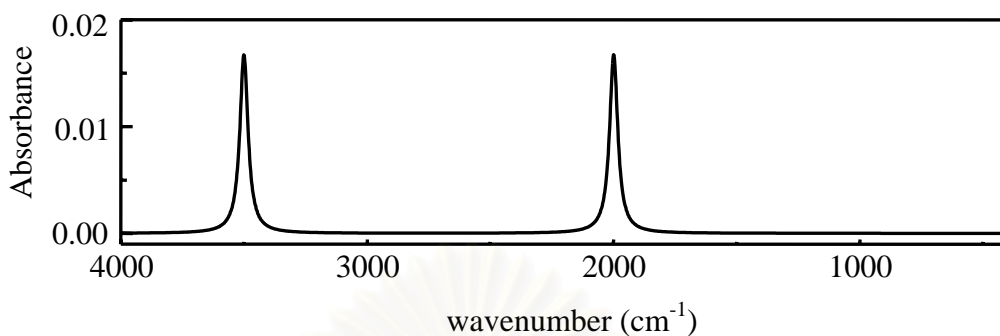


Figure 4.2 Simulated ATR spectrum of medium 1 under optical contact. The simulation parameters are  $n_0 = 4.0$ ,  $n_1 = 1.5$ , and  $\theta = 45^\circ$ .

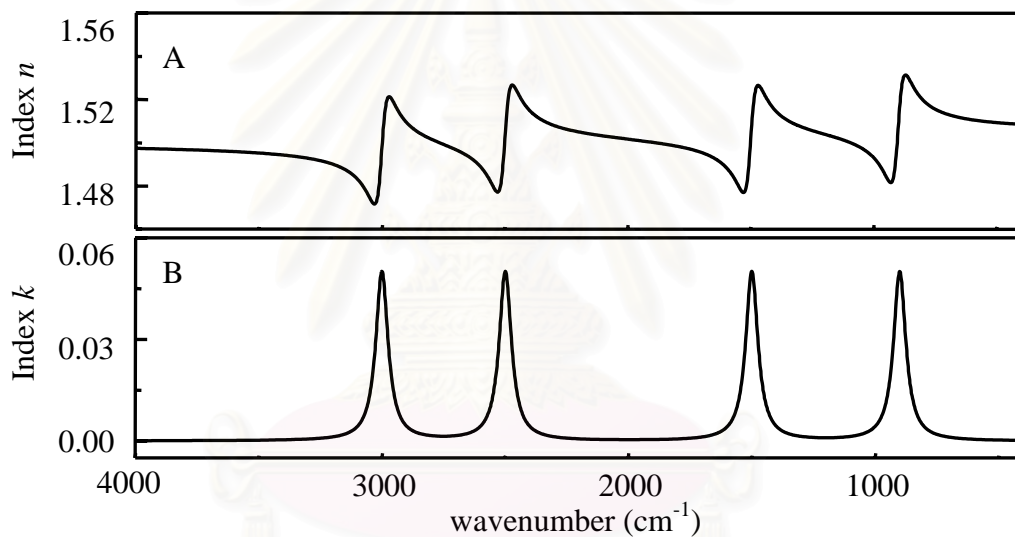


Figure 4.3 Complex refractive index spectrum of medium 2 in mid-infrared region (A) and absorption index spectrum (B).

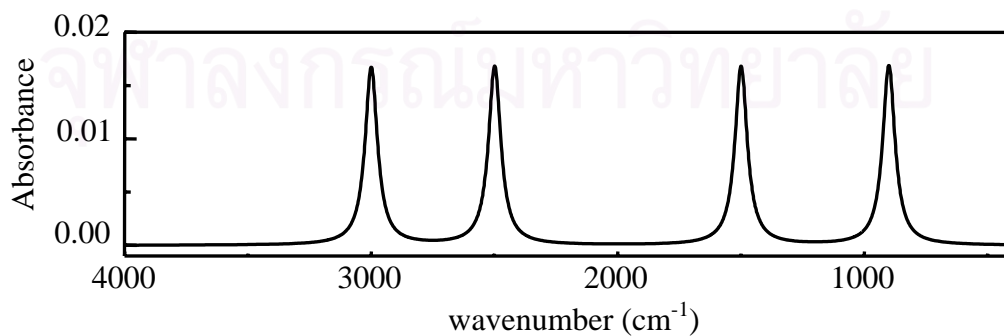


Figure 4.4 Simulated ATR spectrum of medium 2 under optical contact. The simulation parameters are  $n_0 = 4.0$ ,  $n_1 = 1.5$ , and  $\theta = 45^\circ$ .

### 4.1.1 The Influence of an Air Gap

In ATR measurement, it is important to have an optical contact between IRE and sample. If the optical contact is not achieved, an air gap presents. The refractive index mismatch between an air gap ( $n = 0$ ) and a sample ( $n = 1.5$ ) presents. This is cause of the unusual decay behavior of the MSEvF as shown in Figure 2.5. ATR spectra were simulated to demonstrate the influence of an air gap shown in Figure 4.5.

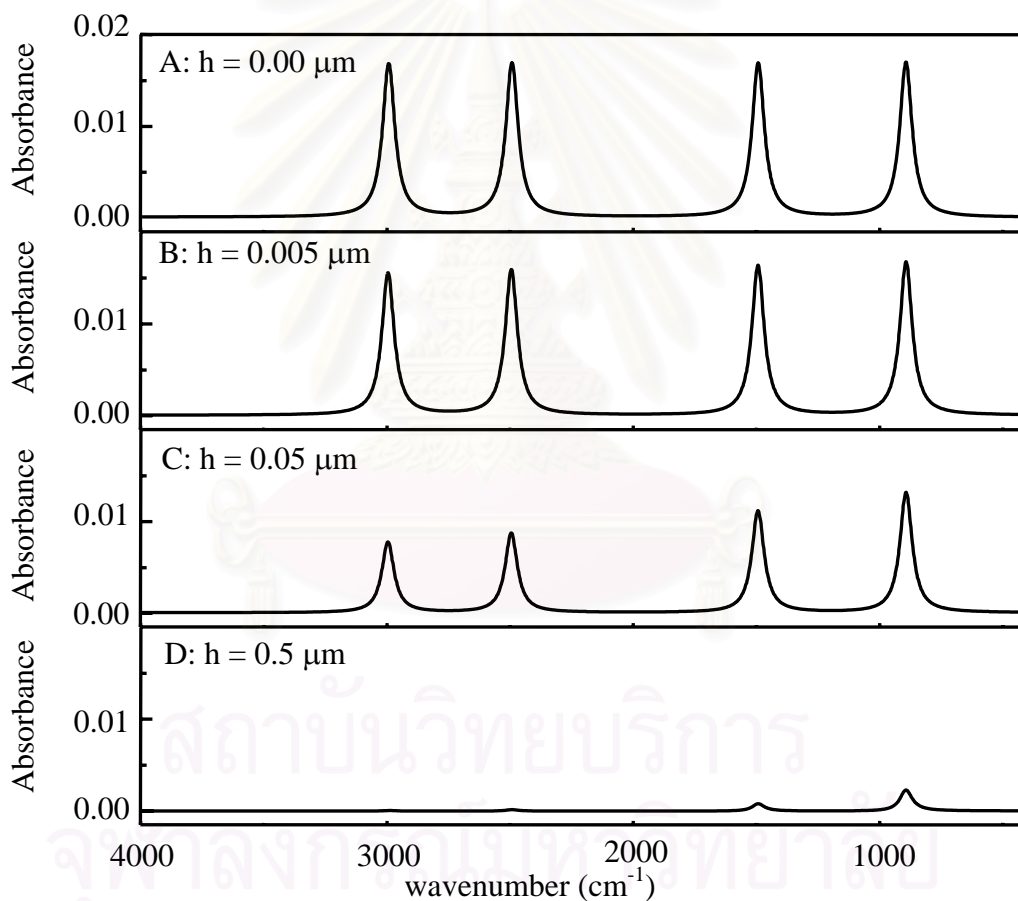


Figure 4.5 ATR spectra of medium 2 at various thickness of the air gap: 0.00 (A), 0.005 (B), 0.05 (C) and 0.5  $\mu\text{m}$  (D). The simulation parameters are the same as those of Figure 4.4.

The simulated spectra of the sample at various thickness of the air gap indicate that when there is no air gap in the system (i.e., optical contact), all absorption bands have the same maximum absorbance. When there is the air gap in the system, the absorbance is decreased. The thicker air gap, the smaller the observed absorbance. Since the strength  $MSEvF$  is significantly decreased when there is an air gap between the sample and the IRE (see Figure 2.5), the interaction between the  $MSEvF$  and the sample is decreased. Under the same air gap, absorbance at high frequency decreases to a greater extent than that at low frequency. This is due to the decay characteristics of  $MSEvF$ . Since the field decays faster at a high frequency (as shown in Figures 2.3 and 2.4), the absorption band at a higher frequency disappears before that at a lower frequency as the air gap becomes thicker.

#### **4.1.2 A Technique for Intensity Enhancement**

Since the refractive index of the air gap ( $n = 1.0$ ) and that of the sample ( $n = 1.5$ ) are different, the refractive index mismatch presents in the system. The decay characteristics of the  $MSEvF$  are changed when there is air gap between the sample and the IRE. It affects the absorbance of the sample as shown in previous topic. The problem of the refractive index mismatch can be solved by replacing the air gap with an organic liquid with a refractive index similar to that of the solid sample. When the refractive index mismatch is eliminated, the decay characteristics of the  $MSEvF$  in this system are the same as that in the system with the optical contact (as shown in Figure 2.6). Therefore, the absorbance of the solid sample is enhanced. Example of absorbance enhancement is shown in Figure 4.6.

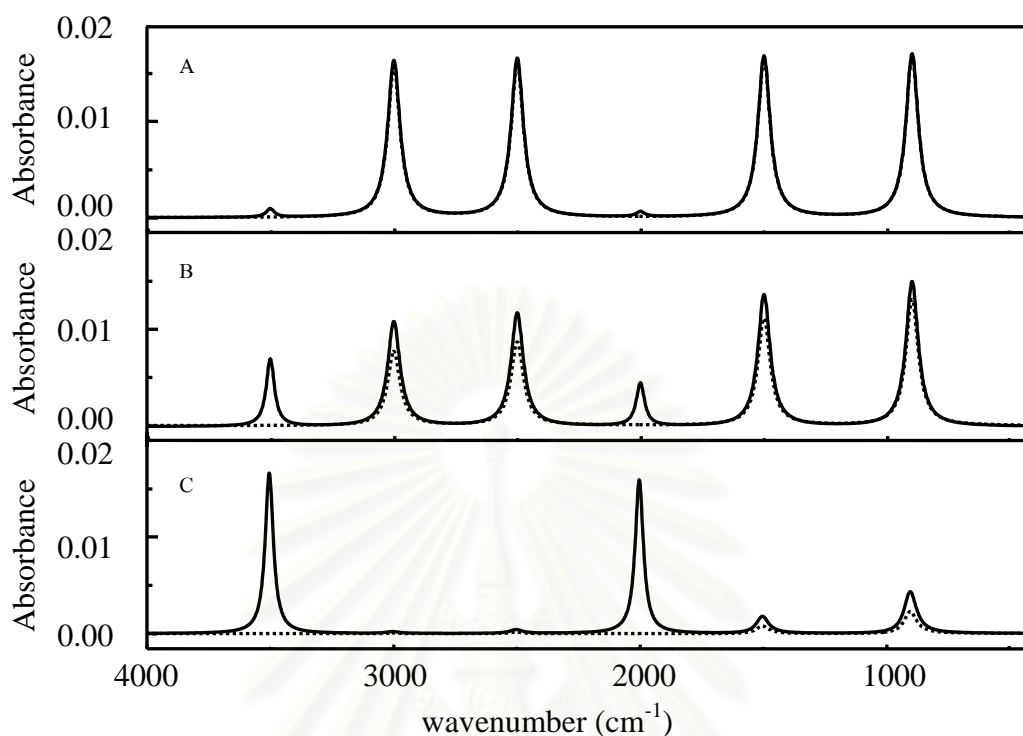


Figure 4.6 Simulated ATR spectra of medium 2 (solid line) at various thickness of medium 1: 0.005 (A), 0.05 (B), and 0.5  $\mu\text{m}$  (C). The dotted lines show spectra of the system at the corresponding thickness of air gap.

In the three-phase system of the air gap (IRE/air gap/medium 2) and that of medium 1 (IRE/medium 1/medium 2) with the same thickness of air gap and medium 1, the characteristic absorbance of medium 2 (i.e., at 3000, 2500, 1500 and 900  $\text{cm}^{-1}$ ) is greater in the three-phase system of medium 1. A greater difference is observed at high frequency and at greater thickness. The observed phenomena indicate the absorbance enhancement when medium with similar refractive index replaces the air gap. The actual experiment, an organic liquid can be employed for improving absorbance of the solid sample in ATR measurement.



### 4.1.3 Calculation of Bulk Spectrum

The spectra obtained from the technique for intensity enhancement are the three-phase system spectra. In the actual experiment, the system consists of IRE, an organic liquid, and a solid sample. The observed spectra consist of both the characteristic absorption of the solid sample and that of the organic liquid. In order to obtain the bulk spectrum of the solid sample, the absorbance of organic liquid must be subtracted from the three-phase spectrum. A subtraction algorithm based on equation 2.16 is employed. The bulk spectra calculated from the system shown in Figure 4.6 are shown in Figures 4.7-4.9.

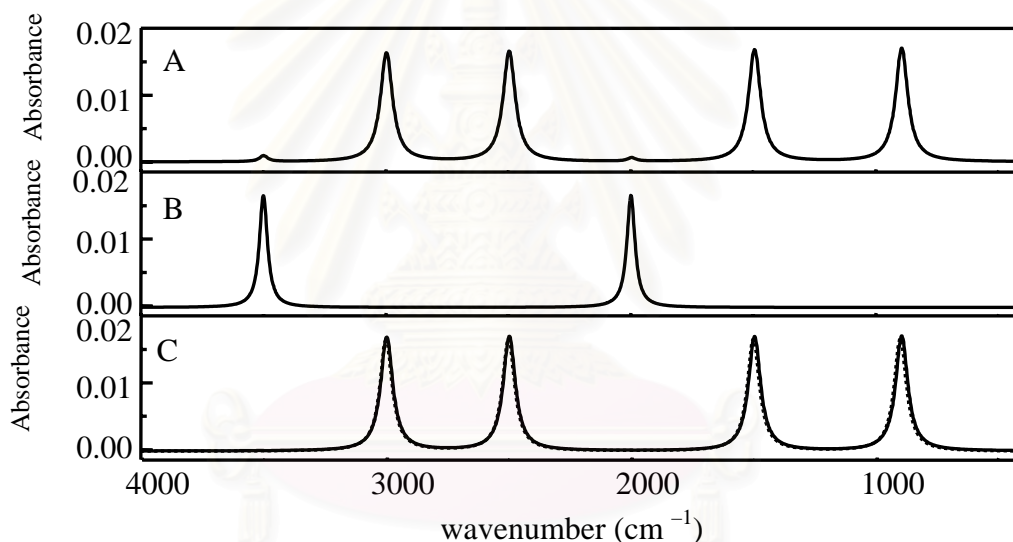


Figure 4.7 Calculated bulk ATR spectrum of medium 2 (C) acquired by subtracting out bulk ATR spectrum of medium 1 (B) from three-phase spectrum of Ge IRE/medium1/medium2 (A) with the thickness of medium 1 of 0.005  $\mu\text{m}$ . The dotted line is simulated bulk ATR spectrum of medium 2.

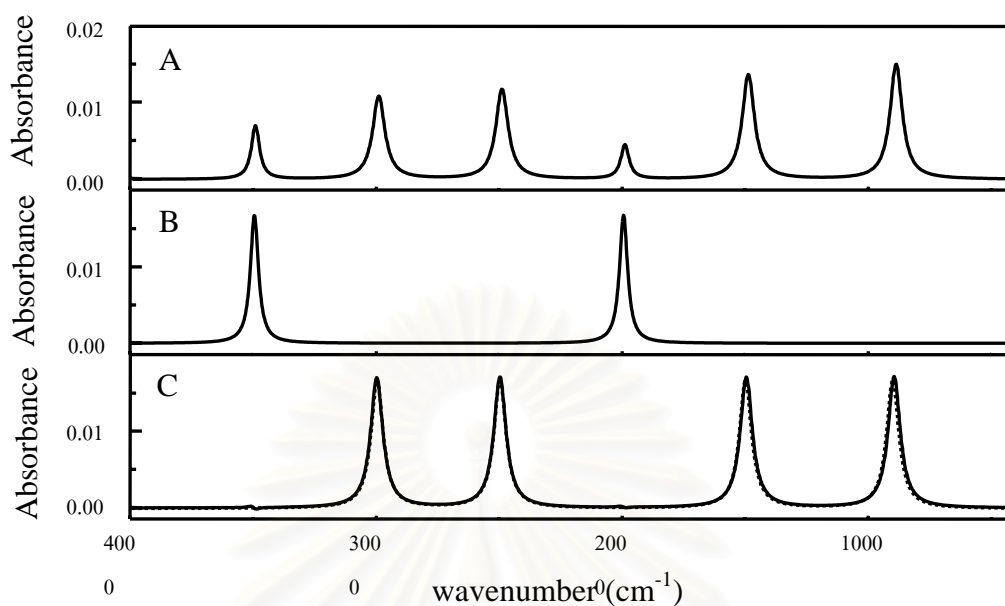


Figure 4.8 Calculated bulk ATR spectrum of medium 2 (C) acquired by subtracting out bulk ATR spectrum of medium 1 (B) from three-phase spectrum of Ge IRE/medium1/medium2 (A) with the thickness of medium 1 of 0.05  $\mu\text{m}$ . The dotted line is simulated bulk ATR spectrum of medium 2.

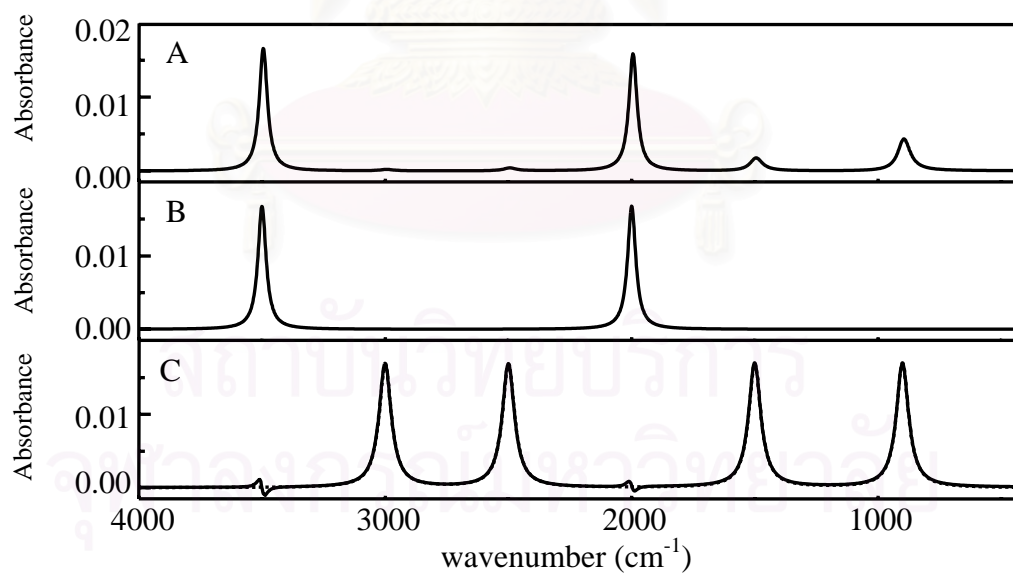


Figure 4.9 Calculated bulk ATR spectrum of medium 2 (C) acquired by subtracting out bulk ATR spectrum of medium 1 (B) from three-phase spectrum of Ge IRE/medium1/medium2 (A) with the thickness of medium 1 of 0.5  $\mu\text{m}$ . The dotted line is simulated bulk ATR spectrum of medium 2.

These calculated bulk spectra indicate that the bulk spectrum of the solid sample (medium 2) can be calculated by the simplified equation of a three-phase system (Equation 2.16). The calculated absorbance is equal to that of the system with an optical contact. However, there are small deviations in the calculated bulk spectra at the characteristic absorption band of medium 1 (at 3500 and 2000  $\text{cm}^{-1}$ ) due to refractive index dispersion. As the thickness of medium 1 increase, the deviations increase. This phenomenon implies that a thin layer of organic liquid should be employed in order to obtain an accurate result.

## **4.2 ATR Spectral Acquisition**

### **4.2.1 The Influence of an Air Gap**

#### **a) Multiple Reflection System**

In order to verify the influence of air gap on the observed ATR spectrum, ATR spectra of the solid sample under different air gap thickness are observed. By applying pressure on the solid sample against IRE, the thickness of the air gap is altered. Spectra of the sample under different pressure are then acquired. ATR spectra of PVC at various the applied pressures are shown in Figure 4.10 and ATR spectra of PC at various the applied pressures are shown in Figure 4.11. Spectra A are the ATR spectrum of solid sample placed into contact with ZnSe IRE without the applied pressure. Spectra B and C are ATR spectra of the same the solid sample with different magnitudes of applied pressure. Spectra C are acquired under a greatest magnitude of applied pressure.

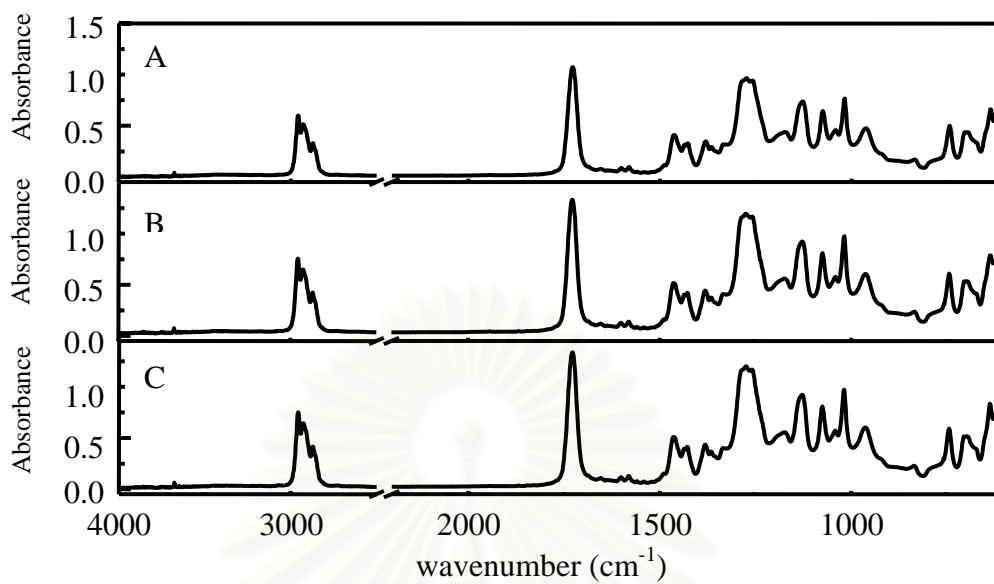


Figure 4.10 ATR spectra of PVC at various applied pressures acquired via multiple reflection IRE accessory with 45° ZnSe IRE.

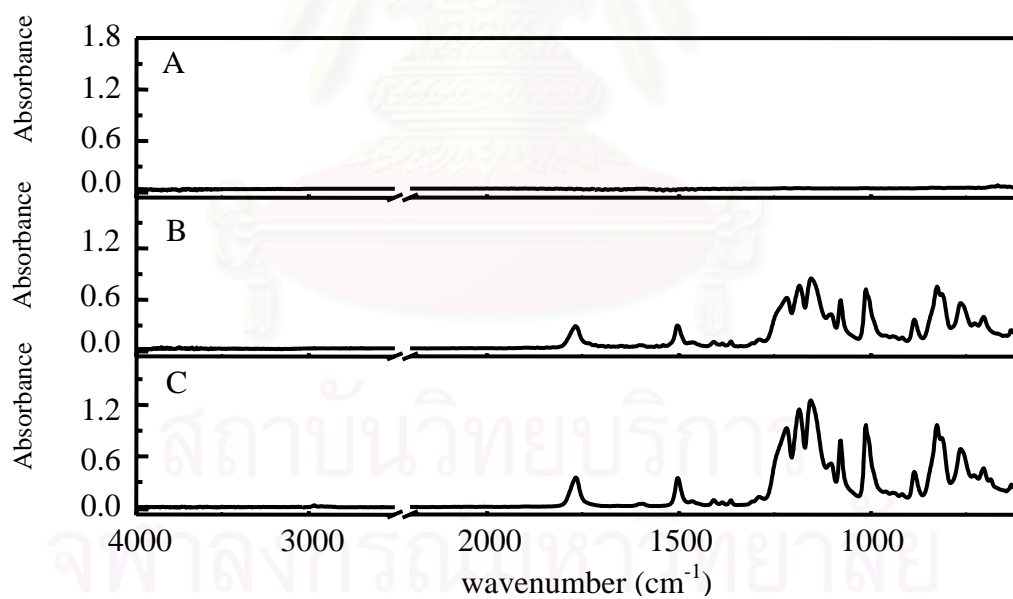


Figure 4.11 ATR spectra of PC at various applied pressures acquired via multiple reflection IRE accessory with 45° ZnSe IRE.

Figure 4.10 indicate that spectra of PVC can be observed although the pressure was not applied. When the PVC sample was pressed against the IRE, the absorbances of PVC are slightly enhanced. Both the absorbances of PVC obtained by applying the low pressure and the highest pressure into PVC sample are the same. This indicates that the low pressure is enough to make a good contact between PVC and IRE. PVC sample is a soft and rubbery solid sample. As a result, an optical contact can be achieved by slight applied pressure.

The PC sample was a virgin compact disc with mirror-flat surface. It is a hard and rigid solid sample. As a result, a good contact with the IRE is not difficult to achieve. When PC was placed against the IRE without the applying pressure, ATR spectrum of PC cannot be observed. However, when PC was pressed against the IRE by various forces, the characteristic absorption band of PC can be observed. The greater force, the greater is the absorbance. These observed spectra indicate that the better the contact, the greater the absorbance of a hard and rigid solid sample. The excessive force, however, may damage the IRE and/or the solid sample. Although a high pressure is applied to the solid sample, an air gap still exists and the optical contact between the solid sample and the IRE is not obtained.

#### **b) Single Reflection System**

A single reflection ATR system, by definition, it makes the absorbance of the sample less than a multiple reflection ATR system. However, the contact efficiency is a crucial factor for obtaining the high quality spectrum. The good contact between the sample and the IRE must be achieved. From observation in multiple reflection system, PVC has a good contact with the IRE, while the contact between PC and the IRE is not good. The contact of PVC and PC with the IRE in single reflection system are illustrated in Figures 4.12 and 4.13, respectively.

From comparison between spectra of PVC acquired by multiple reflection accessory and single reflection accessory, it indicates that the spectrum of PVC with single reflection (spectrum B) is less intense than the spectrum with

multiple reflection (spectrum A). Since the contact of PVC with the IRE is good, the absorbance is proportional to the number of reflections of the infrared beam in the IRE. The absorbance of the flexible sample in multiple reflection system is greater as the number of the reflection increase.

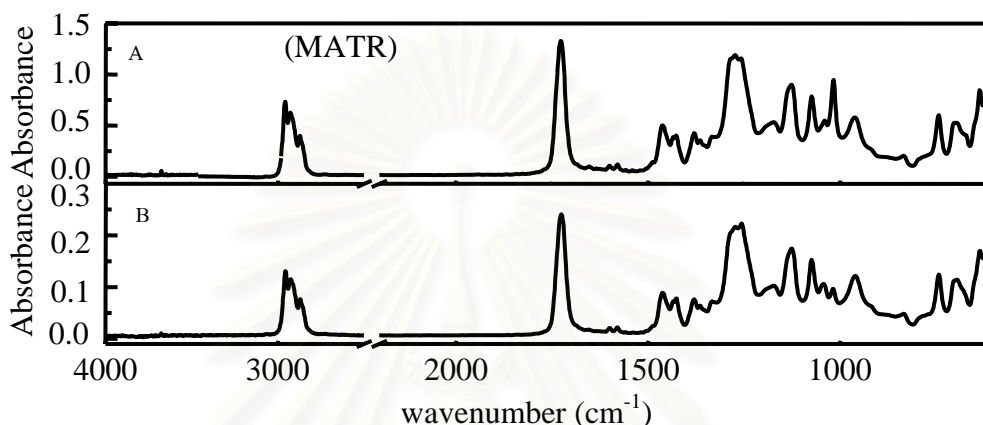


Figure 4.12 ATR spectra of PVC acquired by multiple reflection accessory (A) and single reflection accessory (B) with 45° ZnSe IRE.

In case of the hard and rigid PC sample, spectra of PC collected via multiple reflection (spectrum A) and single reflection (spectrum B) accessories are shown in figure 4.13. The hard and rigid solid sample gave a spectrum with small absorption in a multiple reflection accessory. However, spectrum with strong absorption spectrum is obtained with a single reflection accessory. Since the contact area in a single reflection accessory is small, the solid sample is easier to achieve high contact efficiency. For a hard and rigid solid sample, the absorbance is related to the contact efficiency more than the number of reflection. The absorbance of the hard and rigid solid sample, which is collected via a single reflection accessory, is greater than that collected via a multiple reflection accessory.



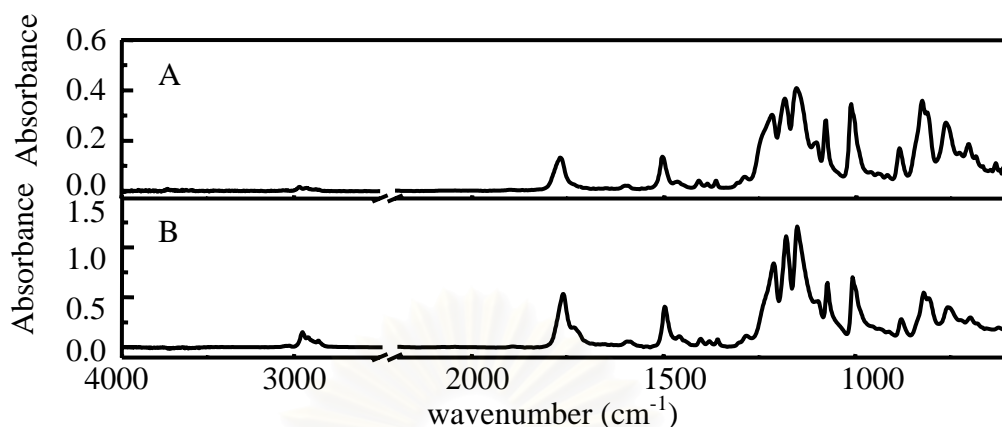


Figure 4.13 ATR spectra of PC acquired by multiple reflection accessory (A) and single reflection accessory (B) with  $45^\circ$  ZnSe IRE

In order to verify the influence of air gap on the observed ATR spectrum in single reflection system, ATR spectra of the solid sample under different pressure are collected via a single reflection accessory. ATR spectra of PVC at various the applied pressures are shown in Figure 4.14 and ATR spectra of PC at various the applied pressures are shown in Figure 4.15. Spectra A are the ATR spectrum of solid sample placed into contact with ZnSe IRE without the applied pressure. Spectra B and C are ATR spectra of the same the solid sample with different magnitudes of applied pressure. Spectra C are acquired under a greatest magnitude of applied pressure.

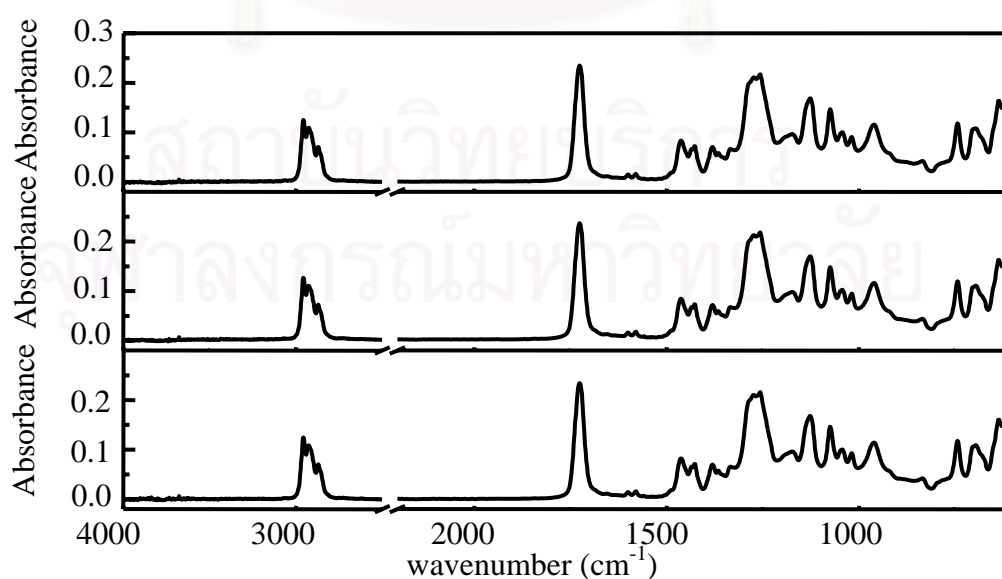


Figure 4.14 ATR spectra of PVC at various applied pressures in single reflection acquired via  $45^\circ$  ZnSe IRE in single reflection system.

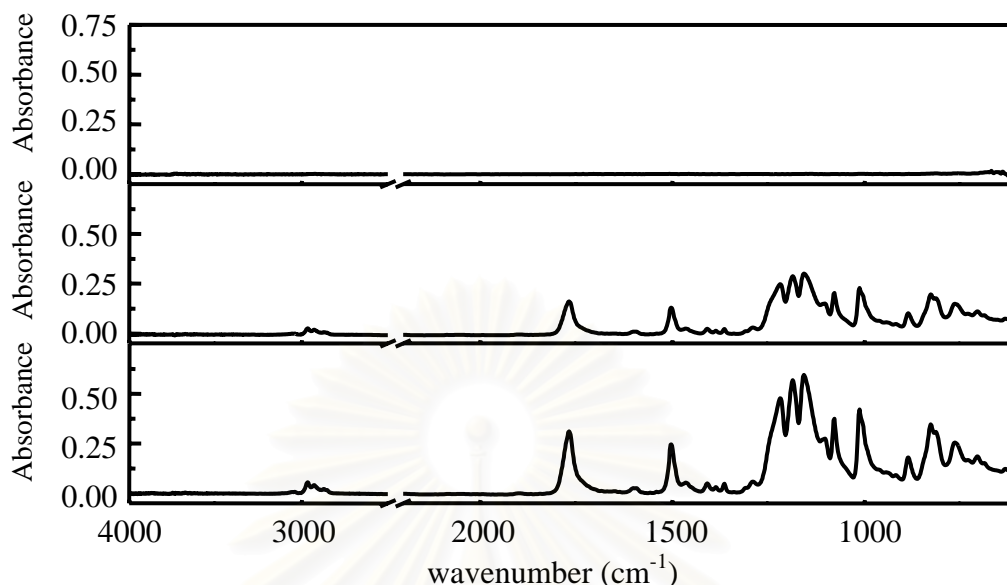


Figure 4.15 ATR spectra of PC at various applied pressures in single reflection acquired via  $45^\circ$  ZnSe IRE in single reflection system.

From Figure 4.14, there are no different in the absorbance of these spectra. This implies that PVC, which is a flexible sample, always has a good contact with the IRE although without any applied pressure.

Figure 4.15 shows ATR spectra of PC at various applied pressures acquired by single reflection ATR accessory. Spectrum A is obtained by placing PC on ZnSe IRE without the applied pressure. No spectral feature of PC can be observed. Spectrum B and C are spectra of PC obtained with increasing pressure. The absorbance of PC is greatly improved as an increasing pressure was applied. Spectrum C is the spectrum of PC where no further absorbance improvement was observed as the pressure was increased. The observed phenomena indicate the applied pressure is necessary for enhancing absorbance of a hard and rigid solid sample in ATR measurement. However, care must be taken since an excessive force may damage the IRE.

## 4.2.2 Absorbance Enhancement

### 4.2.2.1 Influence of Organic Liquid

#### a) Multiple Reflection System

The observed phenomena indicate that when there is an air gap between the solid sample and the IRE, the observed absorbance is smaller. Most solid sample cannot achieve a good contact. Liquid sample, on the other hand, always has a good contact with IRE. As a result, liquid was employed as intermediate layer between the solid sample and the IRE in order to eliminate air gap and improve absorbance. In the case where the solid sample is organic material, the organic liquid is employed as an intermediate layer. Since the refractive index of the organic solid sample is not so much different from that of the organic liquid, the decay characteristic of MSEvF in both samples are same.

Two types of organic liquid were employed for improving the absorbance, *i*-propanol and mineral oil. *i*-Propanol is a low viscosity organic liquid while mineral oil is a high viscosity organic liquid. ATR spectra of *i*-propanol and mineral oil are shown in Figures 4.16 and 4.17.

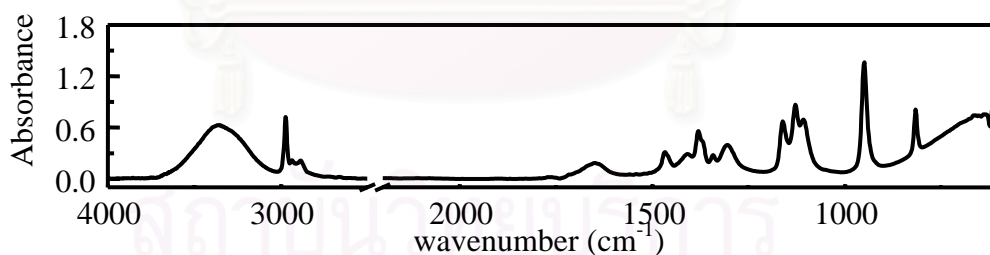


Figure 4.16 ATR spectrum of *i*-propanol acquired via multiple reflection ATR accessory with 45° ZnSe IRE.

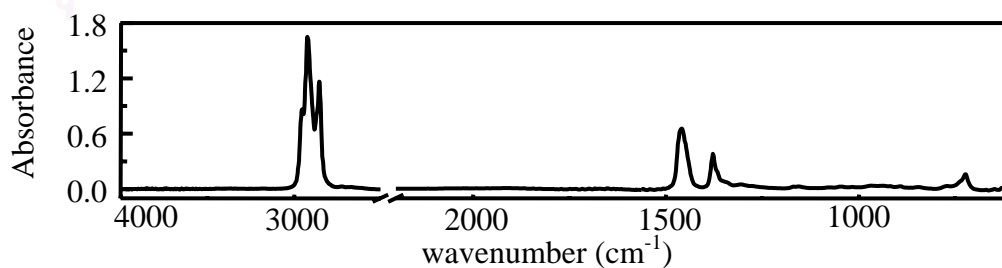


Figure 4.17 ATR spectrum of mineral oil acquired via multiple reflection ATR accessory with 45° ZnSe IRE.

From observed results, PVC has a good contact with the IRE with the applied pressure. In order to verify the goodness of contact of PVC, *i*-propanol and mineral oil were used as intermediate layer between the IRE and the PVC sample. ATR spectra of a three-phase system of ZnSe/*i*-propanol/PVC and ZnSe/mineral oil/PVC acquired by multiple reflection ATR accessory are shown in Figure 4.18 and 4.19, respectively.

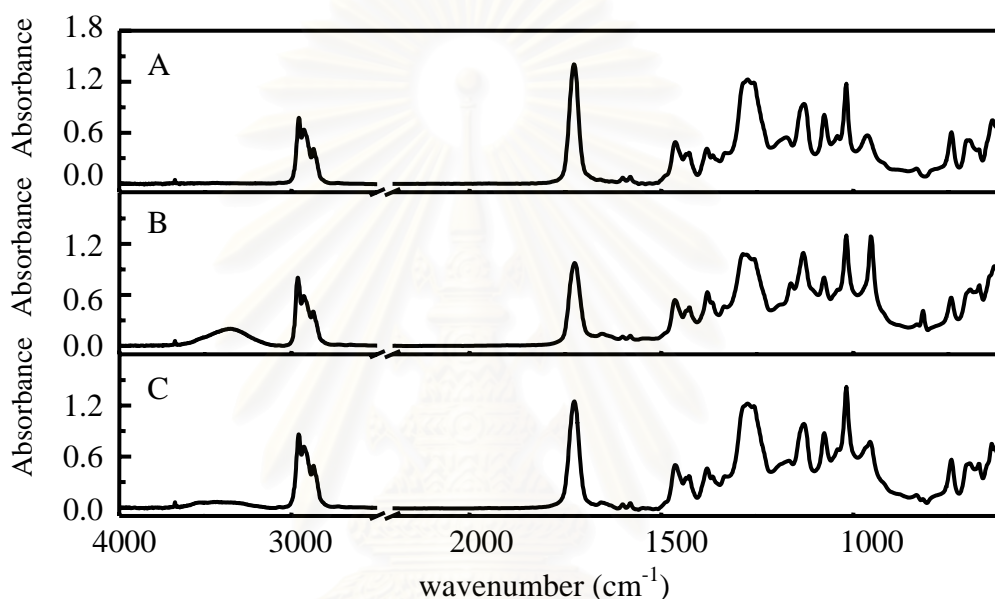


Figure 4.18 ATR spectra of three-phase system of ZnSe/*i*-propanol/PVC acquired by multiple reflection ATR accessory using 45° ZnSe IRE; spectrum of PVC on ZnSe IRE under an applied pressure (A), spectrum of PVC with thin *i*-propanol film (B), and spectrum of PVC with a thinner *i*-propanol film (C).

A comparison between the observed spectrum of PVC in the system without an organic liquid (spectrum A) and that in the system with *i*-propanol (spectrum B and C) indicates that when there is *i*-propanol between PVC and ZnSe IRE, the characteristic absorption of PVC is smaller than that in the system without *i*-propanol. When a greater pressure was applied to PVC and some *i*-propanol evaporates, the thickness of *i*-propanol film was smaller, spectrum C was acquired. A thinner *i*-propanol film can be noticed from the characteristic band of *i*-propanol (i.e., a broad band at 3500 cm<sup>-1</sup>). When *i*-propanol is almost completely evaporated, the

absorption band of PVC is the same absorbance as the absorption band of PVC in the system without *i*-propanol. These phenomena imply that the contact between PVC and the IRE cannot be further improved by *i*-propanol.

Since the contact of PVC with the IRE cannot be improved by *i*-propanol which is low viscosity organic liquid, mineral oil as a high viscosity organic liquid was employed for improving the absorption instead of *i*-propanol. A comparison between absorbance of PVC in system without mineral oil and those with mineral oil are shown in Figure 4.19

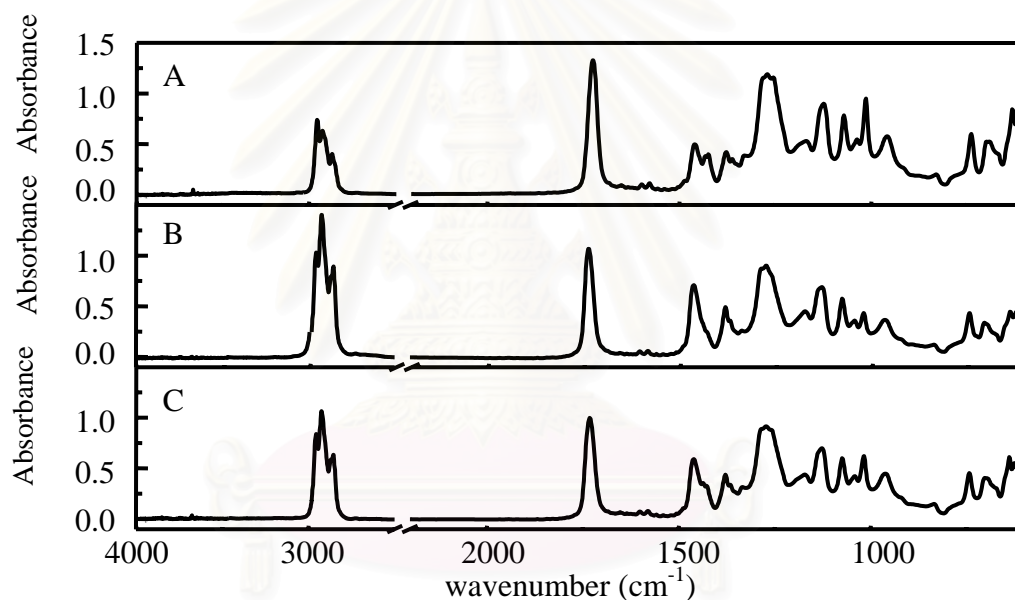


Figure 4.19 ATR spectra of three-phase system of ZnSe/mineral oil/PVC acquired by multiple reflection ATR accessory using 45° ZnSe IRE; spectrum of PVC on ZnSe IRE under an applied pressure (A), spectrum of PVC with thin mineral oil film (B), and spectrum of PVC with a thinner mineral oil (C).

Spectrum A is ATR spectrum of PVC without mineral oil. PVC was pressed against the ZnSe IRE. Spectrum B and C show spectra of the system at the different thickness of mineral oil in the three-phase system. These spectra indicate that there is the excess mineral oil between PVC and the IRE. As a result, the absorbance of PVC is smaller compared to that of in spectrum A. The

applied pressure was increased in order to squeeze the excess mineral oil, the three-phase spectrum of ZnSe/mineral oil/PVC with a thinner mineral oil was acquired (spectrum C). However, the absorbance of the absorption band of PVC in this three-phase system is still smaller than that in the system without mineral oil. Since PVC is a soft and rubbery solid sample, it can easily make a good contact with the IRE. The contact cannot be further improved and the absorbance cannot be further enhanced.

For a hard and rigid solid sample, PC was employed as a solid sample. The contact between the PC sample and the IRE is not good although the pressure was applied to the system. *i*-Propanol and mineral oil were used for enhancing absorbance. Spectral enhancements of PC acquired by *i*-propanol and mineral oil are shown in Figure 4.20 and 4.21, respectively.

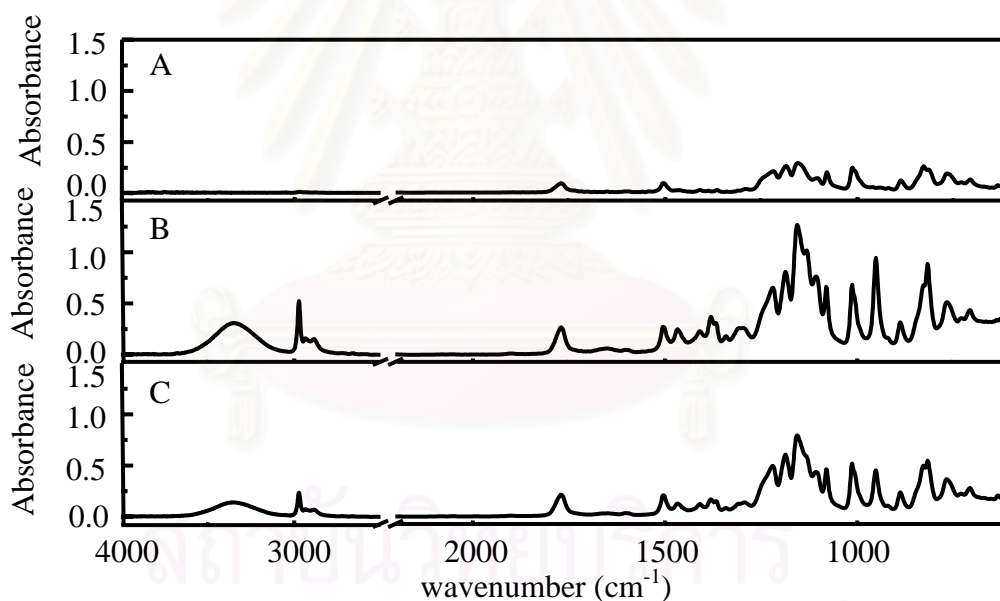


Figure 4.20 ATR spectra of three-phase system of ZnSe/*i*-propanol/PC acquired by multiple reflection ATR accessory using 45° ZnSe IRE; spectrum of PC on ZnSe IRE under an applied pressure (A), spectrum of PC with thin *i*-propanol film (B), and spectrum of PVC with a thinner *i*-propanol film (C).



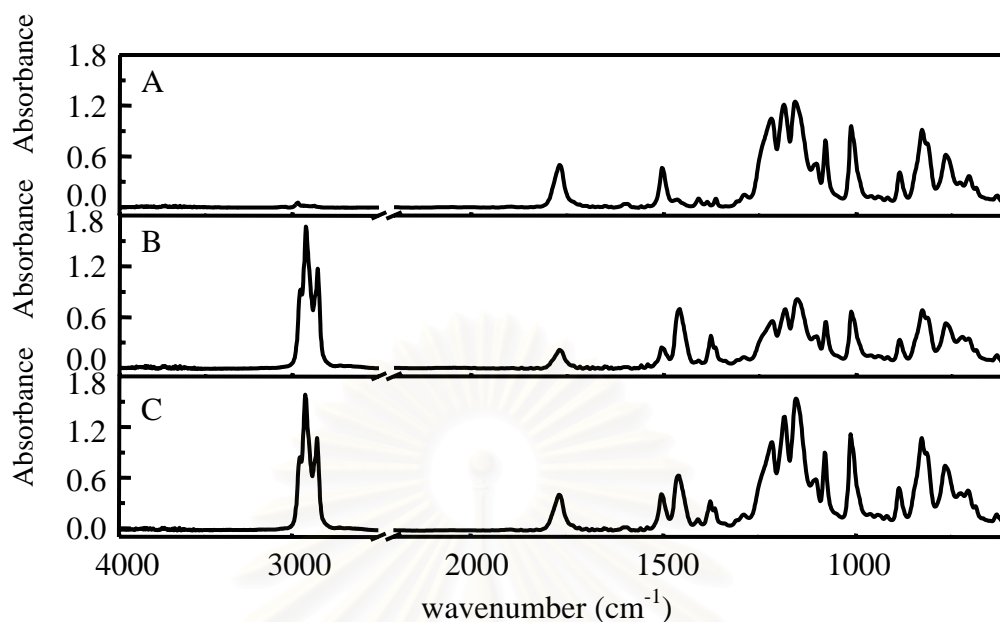


Figure 4.21 ATR spectra of three-phase system of ZnSe/mineral oil/PC acquired by multiple reflection ATR accessory using  $45^\circ$  ZnSe IRE; spectrum of PC on ZnSe IRE under an applied pressure (A), spectrum of PC with thin mineral oil film (B), and spectrum of PC with a thinner mineral oil (C).

Figure 4.20 indicates that *i*-propanol can enhance absorbance of PC. When *i*-propanol evaporates, air gap formation starts somewhere on surface of PC, the absorbance of PC was decreased (spectrum C).

Since *i*-propanol evaporates easily, the measurement is limited by time. A high viscosity organic liquid (mineral oil) was employed instead of *i*-propanol. A comparison between the spectrum of PC in the system without mineral oil and the three-phase system spectrum with thinner mineral oil indicates that the absorbance of mineral oil was slightly decreased, while the absorbance of PC was significantly increased. Mineral oil cannot be squeezed to a very thin liquid film since its viscosity is too high. However, it is possible that the absorbance of PC can be enhanced by thinner mineral oil film.



### b) Single Reflection System

Although the contact between the solid sample and the IRE in a single reflection accessory is good, an air gap may present between the solid sample and the IRE. To verify the goodness of contact and the absorbance enhancement by an organic liquid, two types of organic liquid were employed as intermediate between the solid sample and the IRE. ATR spectra of *i*-propanol and mineral oil acquired via single reflection accessory are shown in Figure 4.22 and 4.23, respectively.

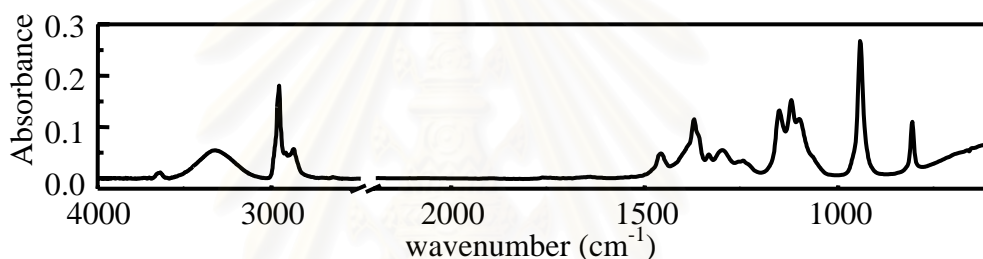


Figure 4.22 ATR spectrum of *i*-propanol acquired via single reflection accessory with 45° ZnSe IRE.

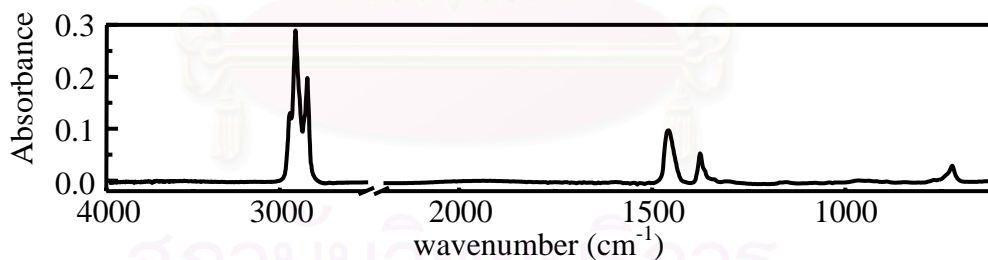


Figure 4.23 ATR spectrum of mineral oil acquired via single reflection accessory with 45° ZnSe IRE.

The spectra, which are illustrated the ability of absorbance enhancement of the PVC sample by *i*-propanol, are shown in Figure 4.24. Spectrum A is spectrum of PVC without *i*-propanol under the applied pressure. An increased pressure is applied onto the sample until no further absorption improvement is observed. Spectrum B and C show spectra of the system with *i*-propanol. The thickness of *i*-propanol in spectrum C is thinner than that in spectrum B. Evaporation of *i*-propanol can be observed by a decreased characteristic absorption of *i*-propanol.

Spectra B and C indicate that *i*-propanol cannot enhance the absorbance of PVC. This phenomenon implies that PVC always has a good contact with the IRE in single reflection accessory. The ability of absorbance enhancement of the PVC sample by mineral oil is illustrated in Figure 4.25.

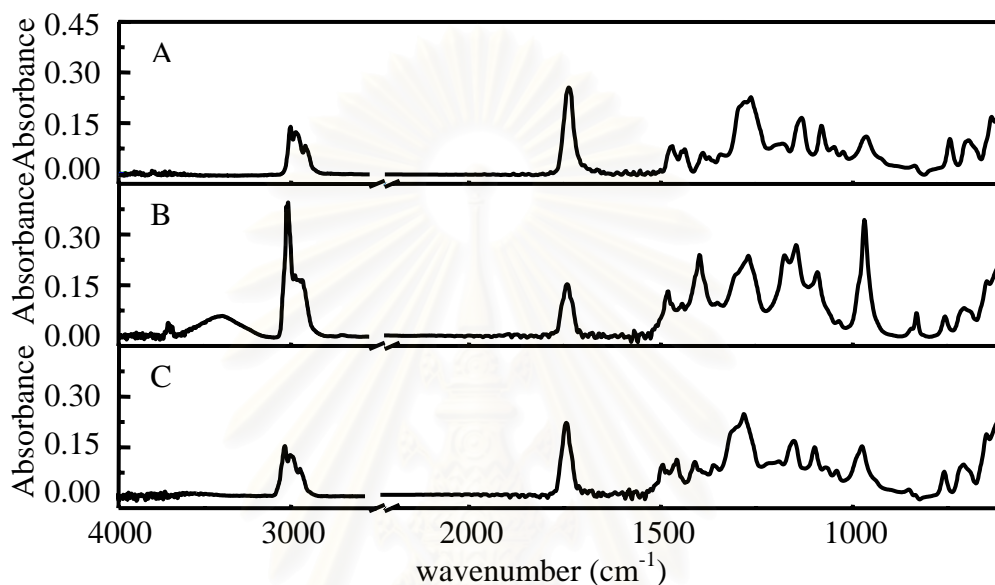


Figure 4.24 ATR spectra of three-phase system of ZnSe/*i*-propanol/PVC acquired by single reflection ATR accessory using 45° ZnSe IRE; spectrum of PVC on ZnSe IRE under an applied pressure (A), spectrum of PVC with thin *i*-propanol film (B), and spectrum of PVC with a thinner *i*-propanol film (C).

สถาบันวิทยบริการ  
จุฬาลงกรณ์มหาวิทยาลัย

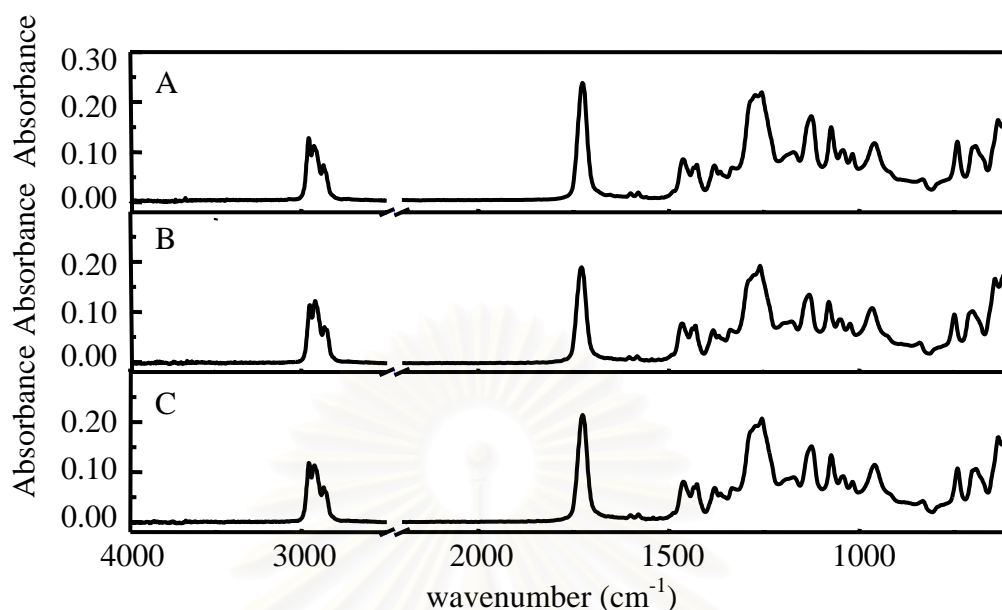


Figure 4.25 ATR spectra of three-phase system of ZnSe/mineral oil/PVC acquired by single reflection ATR accessory using  $45^\circ$  ZnSe IRE; spectrum of PVC on ZnSe IRE under an applied pressure (A), spectrum of PVC with thin mineral oil film (B), and spectrum of PVC with a thinner mineral oil (C).

Figure 4.25 shows ATR spectrum of the three-phase system of ZnSe/ mineral oil/PVC acquired by single reflection ATR accessory. Spectrum A is spectrum of PVC under the applied pressure. Spectrum B and C show absorption improvement of PVC by mineral oil. The Thickness of mineral oil in spectrum C is thinner than that in spectrum B due to the increment of pressure. The absorbance of PVC cannot be enhanced by mineral oil although the thickness of mineral oil was very thin film. The results observed by single reflection measurement correspond to those from multiple reflection measurement. PVC is flexible, it can achieve a good contact with the IRE without applied pressure.

According to the observation, the PC sample cannot have a good contact with the IRE although pressure was applied. In single reflection measurement, the absorbance of PC was significantly increased when the high pressure was applied. However, the air gap may still exist between the sample and the IRE. The present organic liquid may enhance absorbance of PC.

Figure 4.26 shows the absorbance enhancement of PC by *i*-propanol. Spectrum A is spectrum of PC without *i*-propanol. Both spectrum B and C, which are the three-phase system of ZnSe/*i*-propanol/PC. Since the contact between the PC sample and the IRE in single reflection accessory is better when the high pressure was applied, the absorbance of PC is greater improved. If an organic liquid is too thick, the absorbance of PC was not improved, as shown in spectrum B. When *i*-propanol evaporates, the thickness of *i*-propanol is decreased, the absorbance of PC is enhanced. This indicates that the absorbance of PC can be enhanced by *i*-propanol in single reflection measurement.

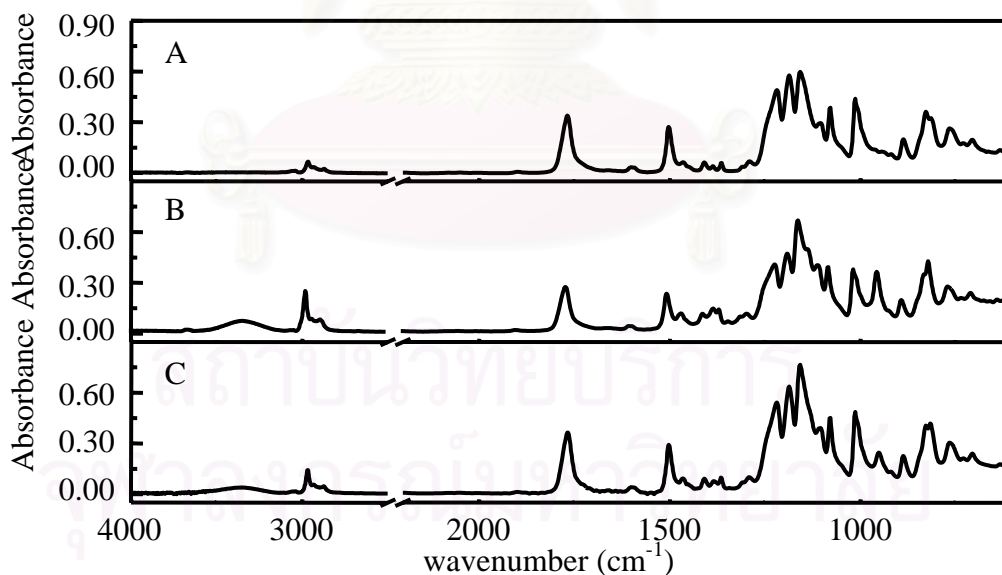


Figure 4.26 ATR spectra of three-phase system of ZnSe/*i*-propanol/PC acquired by single reflection ATR accessory using 45° ZnSe IRE; spectrum of PC on ZnSe IRE under an applied pressure (A), spectrum of PC with thin *i*-propanol film (B), and spectrum of PVC with a thinner *i*-propanol film (C).

Although *i*-propanol can enhance the absorbance of PC in single reflection accessory, *i*-propanol evaporates very fast. The measurement is limited by time. Since mineral oil does not evaporate, mineral oil was used for enhancing the absorbance of PC. The spectra of PC in the system with the present of mineral oil are shown in Figure 4.27.

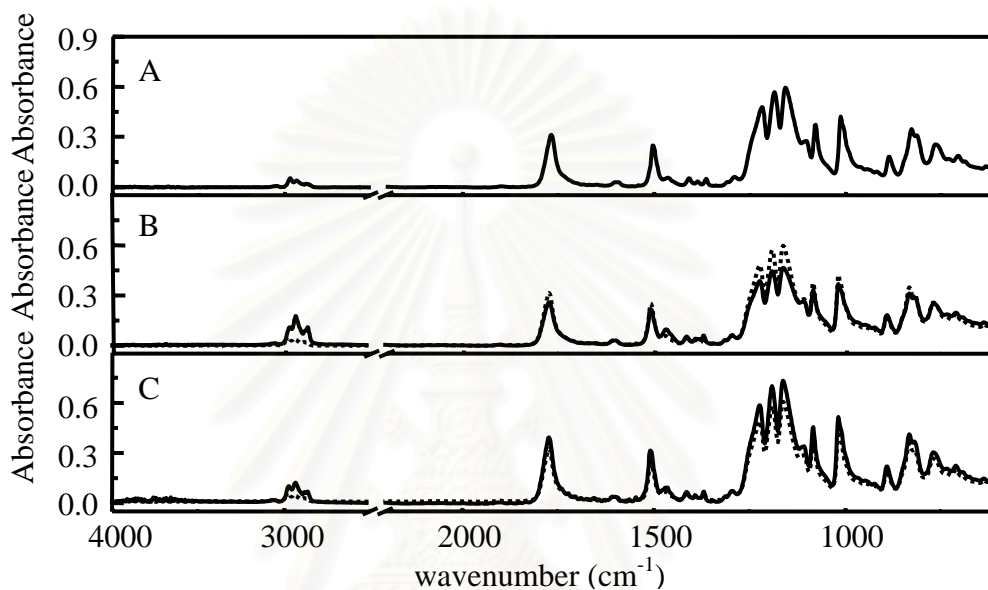


Figure 4.27 ATR spectra of three-phase system of ZnSe/mineral oil/PVC acquired by single reflection ATR accessory using  $45^\circ$  ZnSe IRE; spectrum of PVC on ZnSe IRE under an applied pressure (A), spectrum of PVC with thin mineral oil film (B), and spectrum of PVC with a thinner mineral oil (C).

These spectra indicate the absorbance of PC can be enhanced by mineral oil. However, there is a limitation of mineral oil. If the thickness of mineral oil is too thick, the absorbance of PC was decreased. Figures 4.46 and 4.47 indicate the high absorption of PC under applied pressure. This is due to the influence of small sample size where smooth surface and good contact can be obtained. However, the absorbance of PC can be further enhanced by both *i*-propanol and mineral oil.

### 4.2.2.2 Influence of Surface Roughness

#### a) Multiple Reflection System

The absorbance of the solid sample is related to the contact efficiency. The surface of the sample is rough, the contact with the IRE is not good. Illustration of influence of surface roughness is shown in Figure 4.28.

Figure 4.28 shows ATR spectra of PC at various roughness of the surface. The degree of roughness are PC rough 100 > PC rough 400 > PC rough 1200 > flat PC. All spectra in this Figure were acquired under the applied pressure at the point where no further absorbance increases were observed as the pressure was increased.

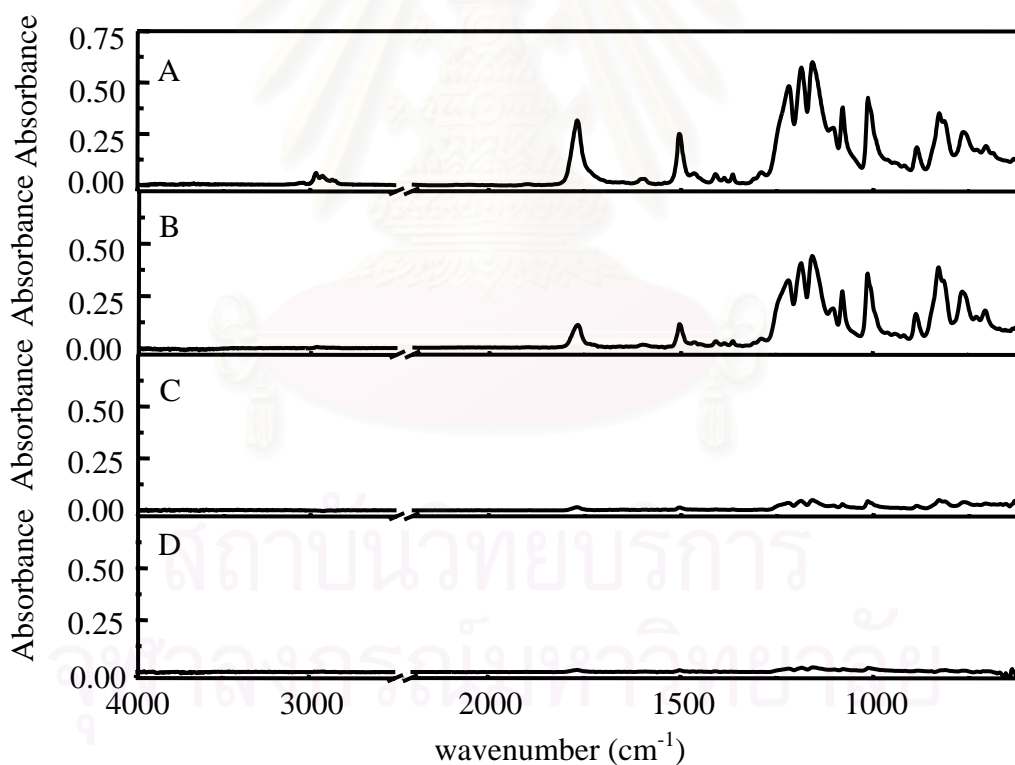


Figure 4.28 ATR spectra of PC at various surface roughness under an applied pressure acquired by multiple reflection ATR accessory using 45° ZnSe IRE; Spectrum of flat PC (A), spectrum of PC rough 1200 (B), spectrum of PC rough 400 (C) and spectrum of PC rough 100 (D).



These spectra indicate that as the roughness is greater, the absorbance becomes smaller. This is because when a greater roughness is attended, the area of contact between the IRE and the solid sample is smaller. Therefore, the interaction between the evanescent field and the sample is smaller than that of the flat surface.

To improve the absorbance of the sample with rough surface, *i*-propanol and mineral oil were employed as intermediate layer between the solid sample and the IRE. ATR spectra of PC with the various roughness of the surface: PC rough 1200, PC rough 400 and PC rough 100 are shown in Figures 4.29 to 4.34.

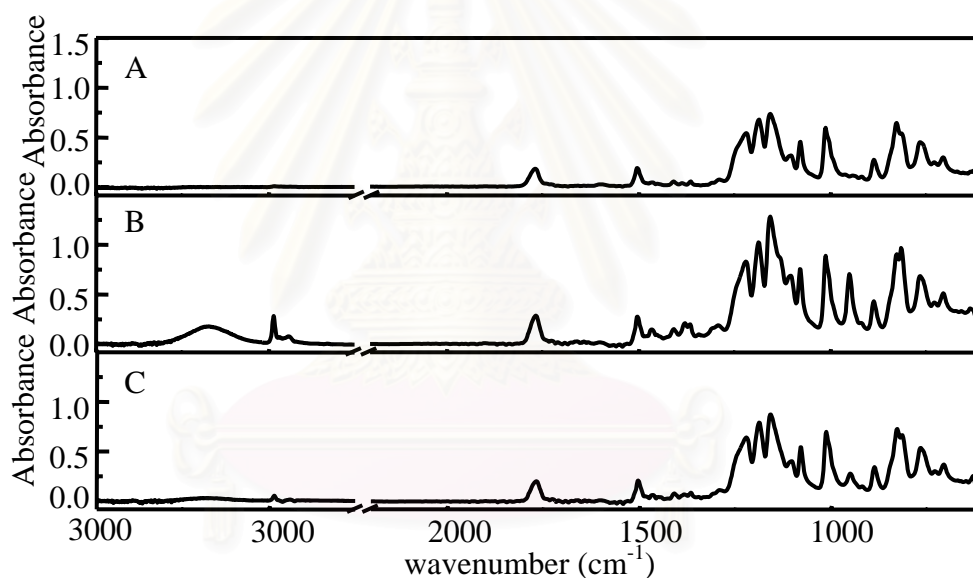


Figure 4.29 ATR spectra of three-phase system of ZnSe/*i*-propanol/PC rough 1200 acquired by multiple reflection ATR accessory using 45° ZnSe IRE; spectrum of PC rough 1200 on ZnSe IRE under an applied pressure (A), spectrum of PC rough 1200 with thin *i*-propanol film (B), and spectrum of PC rough 1200 with thinner *i*-propanol film (C).



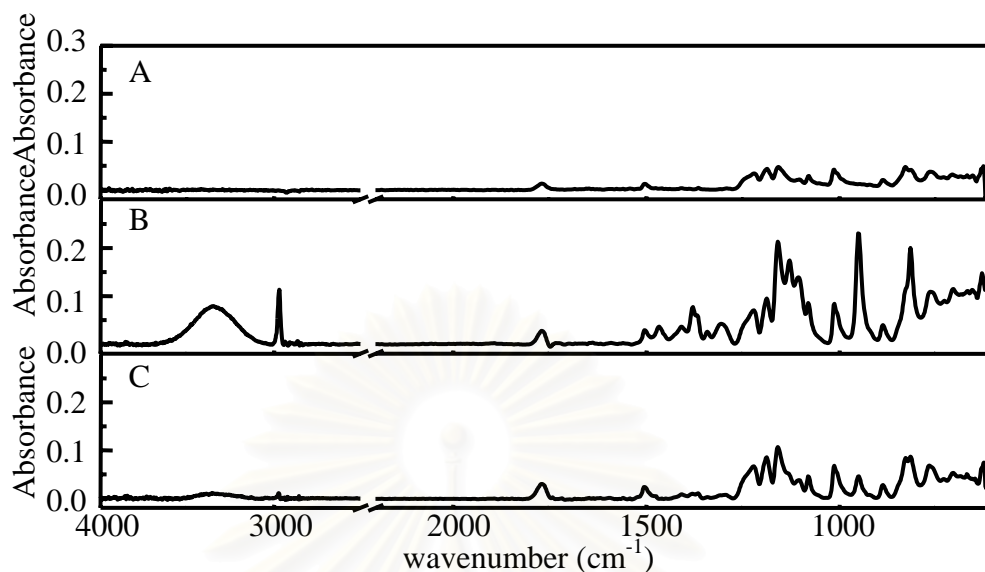


Figure 4.30 ATR spectra of three-phase system of ZnSe/*i*-propanol/PC rough 400 acquired by multiple reflection ATR accessory using 45° ZnSe IRE; spectrum of PC rough 400 on ZnSe IRE under an applied pressure (A), spectrum of PC rough 400 with thin *i*-propanol film (B), and spectrum of PC rough 400 with thinner *i*-propanol film (C).

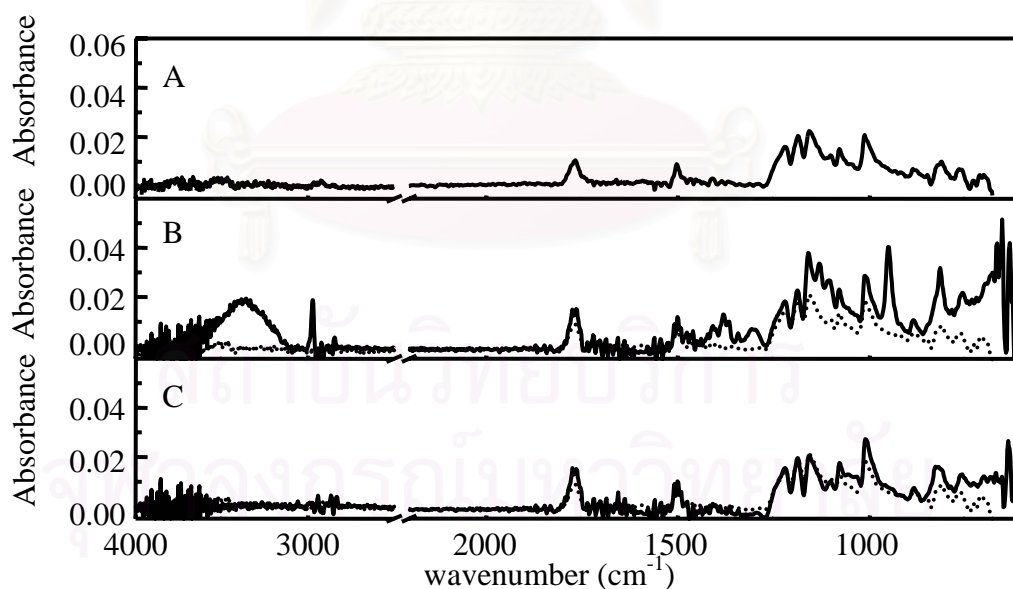


Figure 4.31 ATR spectra of three-phase system of ZnSe/*i*-propanol/PC rough 100 acquired by multiple reflection ATR accessory using 45° ZnSe IRE; spectrum of PC rough 100 on ZnSe IRE under an applied pressure (A), spectrum of PC rough 100 with thin *i*-propanol film (B), and spectrum of PC rough 100 with thinner *i*-propanol film (C).

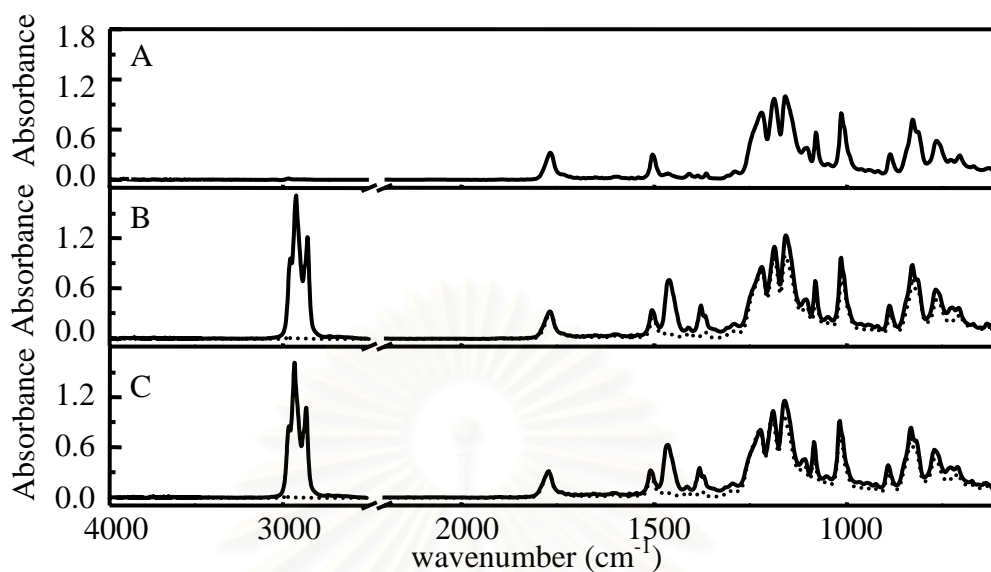


Figure 4.32 ATR spectra of three-phase system of ZnSe/mineral oil/PC rough 1200 acquired by multiple reflection ATR accessory using 45° ZnSe IRE; spectrum of PC rough 1200 on ZnSe IRE under an applied pressure (A), spectrum of PC rough 1200 with thin mineral oil film (B), and spectrum of PC rough 1200 with thinner mineral oil film (C).

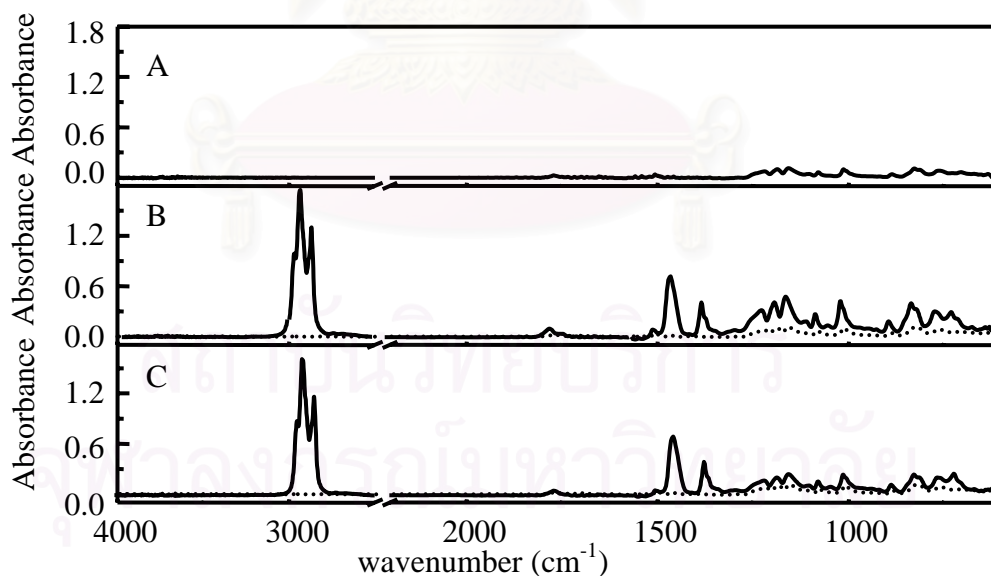


Figure 4.33 ATR spectra of three-phase system of ZnSe/mineral oil/PC rough 400 acquired by multiple reflection ATR accessory using 45° ZnSe IRE; spectrum of PC rough 400 on ZnSe IRE under an applied pressure (A), spectrum of PC rough 400 with thin mineral oil film (B), and spectrum of PC rough 400 with thinner mineral oil film (C).

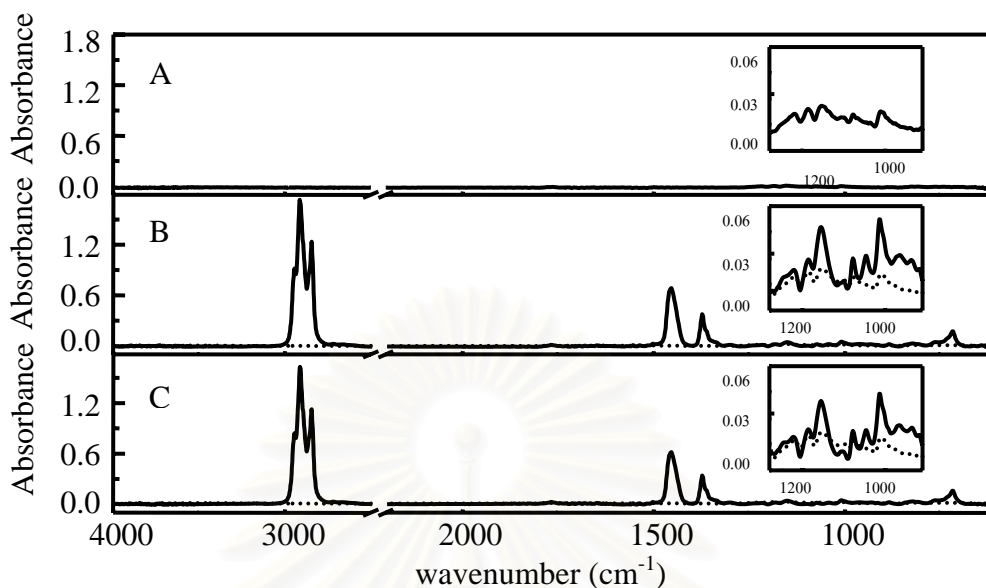


Figure 4.34 ATR spectra of three-phase system of ZnSe/mineral oil/PC rough 100 acquired by multiple reflection ATR accessory using 45° ZnSe IRE; spectrum of PC rough 100 on ZnSe IRE under an applied pressure (A), spectrum of PC rough 100 with thin mineral oil film (B), and spectrum of PC rough 100 with thinner mineral oil film (C). The insets are added for clarity.

These spectra indicate the absorbance of the solid sample with rough surface (PC rough 1200, 400 and 100) is enhanced when an organic liquid was introduced. The absorbance of the solid sample with rough surface can be clearly enhanced by *i*-propanol. However, when *i*-propanol evaporates, the absorbance of sample becomes smaller. This is because an air gap between the sample and the IRE. For absorbance enhancement by mineral oil, it indicates that mineral oil can enhance the absorbance of the solid sample with the rough surface. The thinner is mineral oil, the greater is the absorbance of the solid sample. If the surface of sample is too rough (PC rough 100), the absorbance enhancement is not great. Since the roughness of the solid sample is large, the area of the interaction with the evanescent field is small. As a result, the absorbance of the solid sample with very rough surface is small. When the region of absorption band of PC rough 100 was expanded, the spectral enhancement of PC rough 100 by mineral oil can be observed.

### b) Single Reflection System

The absorbances of PC with various roughness of surface in single reflection system are related to degree of the roughness. The greater the roughness, the smaller the absorbance. Similar to the multiple reflection system, the absorbance of PC with a flat surface is the greatest and the absorbance of PC rough 1200, PC rough 400 and PC rough 100 is smaller. However, the absorbances of PC in single reflection system are greater than in multiple reflection system. This is because the problem of irregularity of sample is decreased. As a result, the contact efficiency is improved.

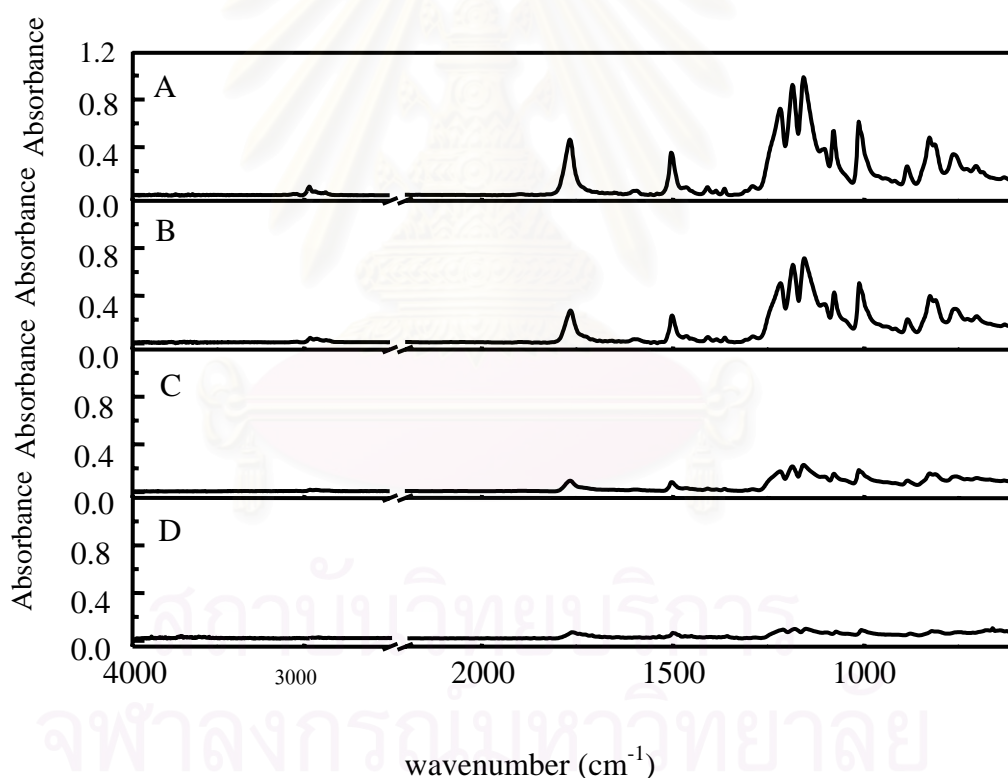


Figure 4.35 ATR spectra of PC with various surface roughness under applied pressure acquired by single reflection system accessory using  $45^\circ$  ZnSe IRE. ATR spectra of flat PC (A), ATR spectra of PC rough 1200 (B), ATR spectra of PC rough 400 (C), and ATR spectra of PC rough 100 (D).

The absorbance of the hard and rigid solid sample with rough surface (PC rough 1200, PC rough 400 and PC rough 100) can be enhanced by *i*-propanol. The spectral enhancement of PC rough 1200, PC rough 400 and PC rough 100 are shown in figure 4.36, 4.37 and 4.38, respectively. Since the contact between the solid sample and the IRE is good, the absorbance is slightly enhanced. Moreover, if the surface is rough, *i*-propanol, which was used as intermediate layer, will evaporate quickly in single reflection accessory. The spectral enhancement is slightly observed.

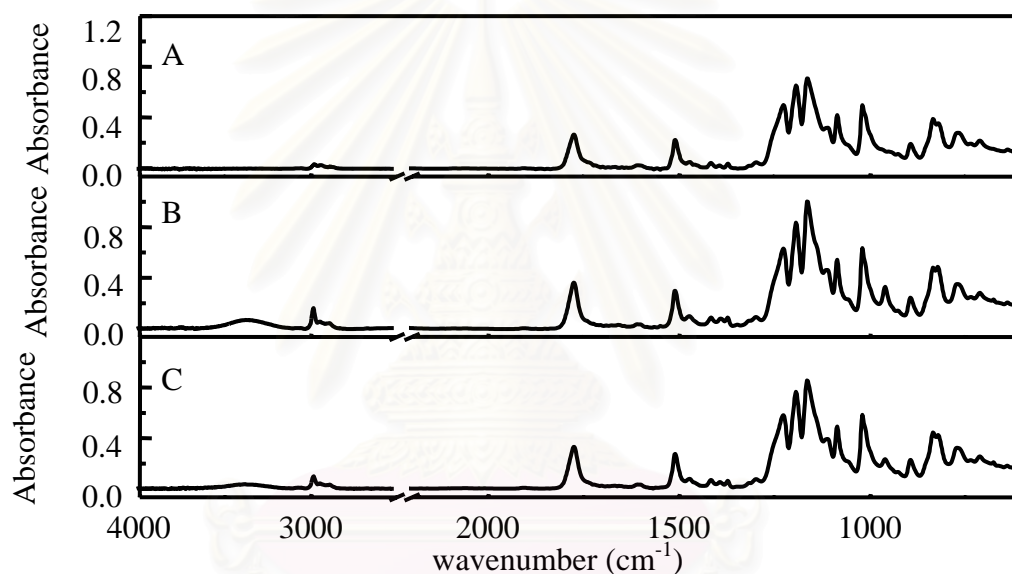


Figure 4.36 ATR spectra of a three-phase system of ZnSe/*i*-propanol/PC rough 1200 acquired by single reflection ATR accessory using 45° ZnSe IRE; spectrum of PC under an applied pressure (A), spectrum of PC rough 1200 with thin *i*-propanol film (B), and spectrum of PC rough 1200 with thinner *i*-propanol film (C).

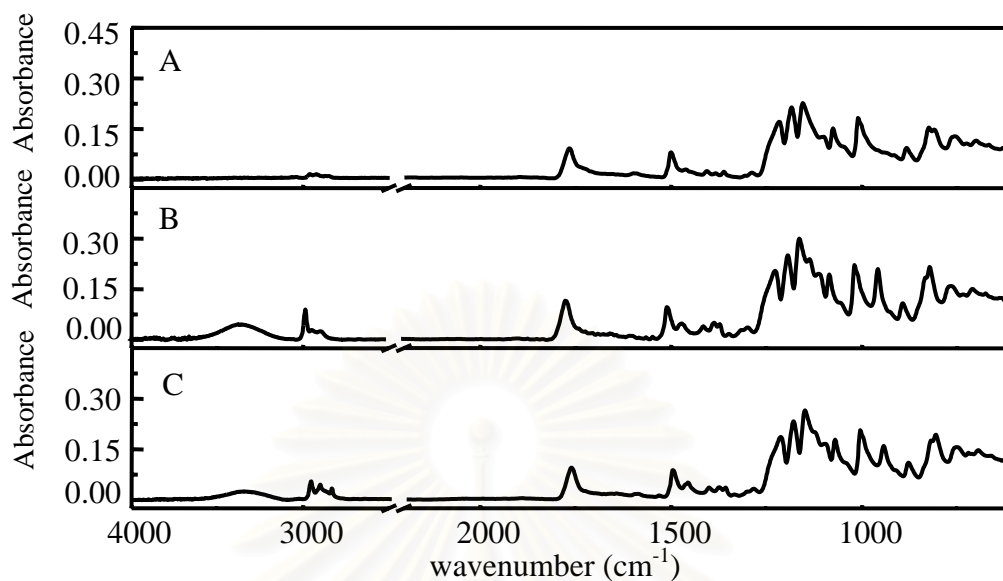


Figure 4.37 ATR spectra of a three-phase system of ZnSe/*i*-propanol/PC rough 400 acquired by single reflection ATR accessory using 45° ZnSe IRE; spectrum of PC under an applied pressure (A), spectrum of PC rough 400 with thin *i*-propanol film (B), and spectrum of PC rough 400 with thinner *i*-propanol film (C).

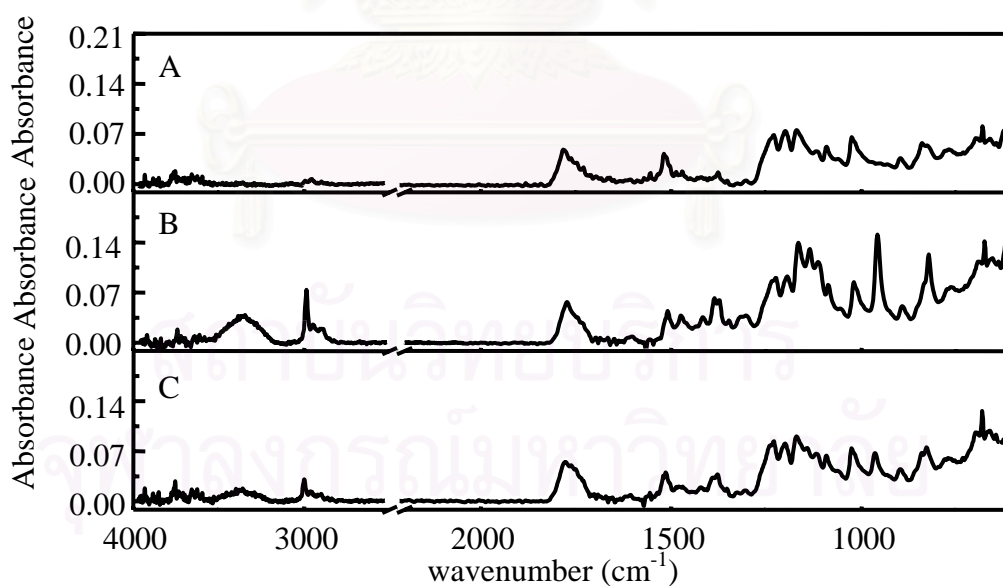


Figure 4.38 ATR spectra of a three-phase system of ZnSe/*i*-propanol/PC rough 100 acquired by single reflection ATR accessory using 45° ZnSe IRE; spectrum of PC under an applied pressure (A), spectrum of PC rough 100 with thin *i*-propanol film (B), and spectrum of PC rough 400 with thinner *i*-propanol film (C).



For spectral enhancement of PC rough 1200, PC rough 400 and PC rough 100 by mineral oil shown in figures 4.39, 4.40 and 4.41, respectively. These spectra indicate that mineral oil can enhance the absorbance of a hard and rigid solid sample with rough surface. When a thinner mineral oil was used, the greater absorbance was observed.

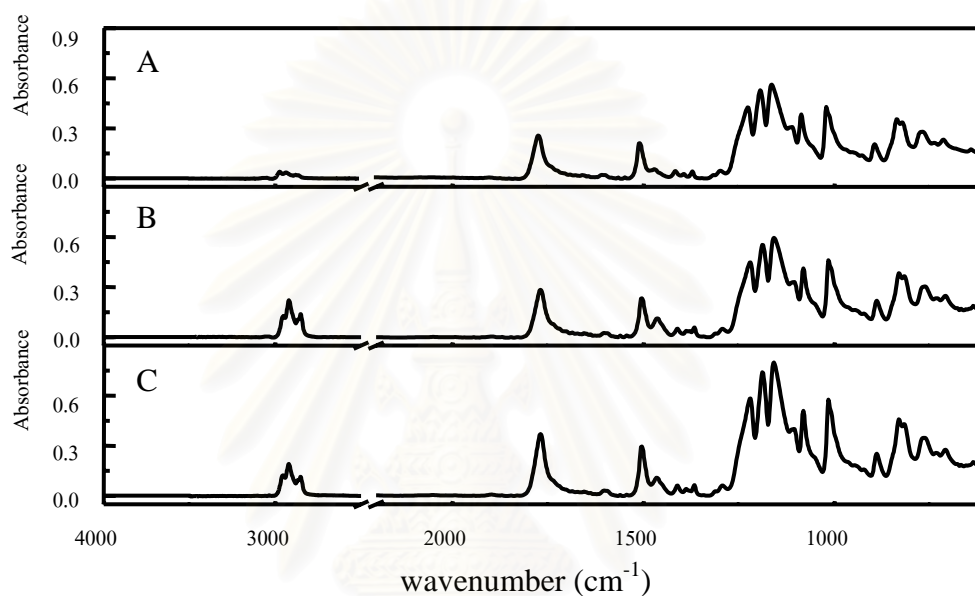


Figure 4.39 ATR spectra of a three-phase system of ZnSe/mineral oil/PC rough 1200 acquired by single reflection ATR accessory using  $45^\circ$  ZnSe IRE; spectrum of PC under an applied pressure (A), spectrum of PC rough 1200 with thin mineral oil film (B), and spectrum of PC rough 1200 with thinner mineral oil film.



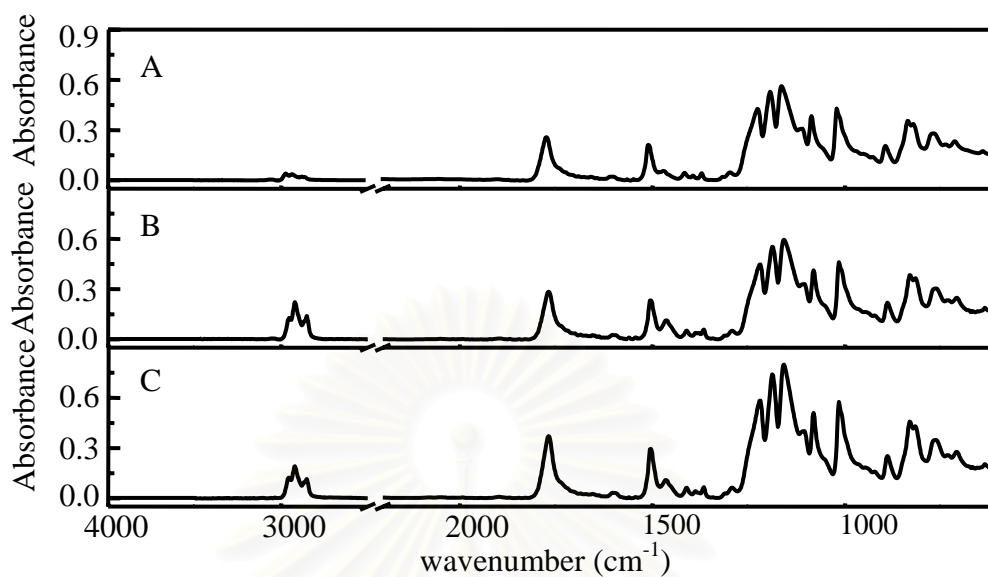


Figure 4.40 ATR spectra of a three-phase system of ZnSe/mineral oil/PC rough 400 acquired by single reflection ATR accessory using 45° ZnSe IRE; spectrum of PC under an applied pressure (A), spectrum of PC rough 400 with thin mineral oil film (B), and spectrum of PC rough 400 with thinner mineral oil film (C).

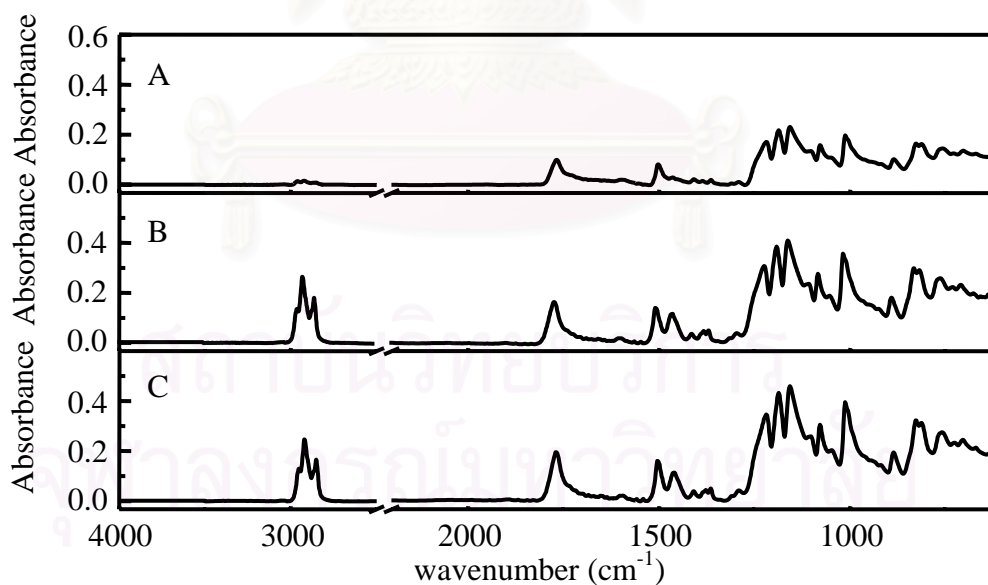


Figure 4.41 ATR spectra of a three-phase system of ZnSe/mineral oil/PC rough 100 acquired by single reflection ATR accessory using 45° ZnSe IRE; spectrum of PC under an applied pressure (A), spectrum of PC rough 100 with thin mineral oil film (B), and spectrum of PC rough 100 with thinner mineral oil film (C).

### 4.2.3 Bulk ATR Spectra from observed Spectra

#### a) Multiple Reflection System

The calculated bulk spectra of PVC in multiple reflection system by subtracting the bulk *i*-propanol spectrum from the three-phase spectrum of ZnSe/mineral oil/PVC using the expression given in Equation 2.16 are shown Figures 4.42 and 4.43. The *i*-propanol in the three-phase system has the calculated thickness of 0.034  $\mu\text{m}$  for Figure 4.42 and 0.017  $\mu\text{m}$  for Figure 4.43. The calculated bulk spectrum of PVC in Figure 4.42 is compared to that in Figure 4.43 shown in Figure 4.44. The Figure indicates that the calculated bulk spectrum of PVC has deviation at frequency of absorption band of *i*-propanol (about 3500  $\text{cm}^{-1}$ ). This deviation is due to refractive index dispersion.

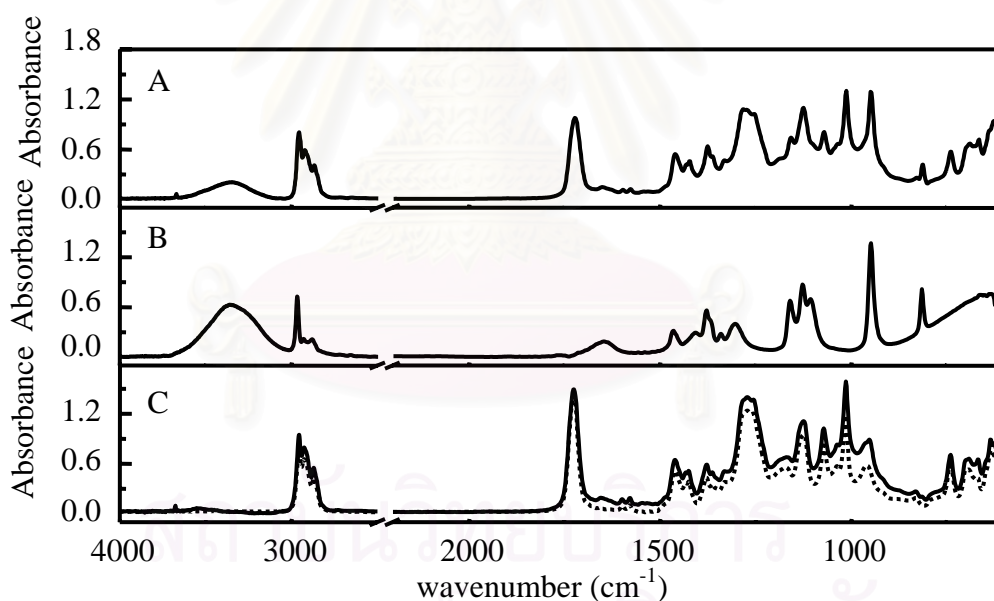


Figure 4.42 Calculated bulk ATR spectrum of PVC acquired by multiple reflection ATR accessory (C) obtained by subtracting bulk ATR spectrum of *i*-propanol (B) from a three-phase system spectrum of ZnSe/*i*-propanol/PVC (A) with 0.034  $\mu\text{m}$  thickness of *i*-propanol. The dotted line is spectrum of PVC under applied pressure.

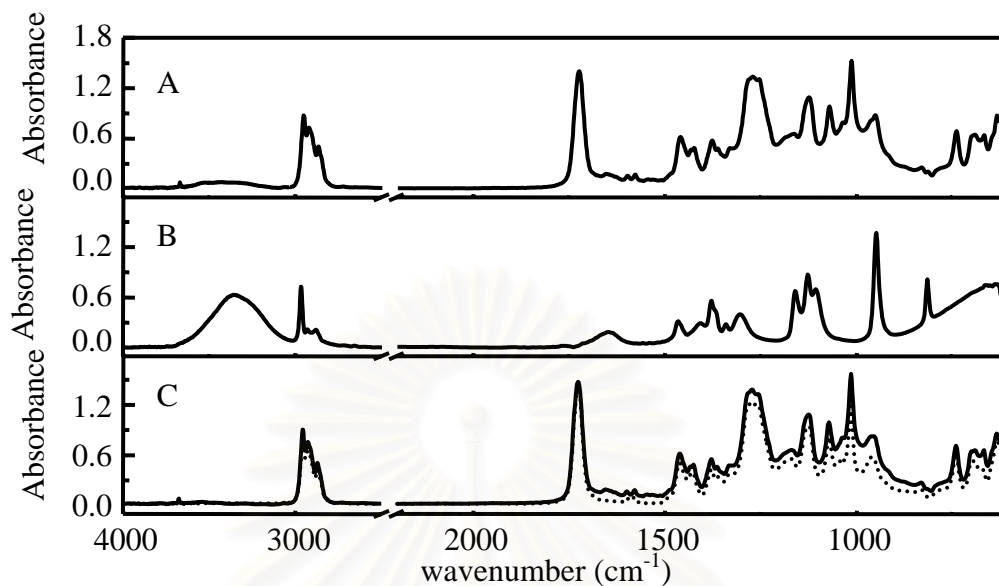


Figure 4.43 Calculated bulk ATR spectrum of PVC acquired by multiple reflection ATR accessory (C) obtained by subtracting bulk ATR spectrum of *i*-propanol (B) from a three-phase system spectrum of ZnSe/*i*-propanol/PVC (A) with 0.017  $\mu\text{m}$  thickness of *i*-propanol. The dotted line is spectrum of PVC under applied pressure.

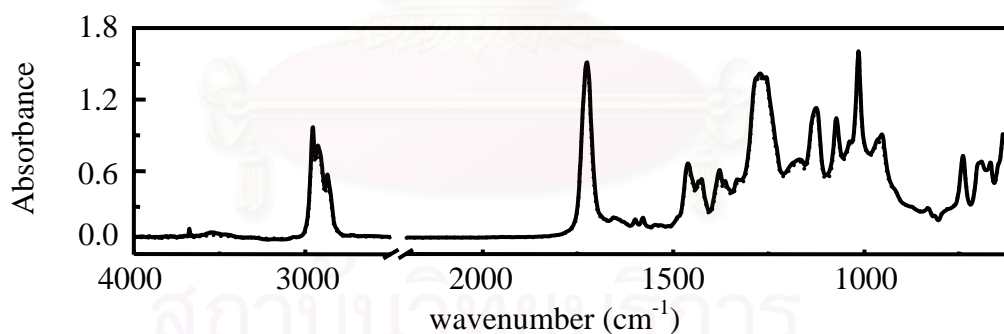


Figure 4.44 Comparison between the calculated bulk ATR spectrum of PVC shown in Figure 4.42 (solid line) and that in Figure 4.43 (dotted line).

The calculated bulk spectra of PVC in multiple reflection system by subtracting the bulk mineral oil spectrum from the three-phase spectrum of ZnSe/mineral oil/PVC using the expression given in Equation 2.16 are shown in Figures 4.45 and 4.46. The mineral oil in the three-phase system has the calculated thickness of 0.210  $\mu\text{m}$  in Figure 4.45 and 0.150  $\mu\text{m}$  in Figure 4.46. Both the calculated bulk spectrum of PVC are compared and shown in Figure 4.47.

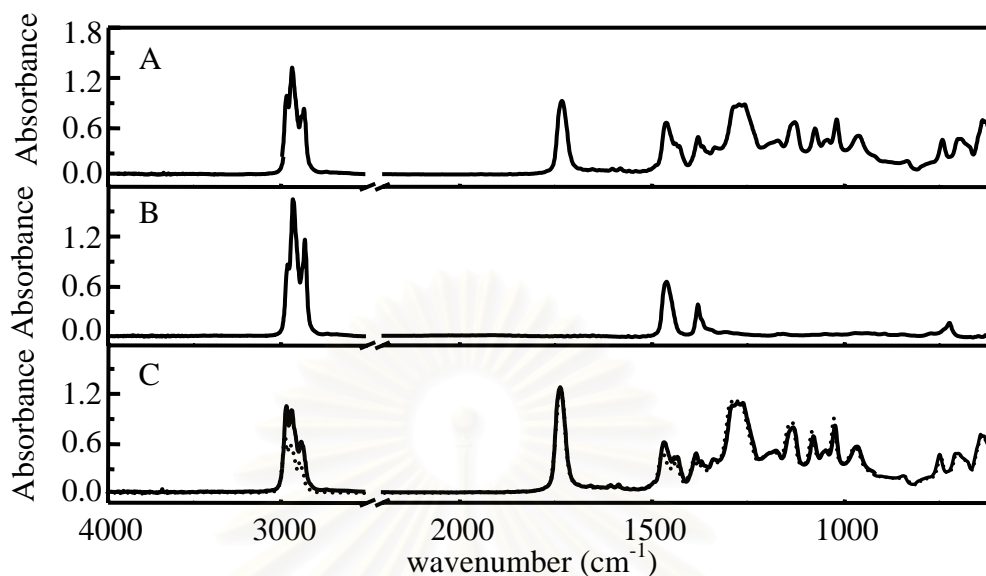


Figure 4.45 Calculated bulk ATR spectrum of PVC acquired by multiple reflection ATR accessory (C) obtained by subtracting bulk ATR spectrum of mineral oil (B) from a three-phase system spectrum of ZnSe/ mineral oil /PVC (A) with 0.210  $\mu\text{m}$  thickness of mineral oil. The dotted line is spectrum of PVC under applied pressure.

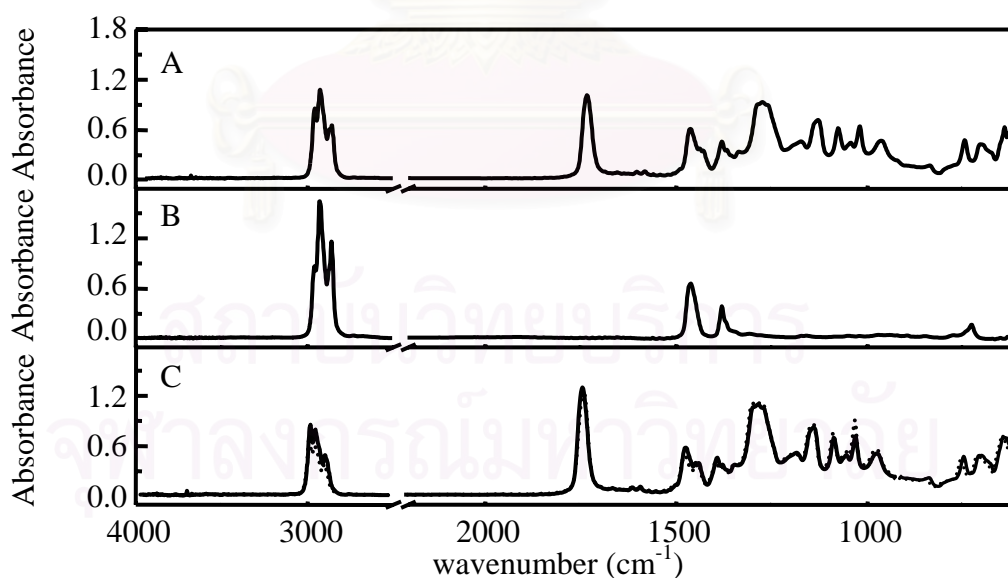


Figure 4.46 Calculated bulk ATR spectrum of PVC acquired by multiple reflection ATR accessory (C) obtained by subtracting bulk ATR spectrum of mineral oil (B) from a three-phase system spectrum of ZnSe/ mineral oil /PVC (A) with 0.150  $\mu\text{m}$  thickness of mineral oil. The dotted line is spectrum of PVC under applied pressure.

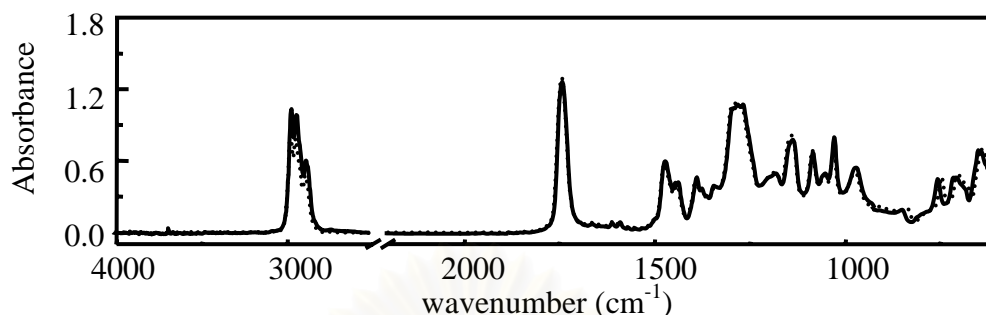


Figure 4.47 Comparison between the calculated bulk ATR spectrum of PVC shown in Figure 4.45 (solid line) and that in Figure 4.46 (dotted line).

From the calculated the bulk ATR spectrum of PVC in the multiple reflection system, the spectra indicate that the calculated bulk spectra are not accurate. This is because the absorbance in the multiple reflection system is too high. Simplified Equation of a three-phase system (Equation 2.16), which was used for calculating bulk spectrum, was defined under a small absorption approximation. Therefore, this calculation based on this equation cannot be applied for PVC acquired by multiple reflection ATR accessory with high absorbance.

Figures 4.48 and 4.49 show the bulk spectra of PC in multiple reflection system obtained by subtracting the bulk *i*-propanol from the three-phase system spectrum of ZnSe/*i*-propanol/PC based on the expression given in Equation 2.16. The *i*-propanol in the three-phase system has the calculated thickness of 0.047  $\mu\text{m}$  for Figure 4.48 and 0.013  $\mu\text{m}$  for Figure 4.49. Both the calculated bulk ATR spectrum of PC are compared and shown in Figure 4.50. The spectra indicate that there are deviations at the characteristic absorption band of *i*-propanol (i.e.,  $\sim 3400\text{ cm}^{-1}$ ). Similar to that of PVC, the deviation is greater as the absorption band of *i*-propanol increase (i.e., thick *i*-propanol film). Moreover, the calculated bulk spectra of PC from different *i*-propanol film thickness are not the same. This observation indicates the limitation of the proposed technique.

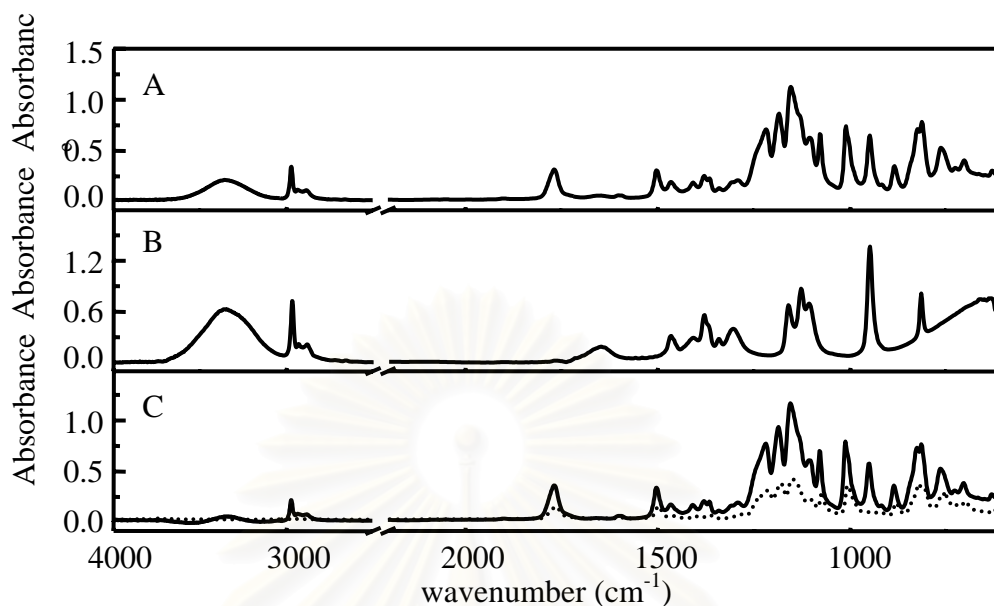


Figure 4.48 Calculated ATR bulk spectrum of PC acquired by multiple reflection accessory with (C) obtained by subtracting ATR bulk spectrum of *i*-propanol (B) from ATR three-phase system spectrum of ZnSe/*i*-propanol/PC with 0.047  $\mu\text{m}$  thickness of *i*-propanol (A). The dotted line is the spectrum of PC under applied pressure.

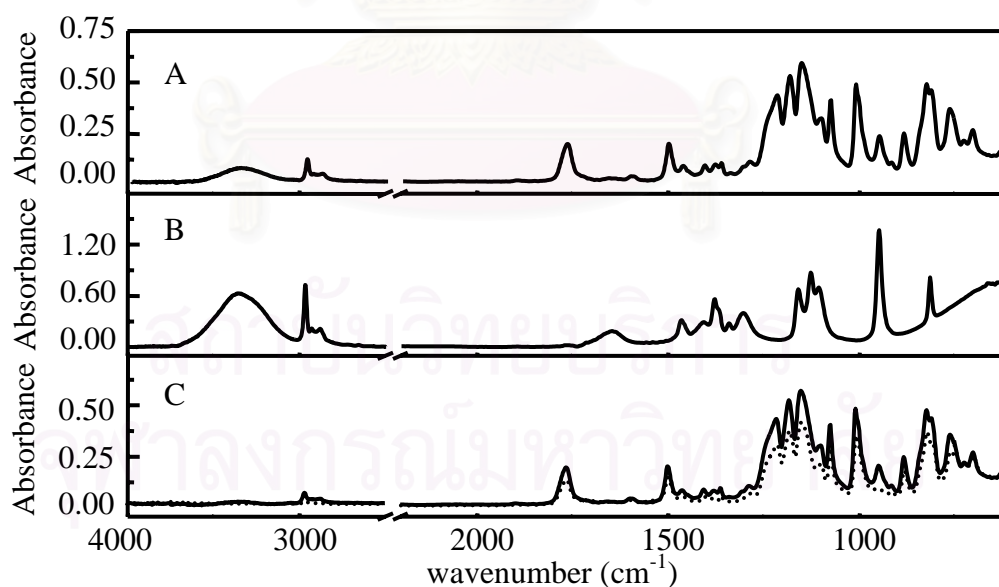


Figure 4.49 Calculated ATR bulk spectrum of PC acquired by multiple reflection accessory with (C) obtained by subtracting ATR bulk spectrum of *i*-propanol (B) from ATR three-phase system spectrum of ZnSe/*i*-propanol/PC with 0.013  $\mu\text{m}$  thickness of *i*-propanol (A). The dotted line is the spectrum of PC under applied pressure.



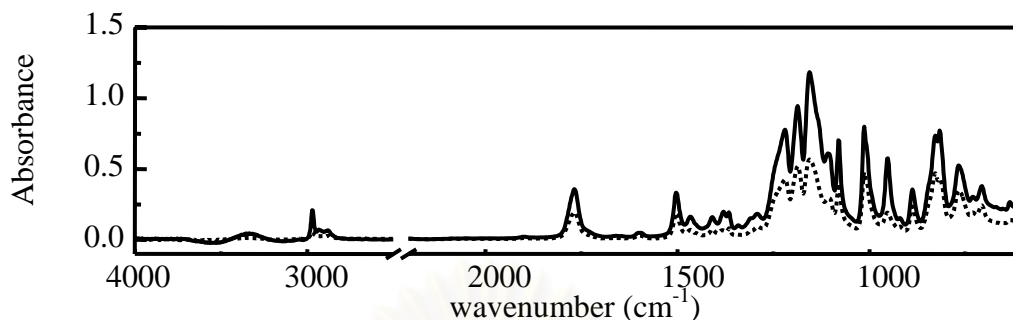


Figure 4.50 Comparison between the calculated bulk ATR spectrum of PC in Figure 4.48 (solid line) and Figure 4.49 (dotted line).

The bulk spectra of PC in multiple reflection system obtained by subtracting the bulk mineral oil from the three-phase system spectrum of ZnSe/mineral oil/PC based on the expression given in Equation 2.16 are shown in Figure 4.51 and 4.52. The mineral oil in the three-phase system has the thickness of 0.33  $\mu\text{m}$  for Figure 4.51 and 0.23  $\mu\text{m}$  for Figure 4.52. Both the calculated bulk ATR spectrum of PC are compared and shown in Figure 4.53.

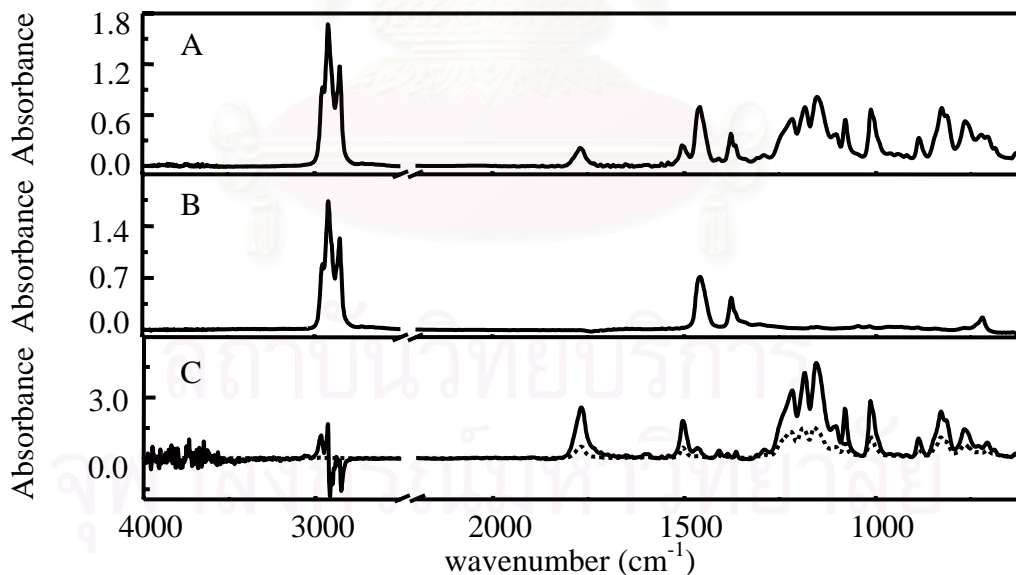


Figure 4.51 Calculated bulk ATR spectrum of PC acquired by multiple reflection ATR accessory (C) obtained by subtracting bulk ATR spectrum of mineral oil (B) from a three-phase system spectrum of ZnSe/mineral oil/PC (A) with 0.330  $\mu\text{m}$  thickness of mineral oil. The dotted line is spectrum of PC under applied pressure.



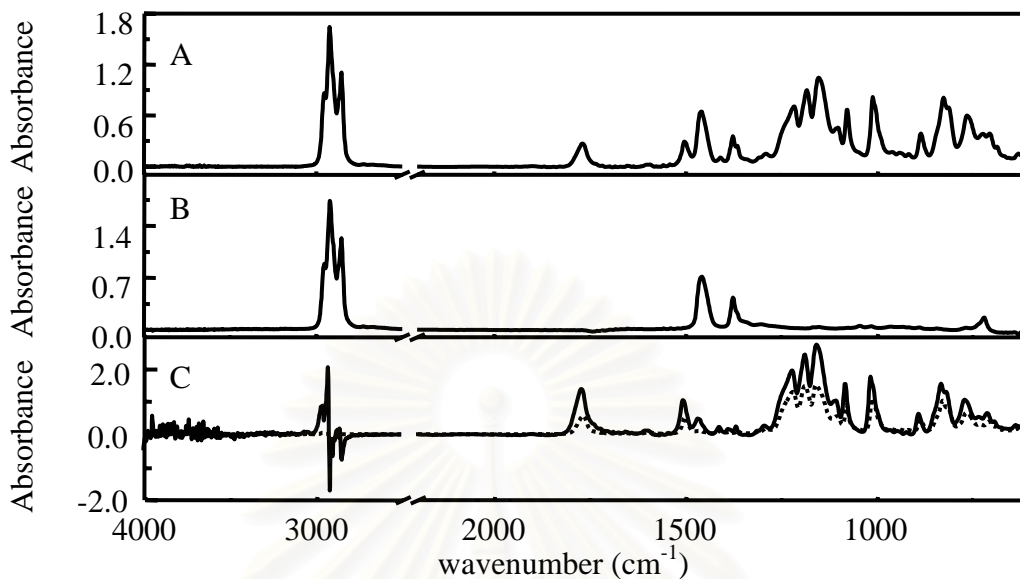


Figure 4.52 Calculated bulk ATR spectrum of PC acquired by multiple reflection ATR accessory (C) obtained by subtracting bulk ATR spectrum of mineral oil (B) from a three-phase system spectrum of ZnSe/ mineral oil /PC (A) with 0.230  $\mu\text{m}$  thickness of mineral oil. The dotted line is spectrum of PC under applied pressure.

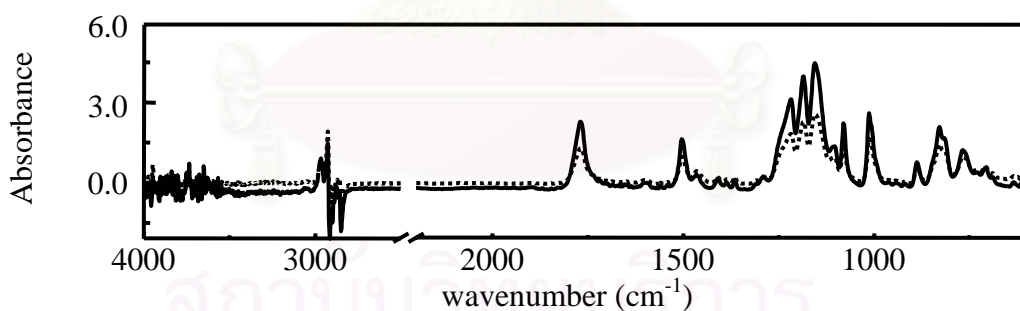


Figure 4.53 Comparison between the calculated bulk ATR spectrum of PC in Figure 4.51 (solid line) and Figure 4.52 (dotted line).

The proposed technique cannot be applied for the calculation of bulk spectrum of PC via the three-phase of ZnSe/mineral oil/PC. There is a great deviation at the characteristic absorption band of mineral oil (at 2800-3000  $\text{cm}^{-1}$ ) as shown in Figure 4.51 and 4.52. Both the calculated bulk spectra of PC are compared in Figure 4.53. The Figure shows that both spectra are different. According to the

observed phenomena, the bulk spectrum of PC cannot be calculated by the three-phase system spectrum in multiple reflection.

For a hard and rigid solid sample with rough surface, the calculated bulk spectra of PC rough 1200, PC rough 400 and PC rough 100 are shown in Figure 4.54, 4.55 and 4.56, respectively. These bulk spectra were calculated from the three-phase system spectra, which used *i*-propanol as intermediate layer. Similar to PVC and PC, there are great deviation, the calculation cannot applied to PC rough 1200, PC rough 400 and PC rough 100 in multiple reflection system.

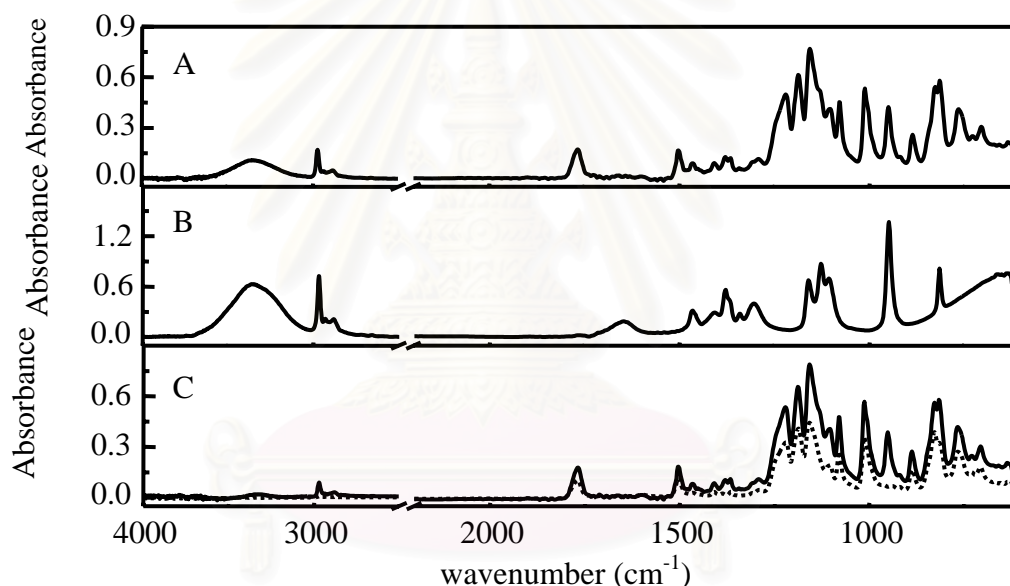


Figure 4.54 Calculated bulk ATR spectrum of PC rough 1200 acquired by multiple reflection ATR accessory (C) obtained by subtracting bulk ATR spectrum of *i*-propanol (B) from a three-phase system spectrum of ZnSe/*i*-propanol/ PC rough 1200 (A) with 0.052  $\mu\text{m}$  thick *i*-propanol. The dotted line is spectrum of PC rough 1200 under applied pressure.

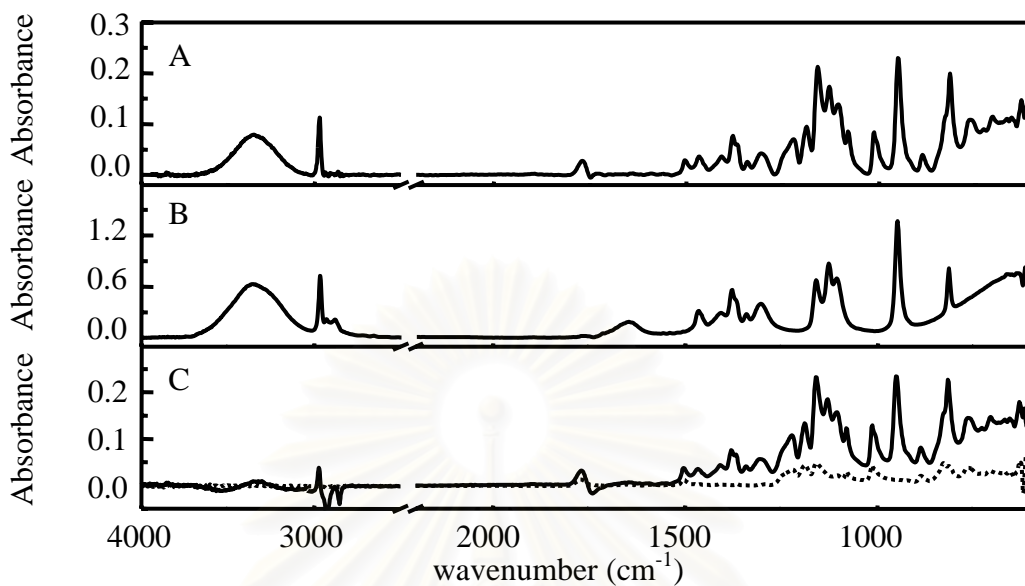


Figure 4.55 Calculated bulk ATR spectrum of PC rough 400 acquired by multiple reflection ATR accessory (C) obtained by subtracting bulk ATR spectrum of *i*-propanol (B) from a three-phase system spectrum of ZnSe/*i*-propanol/ PC rough 400 (A) with 0.038  $\mu\text{m}$  thick *i*-propanol. The dotted line is spectrum of PC rough 400 under applied pressure.

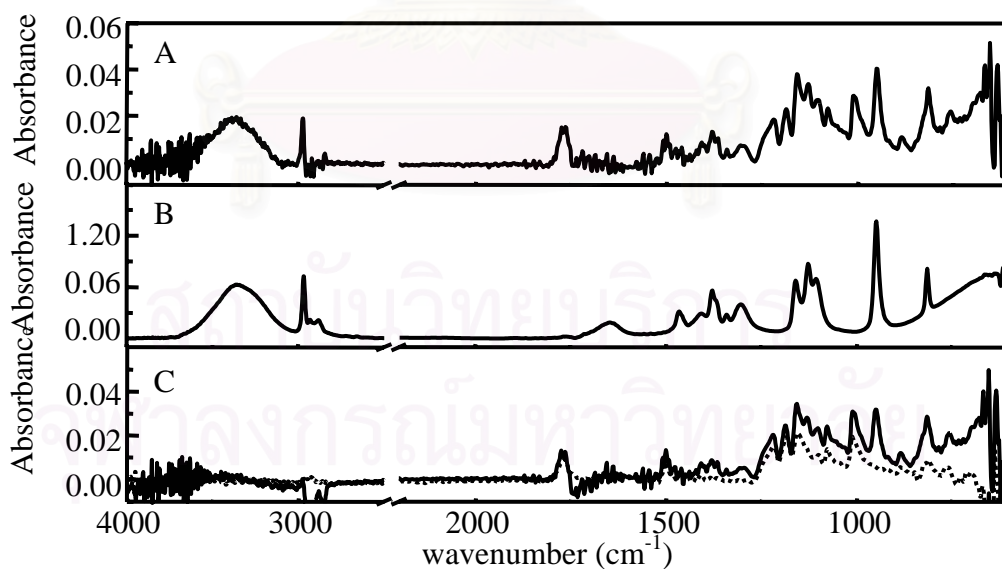


Figure 4.56 Calculated bulk ATR spectrum of PC rough 100 acquired by multiple reflection ATR accessory (C) obtained by subtracting bulk ATR spectrum of *i*-propanol (B) from a three-phase system spectrum of ZnSe/*i*-propanol/ PC rough 100 (A) with 0.061  $\mu\text{m}$  thick *i*-propanol. The dotted line is spectrum of PC rough 100 under applied pressure.

For calculating the bulk spectra of PC rough 1200, PC rough 400, and PC rough 100 from the three-phase spectra with mineral oil as intermediate layer, the calculated bulk spectra of these solid sample are not accurate. There are observable great deviations. The deviations in the calculated bulk spectra of those solid samples with rough surface are similar to those obtained from flat PC.

The calculated spectra indicate that the bulk ATR spectra of solid samples in multiple reflection system cannot be accurately calculated based on Equation 2.16. Since the absorption of the liquid in multiple reflection are too strong. The relationship expressed in Equation 2.16 is based on small absorption.

#### **b) Single Reflection System**

The calculated bulk spectra of PVC collected by single reflection ATR accessory by subtracting the bulk spectrum of *i*-propanol from the three-phase spectrum of ZnSe/*i*-propanol/PVC based on the expression given in Equation 2.16 are shown Figure 4.57 and 4.58. The *i*-propanol film in the three-phase system has the calculated thickness of 0.008  $\mu\text{m}$  for Figure 4.57 and 0.007  $\mu\text{m}$  for Figure 4.58. Both the calculated bulk spectra of PVC are compared and shown in Figure 4.59. Both the calculated bulk spectra of PVC were not the same. Although, a strong absorption is eliminated by single reflection, the calculated bulk spectrum still is not accurate. This is because *i*-propanol evaporates quickly in single reflection system. Therefore, there are both a gas phase spectrum and a liquid phase spectrum of *i*-propanol in the system. It can be observed from absorption band of free OH at frequency 3650  $\text{cm}^{-1}$ . As a result, the bulk of *i*-propanol cannot be accurately obtained. The calculated bulk spectrum of PVC cannot be obtained employed *i*-propanol as a buffer layer.

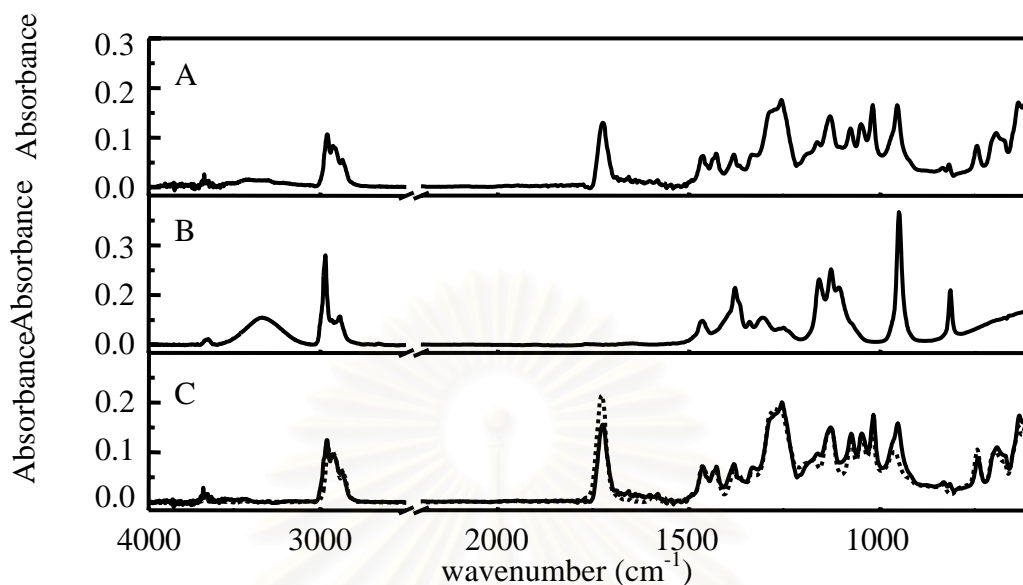


Figure 4.57 Calculated bulk ATR spectrum of PVC acquired by single reflection ATR accessory (C) obtained by subtracting bulk ATR spectrum of *i*-propanol (B) from a three-phase system spectrum of ZnSe/*i*-propanol/PVC (A) with 0.008  $\mu\text{m}$  thickness of *i*-propanol. The dotted line is spectrum of PVC under applied pressure.

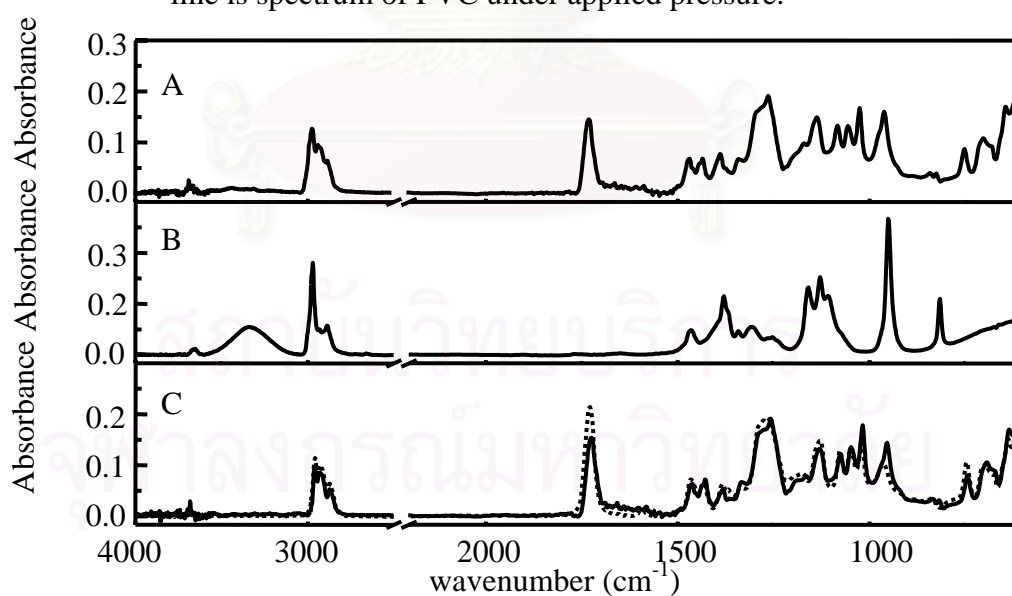


Figure 4.58 Calculated bulk ATR spectrum of PVC acquired by single reflection ATR accessory (C) obtained by subtracting bulk ATR spectrum of *i*-propanol (B) from a three-phase system spectrum of ZnSe/*i*-propanol/PVC (A) with 0.007  $\mu\text{m}$  thickness of *i*-propanol. The dotted line is spectrum of PVC under applied pressure.

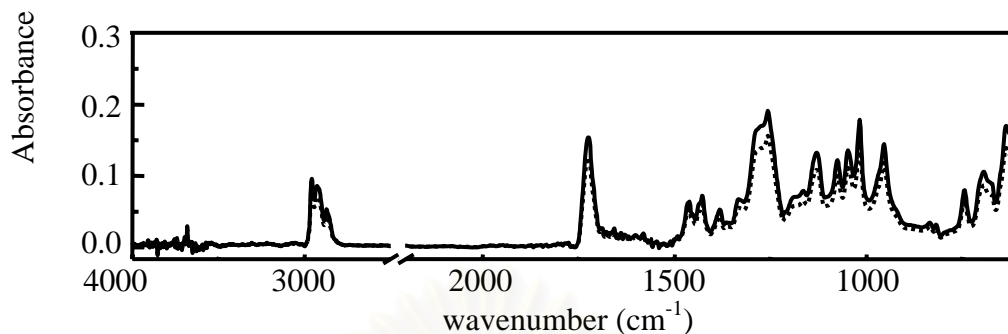


Figure 4.59 Comparison between the calculated bulk spectrum of PVC shown in Figure 4.57 (solid line) and Figure 4.58 (dotted line).

To avoid evaporation problem, an organic liquid with high viscosity such as mineral oil is employed. The calculated bulk spectra of PVC (spectrum C) were obtained by subtracting spectrum of mineral oil (spectrum B) from the three-phase spectrum of ZnSe/mineral oil/PVC (spectrum A) based on Equation 2.16 as shown in Figures 4.60 and 4.61. The mineral oil in the three-phase system has the calculated thickness of 0.043  $\mu\text{m}$  for Figure 4.60 and 0.012  $\mu\text{m}$  for Figure 4.61. The calculated bulk ATR spectra obtained from different buffer layer thickness are the same. The comparison is shown in Figure 4.62. The bulk spectrum of PVC in single reflection system can be calculated by the three-phase system of ZnSe/mineral oil/PVC.



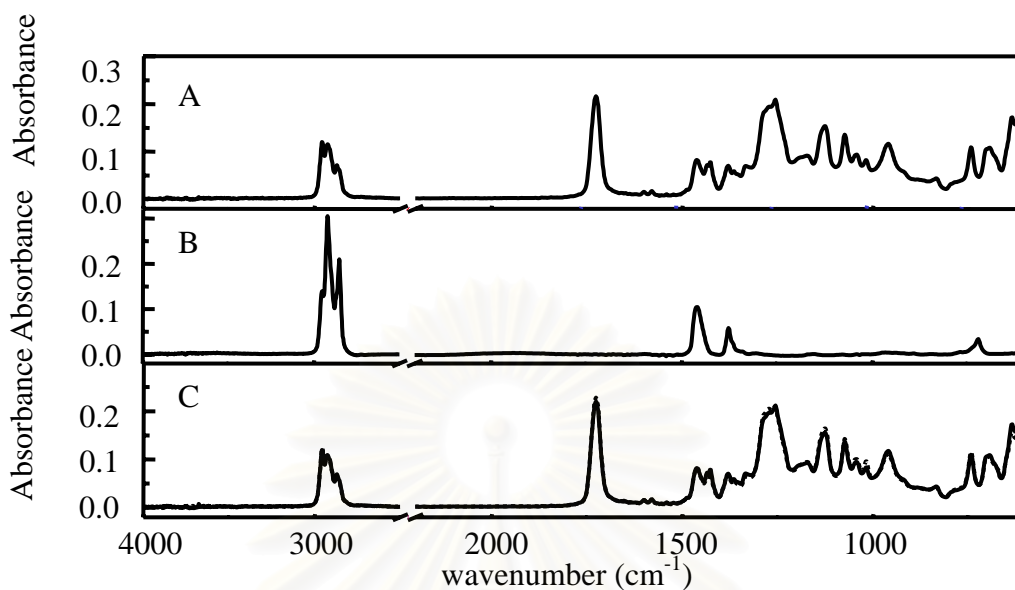


Figure 4.60 Calculated bulk ATR spectrum of PVC acquired by single reflection ATR accessory (C) obtained by subtracting bulk ATR spectrum of mineral oil (B) from a three-phase system spectrum of ZnSe/mineral oil/PVC (A) with 0.043  $\mu\text{m}$  thickness of mineral oil. The dotted line is spectrum of PVC under applied pressure.

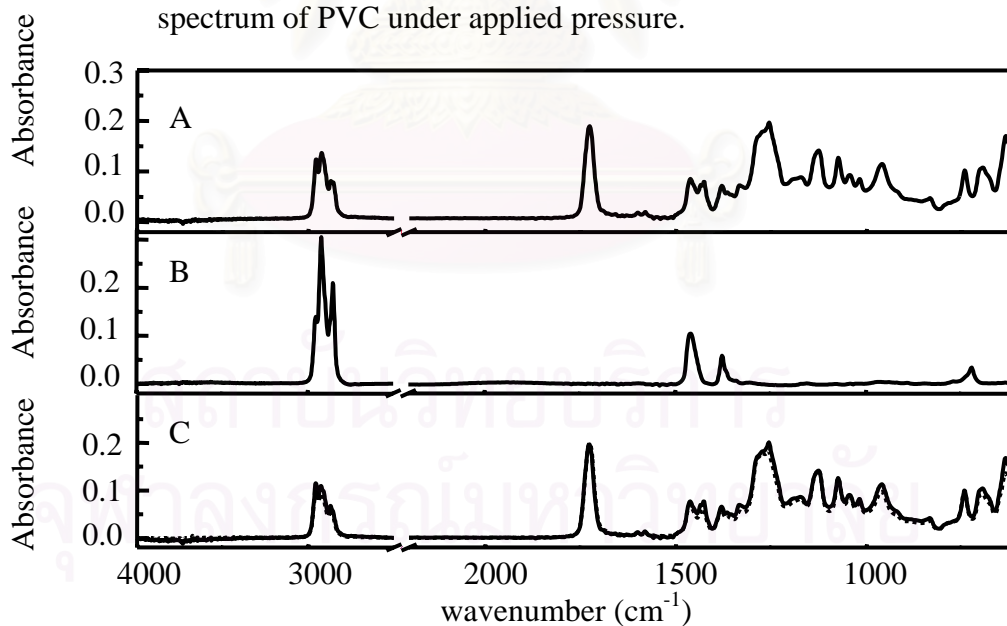


Figure 4.61 Calculated bulk ATR spectrum of PVC acquired by single reflection ATR accessory (C) obtained by subtracting bulk ATR spectrum of mineral oil (B) from a three-phase system spectrum of ZnSe/ mineral oil /PVC (A) with 0.012  $\mu\text{m}$  thickness of mineral oil. The dotted line is spectrum of PVC under applied pressure.

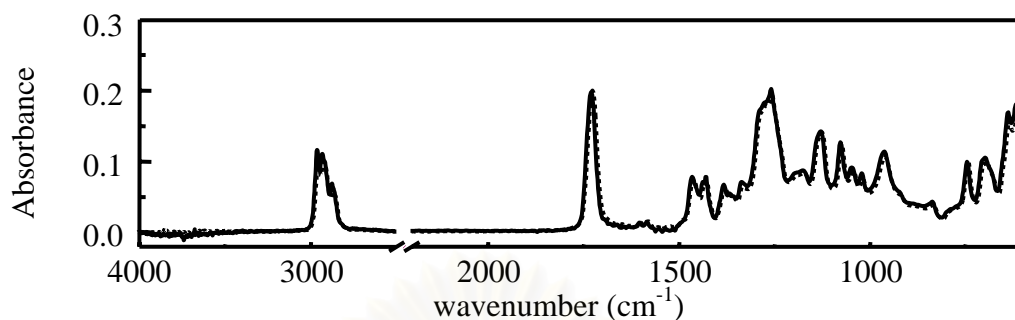


Figure 4.62 Comparison between the calculated bulk spectrum of PVC shown in Figure 4.60 (solid line) and Figure 4.61 (dotted line).

In the case of bulk spectrum calculation from a three-phase system of ZnSe/*i*-propanol/PC, there is a problem of evaporation of *i*-propanol. Similar to the system of ZnSe/*i*-propanol/PVC, the bulk spectrum cannot be accurately calculated. The three-phase spectra and the calculated bulk spectra are shown in Figures 4.63 and 4.64. A comparison of the calculated spectra from different film thickness is shown in Figure 4.65.

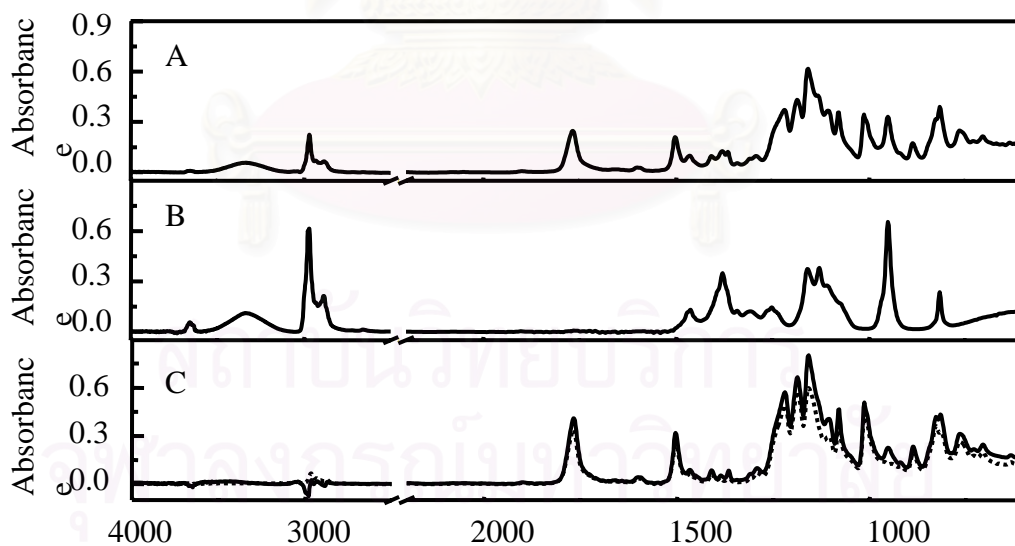


Figure 4.63 Calculated bulk ATR spectrum of PC acquired by single reflection ATR accessory (C) obtained by subtracting bulk ATR spectrum of *i*-propanol (B) from a three-phase system spectrum of ZnSe/*i*-propanol/PC (A) with 0.220  $\mu\text{m}$  thickness of *i*-propanol. The dotted line is spectrum of PC under applied pressure.

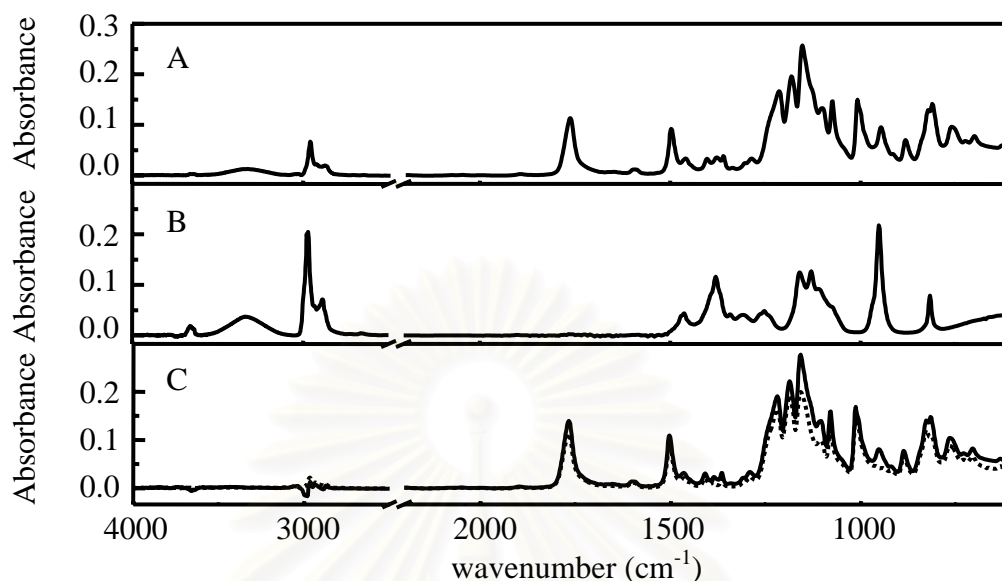


Figure 4.64 Calculated bulk ATR spectrum of PC acquired by single reflection ATR accessory (C) obtained by subtracting bulk ATR spectrum of *i*-propanol (B) from a three-phase system spectrum of ZnSe/*i*-propanol/PC (A) with 0.120  $\mu\text{m}$  thickness of *i*-propanol. The dotted line is spectrum of PC under applied pressure.

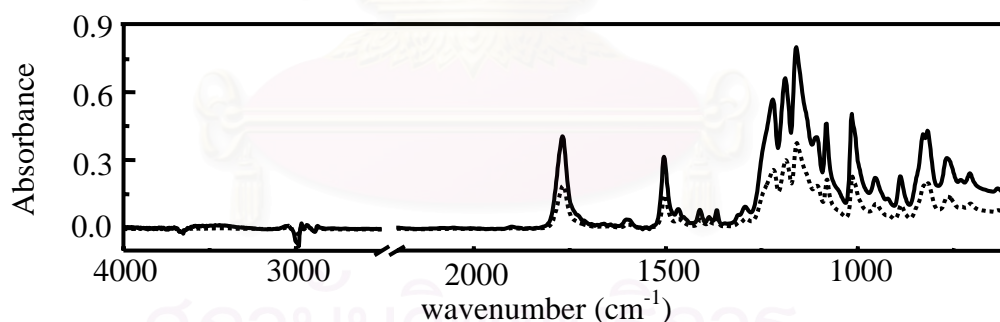


Figure 4.65 Comparison between the calculated bulk spectrum of PC shown in Figure 4.63 (solid line) and Figure 4.64 (dotted line).

Mineral oil was used as an organic liquid layer between PC and the IRE instead of *i*-propanol. The calculated bulk spectra of PC are shown in Figure 4.66 and 4.67. The mineral oil in the three-phase system has the calculated thickness of 0.088  $\mu\text{m}$  for Figure 4.66 and 0.051  $\mu\text{m}$  for Figure 4.67. Each the bulk spectra was compared to the spectrum of PC without mineral oil. However, the calculated bulk spectra from different thickness of liquid layer are not the same and shown in Figure 4.68.

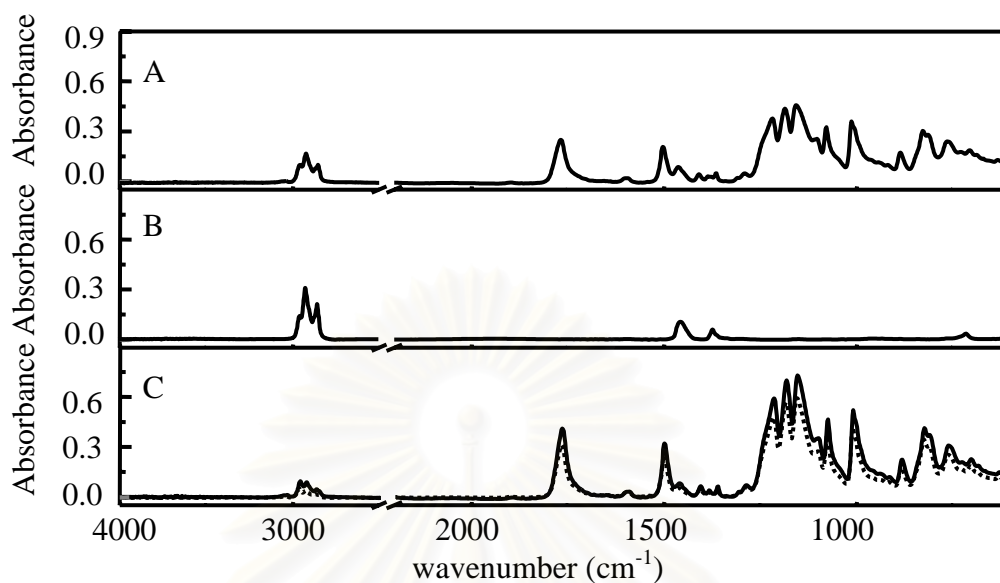


Figure 4.66 Calculated bulk ATR spectrum of PC acquired by single reflection ATR accessory (C) obtained by subtracting bulk ATR spectrum of mineral oil (B) from a three-phase system spectrum of ZnSe/mineral oil/PC (A) with 0.088  $\mu\text{m}$  thickness of mineral oil. The dotted line is spectrum of PC under applied pressure.

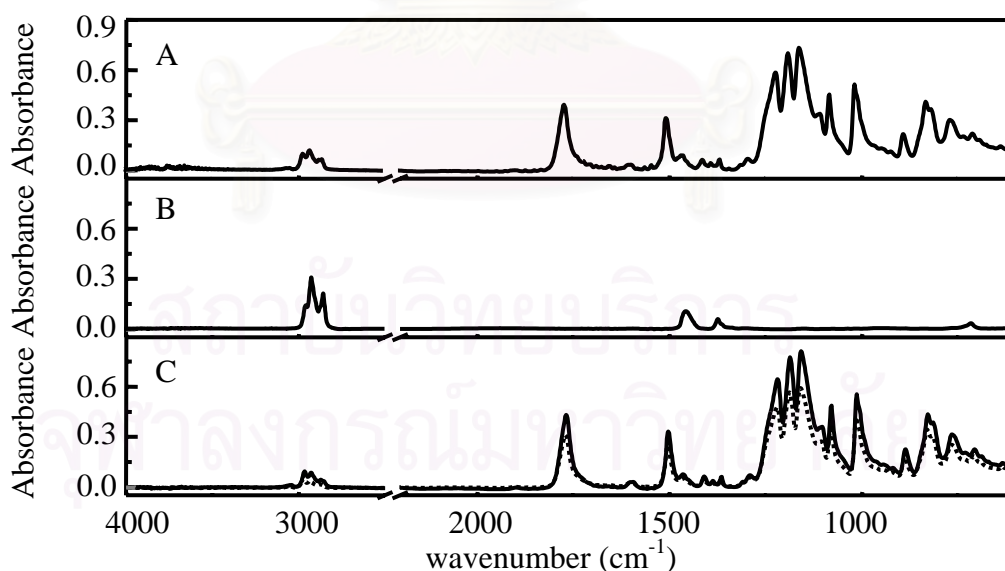


Figure 4.67 Calculated bulk ATR spectrum of PC acquired by single reflection ATR accessory (C) obtained by subtracting bulk ATR spectrum of mineral oil (B) from a three-phase system spectrum of ZnSe/mineral oil/PC (A) with 0.051  $\mu\text{m}$  thickness of mineral oil. The dotted line is spectrum of PC under applied pressure.

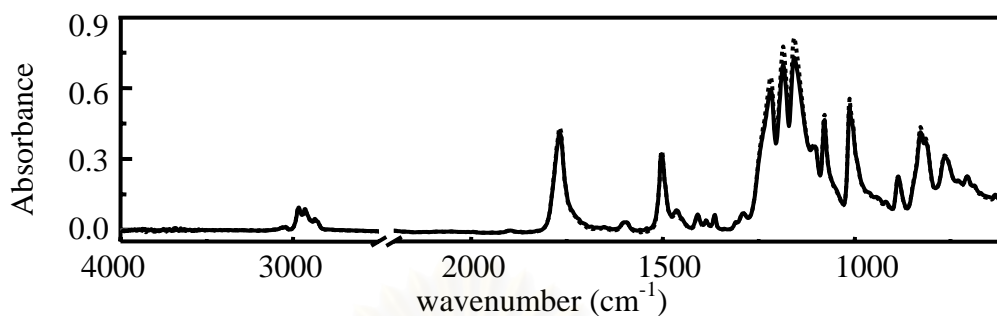


Figure 4.68 Comparison between the calculated bulk spectrum of PC shown in Figure 4.72 (solid line) and Figure 4.73 (dotted line).

These spectra indicate that the calculated bulk spectra of PC based on Equation 2.16 are not valid for system of both ZnSe/*i*-propanol/PC and ZnSe/mineral oil/PC in single reflection system. This is because the absorbance of PC in single reflection system is too strong to calculate the bulk spectrum based on Equation 2.16.

To avoid the strong absorption, Ge IRE was used instead of ZnSe IRE. Ge IRE has a refractive index of 4.0, while ZnSe IRE has a refractive index of 2.4. The refractive index affects the penetration depth of the evanescent wave into the sample. By increase the refractive index of the IRE, the penetration depth decrease. This will decrease the absorbance of the sample. As a result, the absorbance of the sample with Ge as the IRE is smaller than that with ZnSe as the IRE.

The comparison between the absorbance of PVC sample with ZnSe IRE and that with Ge IRE are shown in Figure 4.69. While the absorbance of PC sample with ZnSe IRE is compared to that with Ge IRE as shown in Figure 4.70

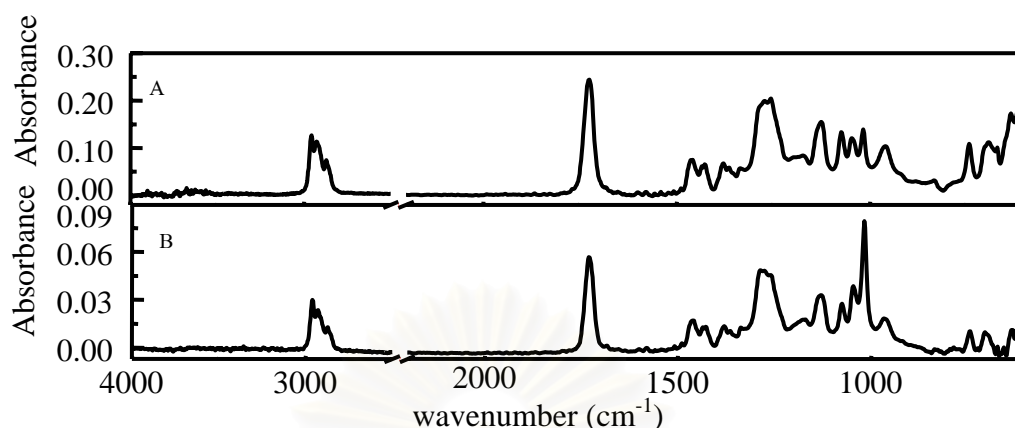


Figure 4.69 ATR spectra of PVC acquired by single reflection ATR accessory using ZnSe IRE (A) and Ge IRE (B) with 45° angle of incidence.

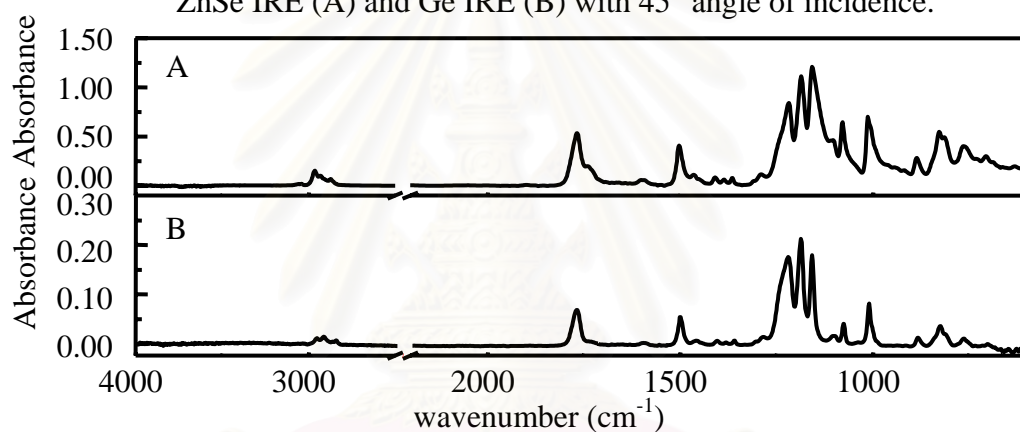


Figure 4.70 ATR spectra of PC acquired by single reflection ATR accessory using ZnSe IRE (A) and Ge IRE (B) with 45° angle of incidence.

Since *i*-propanol cannot be applied to calculate the bulk spectrum of the solid sample in single reflection system, mineral oil was used as intermediate layer between the solid sample and the IRE for calculating the bulk spectrum.

The calculated bulk spectra of PVC, which acquired from the three-phase system of Ge/mineral oil/PVC with thickness of mineral oil of 0.013  $\mu\text{m}$  and 0.005  $\mu\text{m}$  are shown in Figures 4.71 and 4.72. The absorbance in A on C indicate that there are no observable spectral enhancements. This phenomenon indicates that the PVC sample has a good contact with the IRE. Moreover, comparison of both the calculated bulk spectra of PVC shows that the absorbances of both spectra are the same (Figure 4.76). This implies that the bulk spectrum of PVC can be calculated from the three-phase system of Ge/mineral oil/PVC based on Equation 2.16.



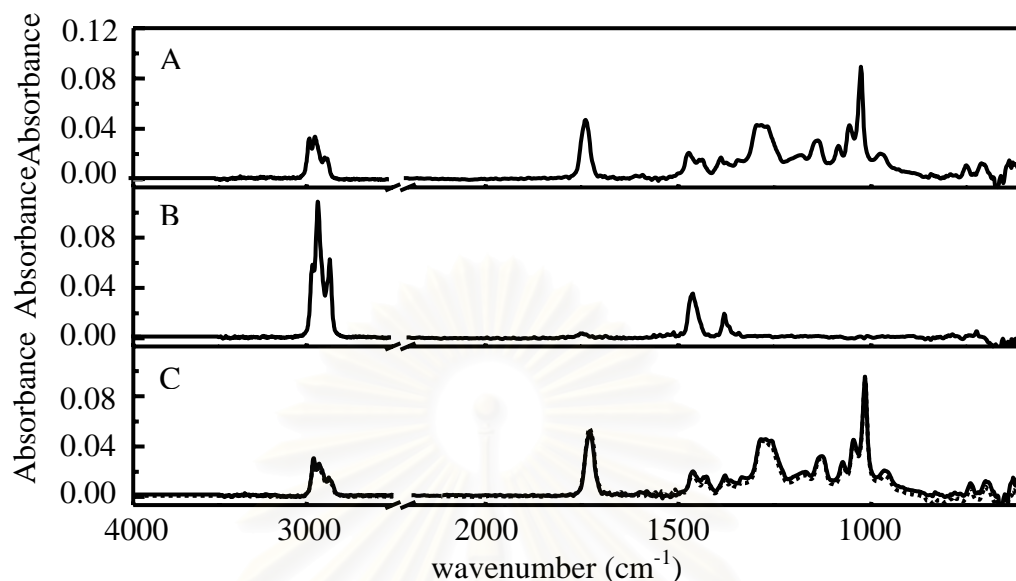


Figure 4.71 Calculated bulk ATR spectrum of PVC acquired by single reflection ATR accessory (C) obtained by subtracting bulk ATR spectrum of mineral oil (B) from a three-phase system spectrum of Ge/ mineral oil /PVC (A) with 0.013  $\mu\text{m}$  thickness of mineral oil. The dotted line is spectrum of PVC under applied pressure.

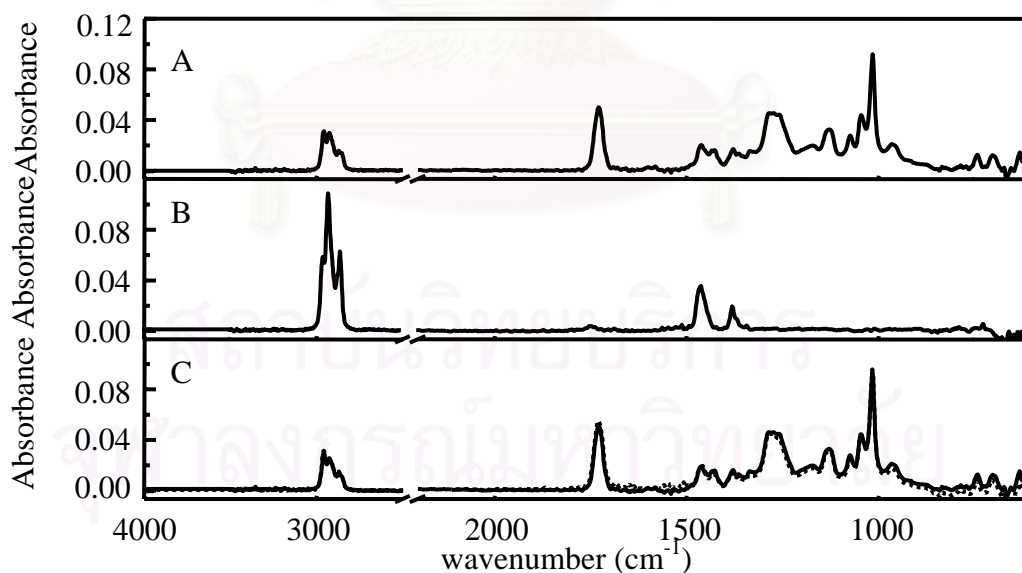


Figure 4.72 Calculated bulk ATR spectrum of PVC acquired by single reflection ATR accessory (C) obtained by subtracting bulk ATR spectrum of mineral oil (B) from a three-phase system spectrum of Ge/ mineral oil /PVC (A) with 0.007  $\mu\text{m}$  thickness of mineral oil. The dotted line is spectrum of PVC under applied pressure.

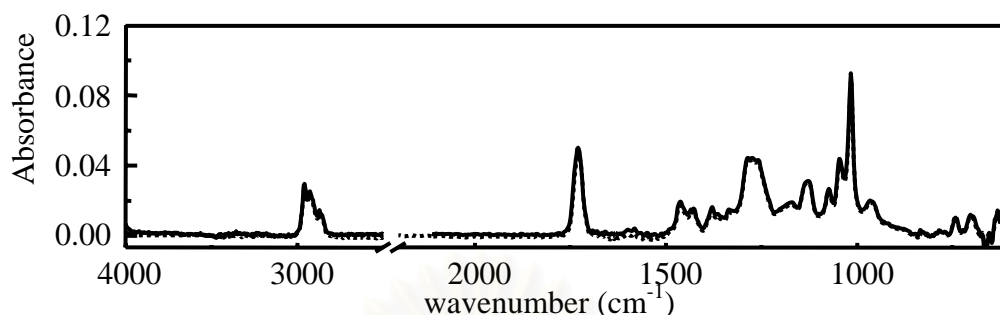


Figure 4.73 Comparison between the calculated bulk spectrum of PVC shown in Figure 4.71 (solid line) and Figure 4.72 (dotted line).

For the hard and rigid solid sample with flat surface, the calculated bulk spectra of PC were acquired from the three-phase system of Ge/mineral oil/PC with thickness of mineral oil of 0.037  $\mu\text{m}$  and 0.025  $\mu\text{m}$  (shown in Figures 4.74 and 4.75). The calculated bulk spectra of PC have greater absorbance than the observed spectra of PC under the applied pressure. This phenomenon indicates that there is an air gap between the PC sample and the IRE. Both the calculated bulk spectra of PC which were acquired from the three-phase system with thickness of mineral oil of 0.037  $\mu\text{m}$  and 0.025  $\mu\text{m}$  are compared and shown in Figure 4.76. The absorbance of both the calculating three bulk spectra are the same. These results indicate that the calculated bulk spectrum of PC based on Equation 2.16 can be applied to the three-phase system of Ge/mineral oil/PC.

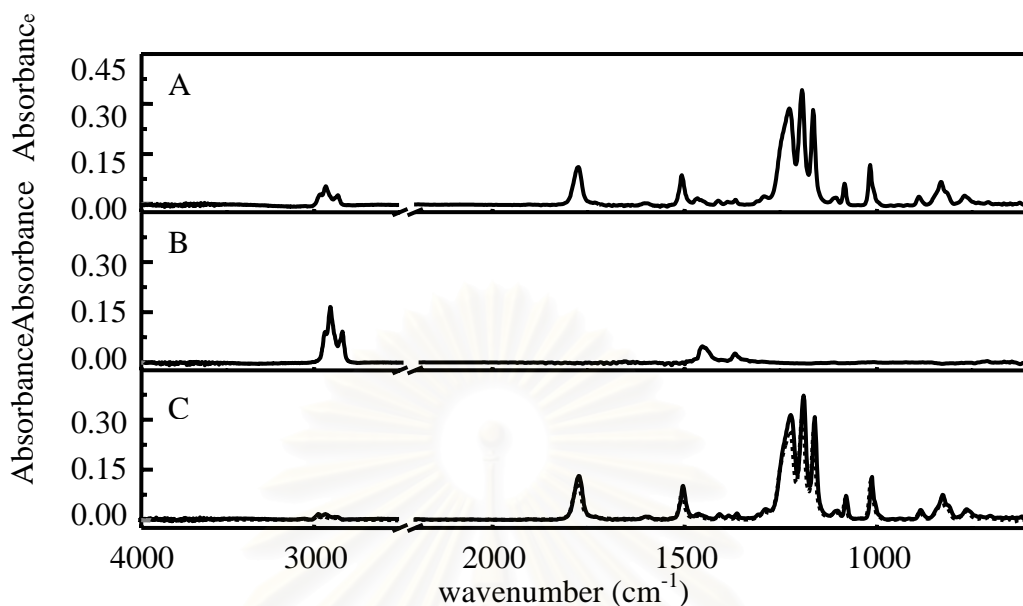


Figure 4.74 Calculated bulk ATR spectrum of PC acquired by single reflection ATR accessory (C) obtained by subtracting bulk ATR spectrum of mineral oil (B) from a three-phase system spectrum of Ge/ mineral oil /PC (A) with 0.037  $\mu\text{m}$  thickness of mineral oil. The dotted line is spectrum of PC under applied pressure.

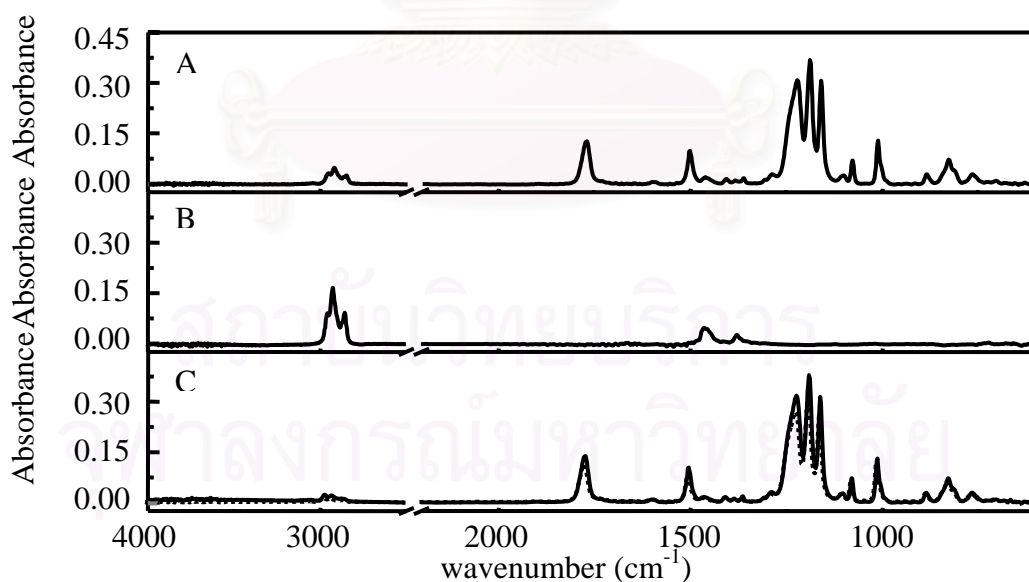


Figure 4.75 Calculated bulk ATR spectrum of PC acquired by single reflection ATR accessory (C) obtained by subtracting bulk ATR spectrum of mineral oil (B) from a three-phase system spectrum of Ge/mineral oil/PC (A) with 0.027  $\mu\text{m}$  thickness of mineral oil. The dotted line is spectrum of PC under applied pressure.

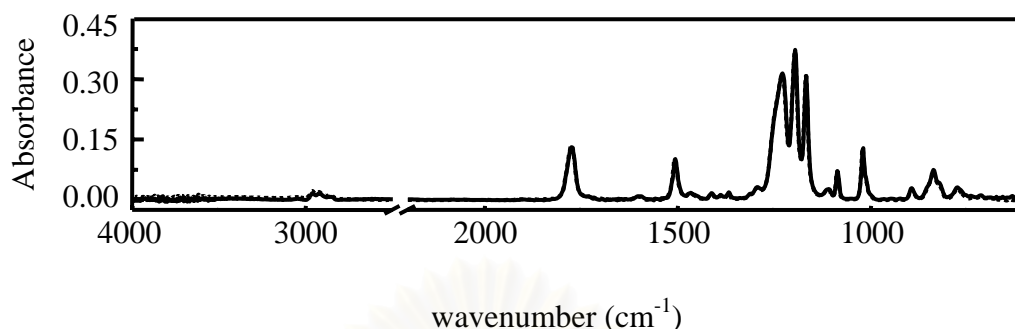


Figure 4.76 Comparison between the calculated bulk spectrum of PC shown in Figure 4.74 (solid line) and Figure 4.75 (dotted line).

For the solid samples with rough surface, the calculated bulk spectra of PC rough 1200 are shown in Figures 4.77 and 4.78. The calculated bulk spectra of PC rough 1200 were obtained from the three-phase of Ge/mineral oil/PC rough 1200 with the calculated thickness of mineral oil of  $0.119\ \mu\text{m}$  for Figure 4.77 and  $0.058\ \mu\text{m}$  for Figure 4.78. The comparison between both the calculated bulk spectra (Figure 4.79) shows that the absorbances of both calculated spectra are not the same.

For PC rough 400 and PC rough 100, like PC rough 1200 system, the calculated bulk spectra have greater absorbance than the observed spectra under the applied pressure. These spectra are shown in Figures 4.80 and 4.81 for PC rough 400 and Figures 4.83 and 4.84 for PC rough 100.

The calculated bulk spectra of PC rough 400 were acquired from the three-phase system of Ge/mineral oil/PC rough 400 with the calculated thickness of mineral oil of  $0.134\ \mu\text{m}$  for Figure 4.80 and  $0.092\ \mu\text{m}$  for Figure 4.81. The absorbance of both the bulk spectra of PC rough 400 are different as shown in Figure 4.82.

For PC rough 100, the calculated bulk spectra have greater absorbance than the observed spectra under the applied pressure. The calculated bulk spectra of PC rough 100 were acquired from the three-phase system of Ge/mineral oil/

PC rough 100 with the calculated thickness of mineral oil of 0.154  $\mu\text{m}$  for Figure 4.83 and 0.092  $\mu\text{m}$  for Figure 4.84. The absorbance of both the bulk spectra of PC rough 100 are very different as shown in Figure 4.85.

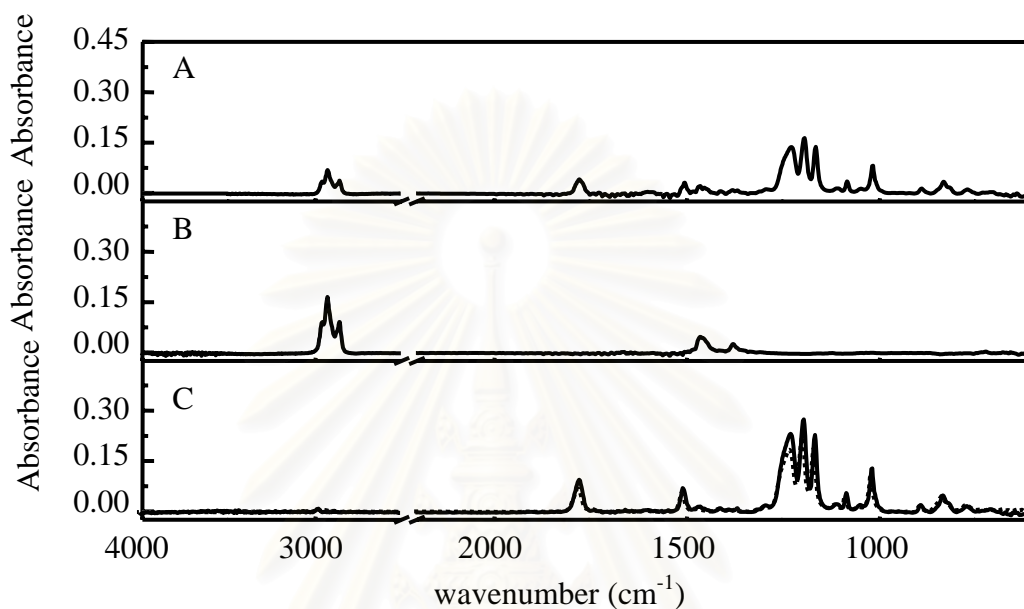


Figure 4.77 Calculated bulk ATR spectrum of PC rough 1200 acquired by single reflection ATR accessory (C) obtained by subtracting bulk ATR spectrum of mineral oil (B) from a three-phase system spectrum of Ge/mineral oil / PC rough 1200 (A) with 0.119  $\mu\text{m}$  thickness of mineral oil. The dotted line is spectrum of PC rough 1200 under applied pressure.

สถาบันวิทยบริการ  
จุฬาลงกรณ์มหาวิทยาลัย

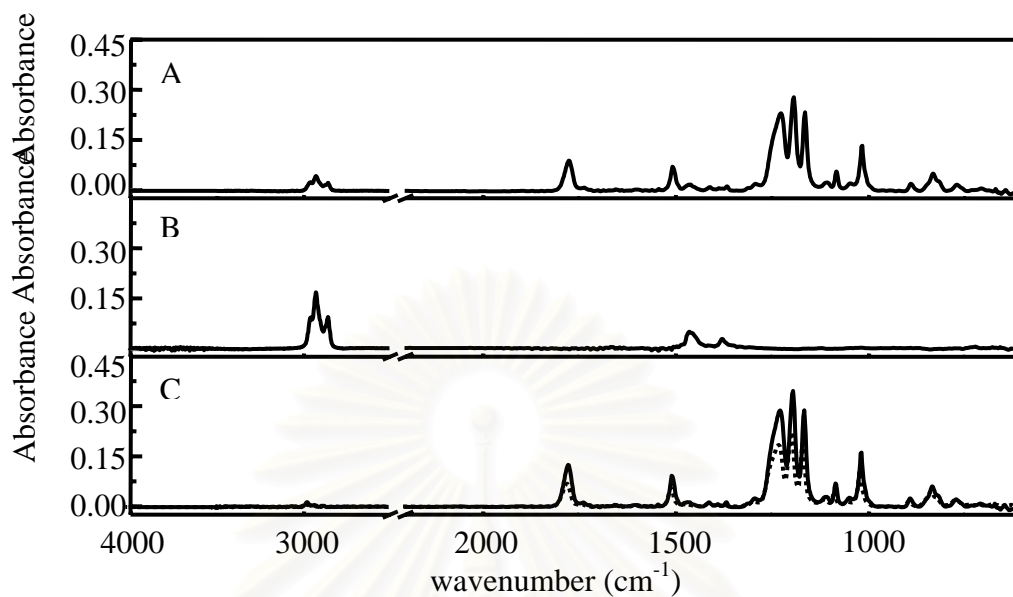


Figure 4.78 Calculated ATR bulk spectrum of PC rough 1200 in single reflection (C) acquired by subtracting ATR bulk spectrum of mineral oil (B) from ATR three-phase system spectrum of Ge IRE/mineral oil/PC rough 1200 with 0.058  $\mu\text{m}$  of the calculated thickness of mineral oil (A). The dotted line is spectrum of PC rough 1200 under applied pressure.

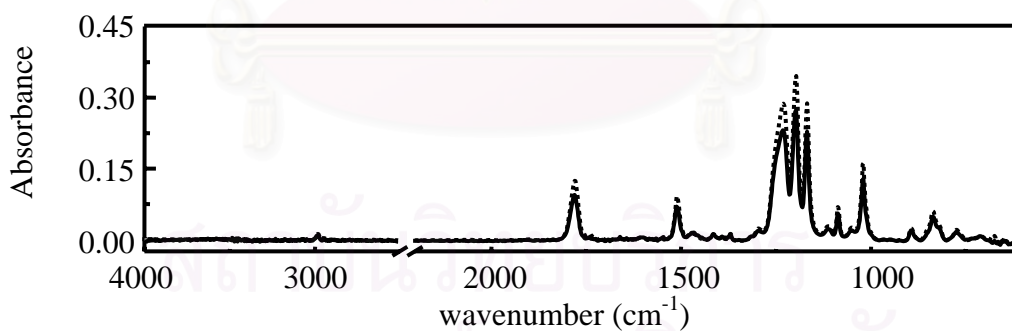


Figure 4.79 Comparison between the calculated bulk spectrum of PC rough 1200 shown in Figure 4.77 (solid line) and Figure 4.78 (dotted line).



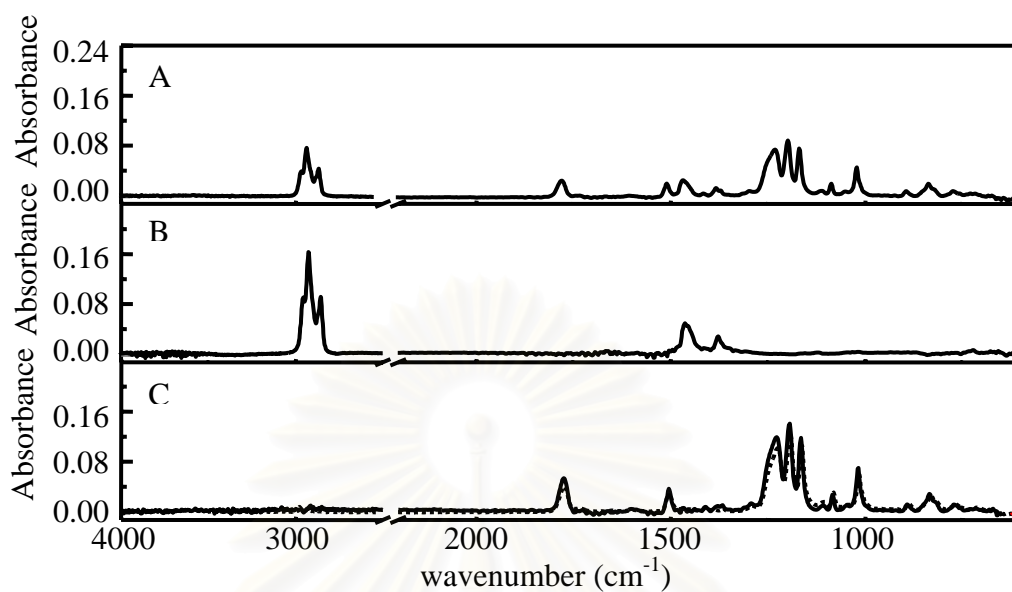


Figure 4.80 Calculated bulk ATR spectrum of PC rough 400 acquired by single reflection ATR accessory (C) obtained by subtracting bulk ATR spectrum of mineral oil (B) from a three-phase system spectrum of Ge/mineral oil / PC rough 400 (A) with 0.134  $\mu\text{m}$  thickness of mineral oil. The dotted line is spectrum of PC rough 400 under applied pressure.

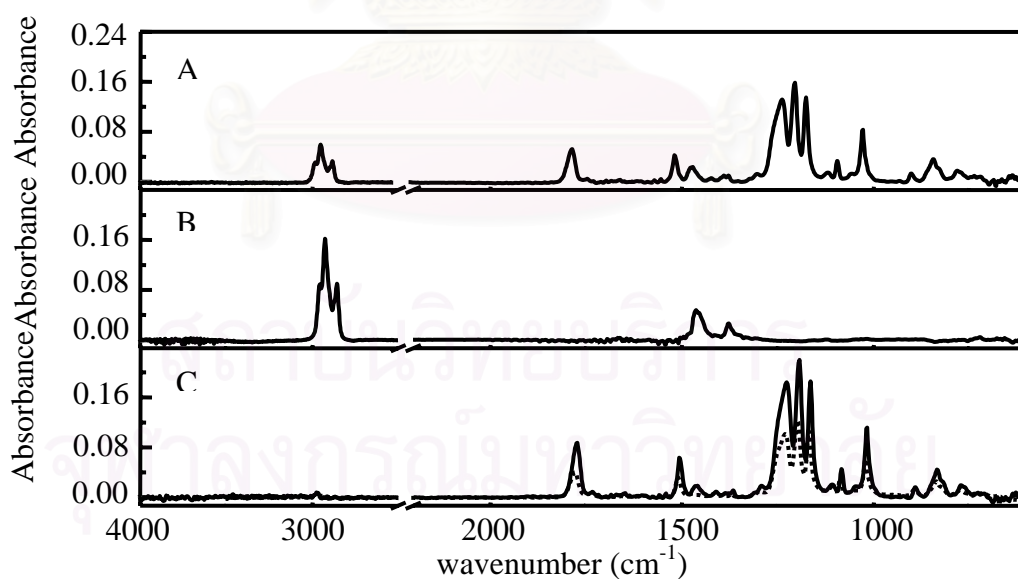


Figure 4.81 Calculated bulk ATR spectrum of PC rough 400 acquired by single reflection ATR accessory (C) obtained by subtracting bulk ATR spectrum of mineral oil (B) from a three-phase system spectrum of Ge/mineral oil / PC rough 400 (A) with 0.092  $\mu\text{m}$  thickness of mineral oil. The dotted line is spectrum of PC rough 400 under applied pressure.

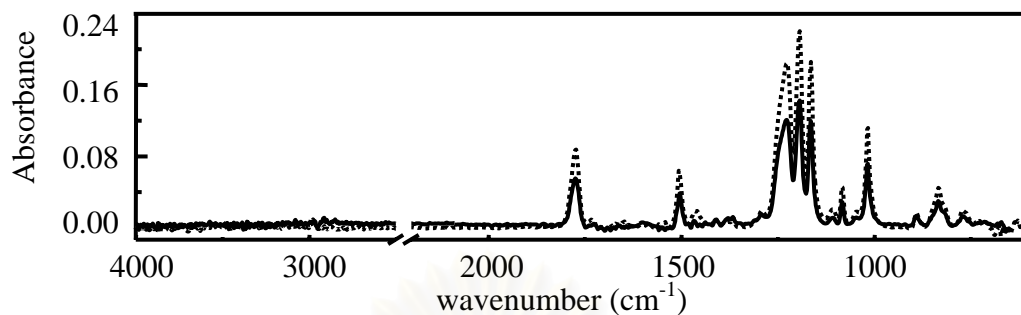


Figure 4.82 Comparison between the calculated bulk spectrum of PC rough 400 shown in Figure 4.80 (solid line) and Figure 4.81 (dotted line).

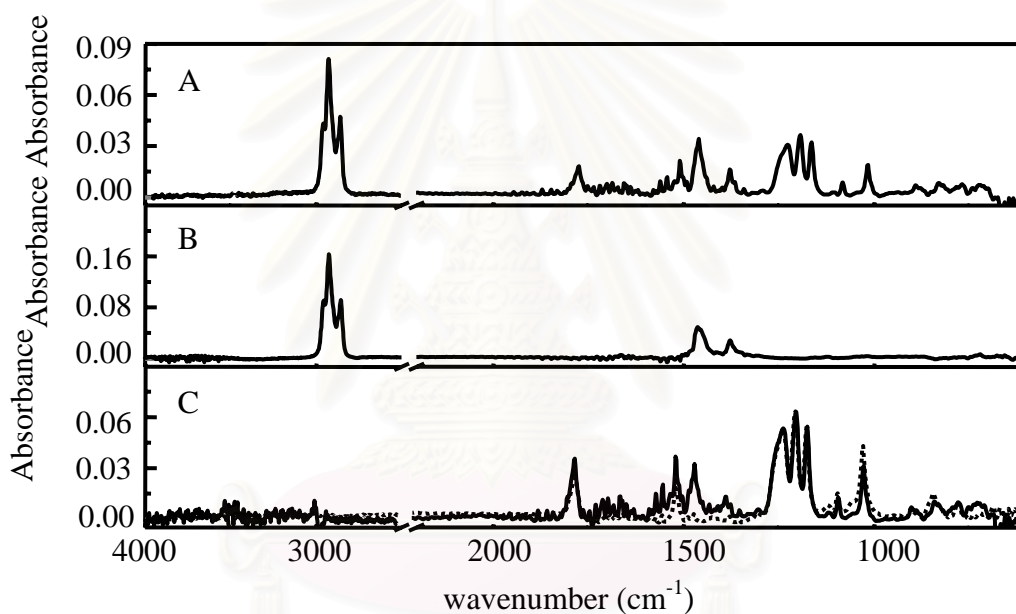


Figure 4.83 Calculated bulk ATR spectrum of PC rough 100 acquired by single reflection ATR accessory (C) obtained by subtracting bulk ATR spectrum of mineral oil (B) from a three-phase system spectrum of Ge/mineral oil / PC rough 100 (A) with  $0.154 \mu\text{m}$  thickness of mineral oil. The dotted line is spectrum of PC rough 100 under applied pressure.

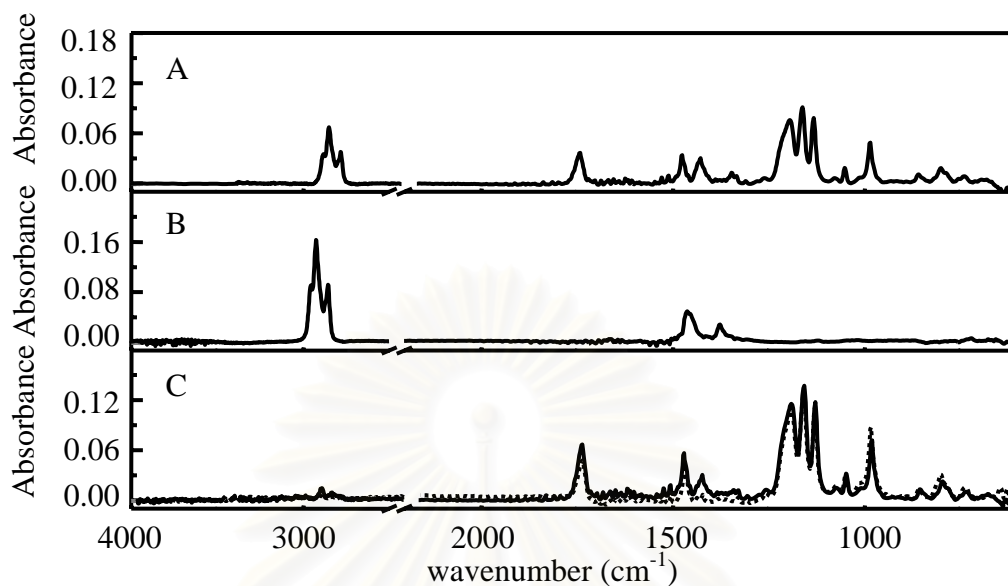


Figure 4.84 Calculated bulk ATR spectrum of PC rough 100 acquired by single reflection ATR accessory (C) obtained by subtracting bulk ATR spectrum of mineral oil (B) from a three-phase system spectrum of Ge/mineral oil / PC rough 100 (A) with 0.106  $\mu\text{m}$  thickness of mineral oil. The dotted line is spectrum of PC rough 100 under applied pressure.

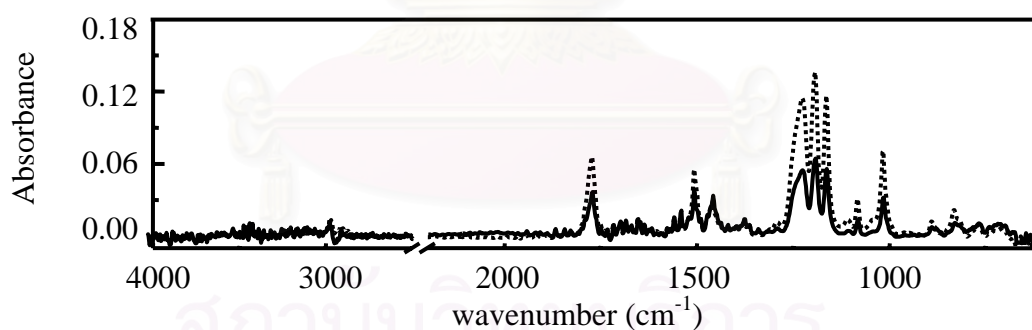


Figure 4.85 Comparison between the calculated bulk spectrum of PC rough 100 shown in Figure 4.83 (solid line) and Figure 4.84 (dotted line).

From all the calculated bulk spectra of the hard and rigid solid sample with various roughnesses, these spectra show that the absorbance of each bulk spectrum obtained from the three-phase system with various thickness of mineral oil is not the same. Since in the rough surface the thickness of mineral oil is irregular, the thickness of mineral oil cannot be accurately calculated. As a result the calculated bulk spectra of hard and rigid solid sample with rough surface cannot be accurately

obtained. These phenomena imply that the calculation of bulk spectra cannot be applied to the system of the hard and rigid solid sample with rough surface.



สถาบันวิทยบริการ  
จุฬาลงกรณ์มหาวิทยาลัย

## CHAPTER V

### CONCLUSIONS

The absorbance of the solid sample was greatly affected by an existence of the air gap between the sample and the IRE. The larger air gap, the smaller is the observed absorbance, especially for a hard and rigid solid sample. If the air gap is large enough, spectrum of the sample cannot be observed. For a hard and rigid solid sample with rough surface, ATR spectrum was rarely observed.

In the measurement using multiple reflection ATR accessory, the hard and rigid solid sample (PC sample) did not have an optical contact with the IRE although the pressure was applied. The soft and rubbery solid sample (PVC sample), on the other hand, had an optical contact with the IRE when the pressure was applied.

In the measurement using single reflection ATR accessory, PC sample does not have an optical contact with the IRE, like multiple reflection. However, absorbance of PC sample in single reflection is greater than that in multiple reflection. On the contrary, the absorbance of PVC sample in single reflection is smaller than that in multiple reflection. This is due to PVC sample has an optical contact with the IRE. The greater the number of reflections, the higher is the absorbance. For PC sample with single reflection, the contact between the IRE and PC sample is better than that in multiple reflection accessory.

The absorbance of PC samples with flat surface and rough surface can be enhanced by organic liquid in both multiple reflection and single reflection. A low viscosity organic liquid (*i*-propanol) can greatly enhance the absorbance of the hard and rigid solid sample. A high viscosity organic liquid (mineral oil) can enhance the absorbance of the hard and rigid solid sample when the thin mineral oil film is used. However, the spectral enhancement of PC by *i*-propanol has limitation on the measurement time since *i*-propanol evaporates rapidly.

In the case of PVC, a soft and rubbery sample, the organic liquid cannot enhance the absorbance. The absorbance of PVC with an organic liquid in the system is always smaller than that in the system without an organic liquid. This is because the soft and rubbery solid sample always has a good contact with the IRE.

The bulk spectrum of the solid sample can be obtained by subtracting an organic liquid from the three-phase spectrum based on the simplified equation of a three-phase system. However, this technique has some limitations. An accurate bulk spectrum of the solid sample can be obtained under small absorption condition only since the simplified equation is defined based on small absorption. The organic liquid used in a three-phase system should be a high viscosity with low evaporation liquid. For an accurate calculated thickness, the used liquid should be very thin. In addition, the technique for calculating bulk spectrum cannot be applied to the solid sample with rough surface since the thickness of the organic liquid in the three-phase system cannot be accurately calculated.



## REFERENCES

1. Harrick, N. J. (Ed.). (1979). Internal Reflection Spectroscopy. New York: Harrick Scientific Corporation.
2. Harrick, N. J. (1960). Surface Chemistry from Spectral Analysis of Totally Internally Reflected Radiation. J. Phys. Chem., 64: 1110-1114.
3. Fahrenfort, J. (1961). Attenuated Total Reflection A New Principle for the Production of Useful Infra-red Reflection Spectra of Organic compounds. Spectrochim. Acta., 17: 698-709.
4. Buffeteau, T., Desbat, B., and Eyquem, D. (1996). Attenuated Total Reflection Fourier Transform Infrared Microspectroscopy: Theory and Application to Polymer Samples. Vib. Spectrosc., 11: 29-36.
5. Krasnokutskaya, I. S., and Finkelshtein, E. I. (1995). Multiple ATR (MATR) Spectroscopy of Vitamin A Compounds. J. Mol. Struct., 349: 313-316.
6. Huang, J., and Urban, M. W. (1993). Novel Approach to Quantitative Depth Profiling of Surfaces Using ATR/FT-IR Measurements. Appl. Spectrosc., 47(7): 973-981.
7. Wojciechowski, C., Dupuy, N., and Legrand, P. (1998). Quantitative Analysis of Water-Soluble Vitamins by ATR-FTIR Spectroscopy. Food Chem., 63: 133-139.
8. Ruddy, V., and McCABE, S. (1990). Detection of Propane by IR-ATR in a Teflon-Clad Fluoride Glass Optical Fiber. Appl. Spectrosc., 44(9): 1461-1463.
9. Sammon, C., Yarwood, J., and Everall, N. (2000). A FTIR-ATR Study of Liquid Diffusion Processes in PET Films: Comparison of Water with Simple Alcohols. Polymer, 41: 2521-2534.
10. Martin, S. T., Kesselman, J. M., and Park, D. S. (1996). Surface Structures of 4-Chlorocatechol Adsorbed on Titanium Dioxide. Environ. Sci. Technol., 30: 2535-2542
11. Neagle, W., and Randell, D. R. (Eds.). (1989). Surface Analysis Techniques and Applications. Cambridge: Thomas Graham House.

12. Shick, R. A., Koenig, J. L., and Ishida, H. (1993). Theoretical Development for Depth Profiling of Stratified Layers Using Variable-Angle ATR. Appl. Spectrosc., 47(8): 1237-1244.
13. Yang, J., and Her, J. W. (1999). Gas-Assisted IR-ATR Probe for Detection of Volatile Compounds in Aqueous Solutions. Anal. Chem., 71: 1773-1779.
14. Yang, J., Her, J. W., and Chen S. H. (1999). Detection of an Infrared Hollow Waveguide as a Sensing Device for Detection of Organic Compounds in Aqueous Solutions. Anal. Chem., 71: 3740-3746.
15. Fieldson, G. T., and Barbari, T. A. (1993). The Use of FTIR-ATR Spectroscopy to Characterize Penetrant diffusion in Polymers. Polymer, 34(6): 1146-1153.
16. Yang, J., and Lin, H. C. (2000). IR Chemical Sensor for Detection of Chlorinated anilines in Aqueous Solutions Based on ATR Waveguides coated with Derivatized Polystyrene. Analyst, 125: 1605-1610.
17. Balik, C. M., and Simendinger III, W. H. (1998). An Attenuated Total Reflectance Cell for Analysis of Small Molecule Diffusion in Polymer Thin Films with Fourier-Transform Infrared Spectroscopy. Polymer, 39(20): 4723-4728.
18. Urban, M. W. (Ed.). (1996). Attenuated Total Reflectance Spectroscopy of Polymer: Theory and Practice. Washington, DC: American Chemical Society.
19. Ekgasit, S. (2000). ATR Spectral Intensity: What is the Upper Limit of Weak Absorption?. Appl. Spectrosc., 54: 756-758.
20. Ekgasit, S., and Padermshoke, A. (2001). Optical Contact in ATR/FT-IR Spectroscopy. Appl. Spectrosc., 55: 1352-1359.
21. Ekgasit, S., and Siesler, H. W. (1998). Simplified Equation for ATR Spectral Intensity of a Three-Phase System. Appl. Spectrosc., 52(3): 367-374.
22. Hansen, W. N. (Ed.). (1973). in Advance in Electrochemistry and Electrochemical Engineering. New York: John Wiley & Sons.

23. Hansen, W. N. (1968). Electric Fields Produced by the Propagation of Plane Coherent Electromagnetic Radiation in a Stratified Medium. J. Opt. Soc. Am., 58(3): 380-390.



สถาบันวิทยบริการ  
จุฬาลงกรณ์มหาวิทยาลัย



## APPENDICES

สถาบันวิทยบริการ  
จุฬาลงกรณ์มหาวิทยาลัย

**APPENDIX A**  
**PROGRAM FOR GENERATING REFRACTIVE INDEX**  
**SPECTRUM AND ABSORPTION INDEX**  
**SPECTRUM OF MEDIUM 1**

**1. nk\_Input\_Data.m**

```
% This is a data file of generation of n and k spectra.
% The following are necessary information for the calculation.
% file_out: filename for output with dot '.'
% wn_start: start wavenumber for calculation
% wn_end: end wavenumber for calculation
% wn_step: spectral resolution
% PEAK_POSITION: position of each peak
% K_MAX: maximum absorption index, k, of each peak
% HWHH: half width at half height of each peak
% N_INFINITY: refractive index, n at non-absorbing wavenumber
%
% ***Important***
% Number of PEAK_POSITION, K_MAX, HWHH must be the same.
%
global PEAK_POSITION K_MAX HWHH N_INFINITY

file_out = 'liquid film.'; %output filename with dot '.'
wn_start = 4000; %start wavenumber for calculation
wn_end = 400; %end wavenumber for calculation
wn_step = -2; %spectral resolution
PEAK_POSITION = [2000 3500]; %position of each peak
K_MAX = [0.05 0.05]; %maximum peak height
HWHH = [20 20]; %half width at half height
N_INFINITY = 1.5; %n at non-absorbing wavenumber
```

**2. nk\_SpectSim.m**

```
% This program is for generating the complex refractive index spectrum
%(refractive index: n, absorption index: k).
%
nk_Input_Data.m;
wn=((wn_start:wn_step:wn_end));
```

```
[n,k] = Eq_nk_Gen((wn_start:wn_step:wn_end));
```

```
%write data to ASCII file
fwid=fopen(strep(file_out,'.','n'),'w');
fprintf(fwid,'%10.6f %10.6f\n',[wn,n]);
status=fclose(fwid);
fwid=fopen(strep(file_out,'.','k'),'w');
fprintf(fwid,'%10.6f %10.6f\n',[wn,k]);
status=fclose(fwid);
```

```
%plot the results
clf;
subplot(2,1,1);plot(wn,n);
axis([400 4000 -inf inf]);
title('refractive index');
subplot(2,1,2);plot(wn,k);
axis([400 4000 -inf inf]);
title('absorption index');
```

### 3. Eq\_nk\_Gen.m

% This is the equation for generating the complex refractive index spectrum  
% (refractive index: n, absorption index:k).

```
function [n,k]=Equation_nk_Gen(wnj)
global PEAK_POSITION K_MAX HWHH N_INFINITY
```

```
n=N_INFINITY.*[ones(size(wnj))];
k=[zeros(size(wnj))];
for i=1:size(PEAK_POSITION,2)
    n1=(wnj-PEAK_POSITION(i)).*K_MAX(i)*HWHH(i);
    n2=(wnj-PEAK_POSITION(i)).^2 + HWHH(i)^2;
    n3=(wnj+PEAK_POSITION(i)).*K_MAX(i)*HWHH(i);
    n4=(wnj+PEAK_POSITION(i)).^2 + HWHH(i)^2;
    k1=K_MAX(i)*HWHH(i)^2;
    k2=n2;
    k3=k1;
    k4=n4;
    n = n - n1./n2 + n3./n4; %refractive index
    k = k + k1./k2 - k3./k4; %absorption index
end
```



**APPENDIX B**

**PROGRAM FOR GENERATING REFRACTIVE INDEX**

**SPECTRUM AND ABSORPTION INDEX**

**SPECTRUM OF MEDIUM2**

**1. nk\_Input\_Data.m**

```
% This is a data file of generation of n and k spectra.
% The following are necessary information for the calculation.
% file_out: filename for output with dot '.'
% wn_start: start wavenumber for calculation
% wn_end: end wavenumber for calculation
% wn_step: spectral resolution
% PEAK_POSITION: position of each peak
% K_MAX: maximum absorption index, k, of each peak
% HWHH: half width at half height of each peak
% N_INFINITY: refractive index, n at non-absorbing wavenumber
%
% ***Important***
% Number of PEAK_POSITION, K_MAX, HWHH must be the same.
%
global PEAK_POSITION K_MAX HWHH N_INFINITY

file_out = 'solid.'; % output filename with dot '.'
wn_start = 4000; % start wavenumber for calculation
wn_end = 400; % end wavenumber for calculation
wn_step = -2; % spectral resolution
PEAK_POSITION = [900 1500 2500 3000]; % position of each peak
K_MAX = [0.05 0.05 0.05 0.05]; % maximum peak height
HWHH = [30 30 30 30]; % half width at half height
N_INFINITY = 1.5; % n at non-absorbing wavenumber
```

**2. nk\_SpectSim.m**

```
% This program is for generating the complex refractive index spectrum
% (refractive index: n, absorption index: k).
%
nk_input_data;
wn=((wn_start:wn_step:wn_end));
```

```
[n,k] = Eq_nk_Gen((wn_start:wn_step:wn_end));
```

```
%write data to ASCII file
fwid=fopen(strep(file_out,'.','n'),'w');
fprintf(fwid,'%10.6f %10.6f\n',[wn,n]);
status=fclose(fwid);
fwid=fopen(strep(file_out,'.','k'),'w');
fprintf(fwid,'%10.6f %10.6f\n',[wn,k]);
status=fclose(fwid);
```

```
%plot the results
clf;
subplot(2,1,1);plot(wn,n);
axis([400 4000 -inf inf]);
title('refractive index');
subplot(2,1,2);plot(wn,k);
axis([400 4000 -inf inf]);
title('absorption index');
```

### 3. Eq\_nk\_Gen.m

% This is the equation for generating the complex refractive index spectrum  
% (refractive index:., absorption index:k).

```
function [n,k]=Equation_nk_Gen(wnj)
global PEAK_POSITION K_MAX HWHH N_INFINITY
```

```
n=N_INFINITY.*[ones(size(wnj))];
k=[zeros(size(wnj))];
for i=1:size(PEAK_POSITION,2)
    n1=(wnj-PEAK_POSITION(i)).*K_MAX(i)*HWHH(i);
    n2=(wnj-PEAK_POSITION(i)).^2 + HWHH(i)^2;
    n3=(wnj+PEAK_POSITION(i)).*K_MAX(i)*HWHH(i);
    n4=(wnj+PEAK_POSITION(i)).^2 + HWHH(i)^2;
    k1=K_MAX(i)*HWHH(i)^2;
    k2=n2;
    k3=k1;
    k4=n4;
    n = n - n1./n2 + n3./n4; %refractive index
    k = k + k1./k2 - k3./k4; %absorption index
end
```

## APPENDIX C

### PROGRAM FOR SIMULATING ATR SPECTRA IN TWO-PHASE SYSTEM

#### 1. Medium 1

##### 1.1 SpectSim\_2P\_data.m

```
% This is the data file for spectral simulation in Two-Phase System (incident
%medium/absorbing medium)
% The detail description for all parameters can be found in Hansen's Papers.
% W.N.Hansen,J.Opt.Soc.Am, 58(3),380(1966).
%
% ***** THE INPUT INFORMATION *****
%file_out: filename (with dot '.') for output file
%n0: refractive index of the incident medium
%file_film: filename for complex refractive index spectrum (with dot '.') of absorbing
%medium
%polarize: degree_of_polarization; -1=s, 0=non, 1=p
%t0: angle of incidence (degree)
%
file_out = char('2P_liquid.');
```

##### 1.2 SpectSim\_2P\_main.m

```
% This is the program file for spectral simulation in Two-Phase System (incident
medium/absorbing medium)
% The detail description for all parameters can be found in Hansen's Papers.
% W.N.Hansen,J.Opt.Soc.Am, 58(3),380(1966).
%
clear;
SpectSim_2P_data;
%Load n and k spectra of film
temp = load(strrep(file_film, '.', '.n'));
wnf = temp(:,1); nf = temp(:,2);
temp = load(strrep(file_film, '.', '.k'));
kf = temp(:,2);
```

```

%Perform calculation based on Optical Theory
disp('CALCULATION STARTED');
angle = angle*pi/180;
nkf = complex(nf,kf);
[Rp,Rs, Tp, Ts] = Hansen_2Phase(wnf,angle,n0,nkf);
Rps = ((1+polarize)*Rp+(1-polarize)*Rs)/2; %reflectance
Aps = 1 - Rps; % Absorptance
Abs = -log10(Rps); % Absorbance
disp('CALCULATION ENDED');

%Exporting the Output
%Writing to ASCII Files
disp('START WRITING ASCII FILES');
file_name=strep(file_out,','.Abs'); %export Absorbance
data_out=[wnf Abs];
dlmwrite(file_name,data_out,'\t');
disp('STOP WRITING ASCII FILES');

plot(wnf,Abs)

```

### 1.3 Hansen\_2Phase.m

```

function [Rp,Rs, Tp, Ts] = Hansen_2Phase(wn,t0,n0,nkf)
%
% This function is for calculating Reflectance and Transmittance
% from Hansen formulation.
% W.N.Hansen,J.Opt.Soc.Am, 58(3),380(1966).
%
cost1=sqrt(1-(sin(t0)*n0./nkf).^2);
beta=2*pi.*(wn/10000).*cost1.*nkf;
%p-polarized component
g0=cos(t0)/n0;
g1=cost1./nkf;
r01=(g0-g1)/(g0+g1);
t01=2*g0/(g0+g1);
Rp=(abs(r01)).^2;
Tp=(real(g1)/g0).*(abs(t01)).^2;
%s-polarized component
g0=n0*cos(t0);
g1=nkf.*cost1;
r01=(g0-g1)/(g0+g1);
t01=2*g0/(g0+g1);
Rs=(abs(r01)).^2;

```

```
Ts=(real(g1)/g0).*(abs(t01)).^2;
```

## 2. Medium 2

### 2.1 SpectSim\_2P\_data.m

```
% This is the data file for spectral simulation in Two-Phase System (incident
% medium/absorbing medium)
% The detail description for all parameters can be found in Hansen's Papers.
% W.N.Hansen,J.Opt.Soc.Am, 58(3),380(1966).
%
% ***** THE INPUT INFORMATION *****
% file_out: filename (with dot '.') for output file
% n0: refractive index of the incident medium
% file_film: filename for complex refractive index spectrum (with dot '.') of absorbing
% medium
% polarize: degree_of_polarization; -1=s, 0=non, 1=p
% t0: angle of incidence (degree)
%
file_out = char('2P_solid.');
```

```
n0 = 4.0;
```

```
file_film = char('solid.');
```

```
polarize = 0;
```

```
angle = 45;
```

### 2.2 SpectSim\_2P\_main.m

```
% This is the program file for spectral simulation in Two-Phase System (incident
% medium/absorbing medium)
% The detail description for all parameters can be found in Hansen's Papers.
% W.N.Hansen,J.Opt.Soc.Am, 58(3),380(1966).
%
clear;
SpectSim_2P_data;
%Load n and k spectra of film
temp = load(strrep(file_film, '.', '.n'));
wnf = temp(:,1); nf = temp(:,2);
temp = load(strrep(file_film, '.', '.k'));
kf = temp(:,2);

%Perform calculation based on Optical Theory
disp('CALCULATION STARTED');
```

```

angle = angle*pi/180;
nkf = complex(nf,kf);
[Rp,Rs, Tp, Ts] = Hansen_2Phase(wnf,angle,n0,nkf);
Rps = ((1+polarize)*Rp+(1-polarize)*Rs)/2; %reflectance
Aps = 1 - Rps;          % Absorptance
Abs = -log10(Rps);     % Absorbance
disp('CALCULATION ENDED');

%Exporting the Output
%Writing to ASCII Files
disp('START WRITING ASCII FILES');
file_name=strrep(file_out,','.Abs'); %export Absorbance
data_out=[wnf Abs];
dlmwrite(file_name,data_out,'\t');
disp('STOP WRITING ASCII FILES');

plot(wnf,Abs)

```

### 2.3 Hansen\_2Phase.m

```

function [Rp,Rs, Tp, Ts] = Hansen_2Phase(wn,t0,n0,nkf)
%
% This function is for calculating Reflectance and Transmittance
% from Hansen formulation.
% W.N.Hansen,J.Opt.Soc.Am, 58(3),380(1966).
%
cost1=sqrt(1-(sin(t0)*n0./nkf).^2);
beta=2*pi.*(wn/10000).*cost1.*nkf;
%p-polarized component
g0=cos(t0)/n0;
g1=cost1./nkf;
r01=(g0-g1)/(g0+g1);
t01=2*g0/(g0+g1);
Rp=(abs(r01)).^2;
Tp=(real(g1)/g0).*(abs(t01)).^2;
%s-polarized component
g0=n0*cos(t0);
g1=nkf.*cost1;
r01=(g0-g1)/(g0+g1);
t01=2*g0/(g0+g1);
Rs=(abs(r01)).^2;
Ts=(real(g1)/g0).*(abs(t01)).^2;

```



**APPENDIX D**  
**PROGRAM FOR SIMULATING ATR SPECTRA**  
**OF MEDIUM 2 WITH AIR GAP**

**1. nk\_Input\_Data.m**

```
% This is a data file of generation of n and k spectra.
% The following are necessary information for the calculation.
% file_out: filename for output with dot '.'
% wn_start: start wavenumber for calculation
% wn_end: end wavenumber for calculation
% wn_step: spectral resolution
% PEAK_POSITION: position of each peak
% K_MAX: maximum absorption index, k, of each peak
% HWHH: half width at half height of each peak
% N_INFINITY: refractive index, n at non-absorbing wavenumber
%
% ***Important***
% Number of PEAK_POSITION, K_MAX, HWHH must be the same.
%
global PEAK_POSITION K_MAX HWHH N_INFINITY

file_out = 'Air gap.'; %output filename with dot '.'
wn_start = 4000; %start wavenumber for calculation
wn_end = 400; %end wavenumber for calculation
wn_step = -2; %spectral resolution
PEAK_POSITION = [1]; %position of each peak
K_MAX = [0]; %maximum peak height
HWHH = [30 30 30 30]; %half width at half height
N_INFINITY = 1.0; %n at non-absorbing wavenumber
```

**2. nk\_SpectSim.m**

```
% This program is for generating the complex refractive index spectrum
% (refractive index: n, absorption index: k).
%
nk_Input_Data.m;
wn=((wn_start:wn_step:wn_end)');
[n,k] = Eq_nk_Gen((wn_start:wn_step:wn_end)');
```

```

%write data to ASCII file
fwid=fopen(strep(file_out,','.n'),'w');
fprintf(fwid,'%10.6f %10.6f\n',[wn,n]);
status=fclose(fwid);
fwid=fopen(strep(file_out,','.k'),'w');
fprintf(fwid,'%10.6f %10.6f\n',[wn,k]);
status=fclose(fwid);

%plot the results
clf;
subplot(2,1,1);plot(wn,n);
axis([400 4000 -inf inf]);
title('refractive index');
subplot(2,1,2);plot(wn,k);
axis([400 4000 -inf inf]);
title('absorption index');

```

### 3. Eq\_nk\_Gen.m

% This is the equation for generating the complex refractive index spectrum  
 % (refractive index: n, absorption index: k).

```

function [n,k]=Equation_nk_Gen(wnj)
global PEAK_POSITION K_MAX HWHH N_INFINITY

n=N_INFINITY.*[ones(size(wnj))];
k=[zeros(size(wnj))];
for i=1:size(PEAK_POSITION,2)
    n1=(wnj-PEAK_POSITION(i)).*K_MAX(i)*HWHH(i);
    n2=(wnj-PEAK_POSITION(i)).^2 + HWHH(i)^2;
    n3=(wnj+PEAK_POSITION(i)).*K_MAX(i)*HWHH(i);
    n4=(wnj+PEAK_POSITION(i)).^2 + HWHH(i)^2;
    k1=K_MAX(i)*HWHH(i)^2;
    k2=n2;
    k3=k1;
    k4=n4;
    n = n - n1./n2 + n3./n4; %refractive index
    k = k + k1./k2 - k3./k4; %absorption index
end

```

#### 4. SpectSim\_3P\_data.m

```

% This is the data file for spectral simulation in Three-Phase System
% The detail description for all parameters can be found in Hansen's Papers.
% W.N.Hansen,J.Opt.Soc.Am, 58(3),380(1966).
%
% ***** THE INPUT INFORMATION *****
% file_out: filename (with dot '.') for output file
% n0: refractive index of the incident medium
% file_film: filename for complex refractive index spectrum of absorbing medium (with
% dot '.')
% film_thick: film thickness in micrometer
% file_subs: filename for complex refractive index spectrum of substrate medium (with
% dot '.')
% polarize: degree_of_polarization; -1=s, 0=non, 1=p
% t0: angle of incidence (degree)
%
file_out = char('h0_5airsolid. ');
n0 = 4;
file_film = char('Air gap');
film_thick = 0.5;
file_subs = char('solid. ');
polarize = 0;
angle = 45;

```

#### 5. SpectSim\_3P\_main.m

```

% This is the program file for spectral simulation in Three-Phase System (incident
% medium/absorbing medium)
% The detail description for all parameters can be found in Hansen's Papers.
% W.N.Hansen,J.Opt.Soc.Am, 58(3),380(1966).
%
clear;
SpectSim_3P_data.m;
% Load n and k spectra of film
temp = load(strrep(file_film, '.', '.n'));
wnf = temp(:,1); nf = temp(:,2);
temp = load(strrep(file_film, '.', '.k'));
kf = temp(:,2);
% Load n and k spectra of substrate
temp = load(strrep(file_subs, '.', '.n'));
wns = temp(:,1); ns = temp(:,2);
temp = load(strrep(file_subs, '.', '.k'));

```

```

ks = temp(:,2);
resolution_compatibility(wnf,wns);
%Perform calculation based on Optical Theory
disp('CALCULATION STARTED');
angle = angle*pi/180;
nkf = complex(nf,kf);
nks = complex(ns,ks);
Dp = PenetrnDepth(wnf,n0,nf,angle);
[Rp,Rs,Tp,Ts] = Hansen_3Phase(wnf,angle,n0,nkf,film_thick,nks);
Rps = ((1+polarize)*Rp+(1-polarize)*Rs)/2; %reflectance
Aps = 1 - Rps; % Absorptance
Abs = -log10(Rps); % Absorbance
disp('CALCULATION ENDED');

file_name=strrep(file_out,'.','Abs'); %export Absorbance
data_out=[wnf Abs];
dlmwrite(file_name,data_out,'\t');
file_name=strrep(file_out,'.','Dp'); %export Absorbance
data_out=[wnf Dp];
dlmwrite(file_name,data_out,'\t');
disp('STOP WRITING ASCII FILES');

clf,
plot(wns,Abs)

```

## 6. PenetrnDepth.m

% This is program for calculating the penetration depth

```

function Dp = PenetrnDepth(wn,n0,nf,t0);
Dp=1./(2*pi*(wn/10000)*n0.*sqrt(sin(t0)^2-nf.^2/n0^2));

```

## 7. Hansen\_3Phase.m

```

function [Rp,Rs,Tp,Ts] = Hansen_3Phase(wn,t0,n0,nkf,h,nks)
%
% This is a function for calculation spectral intensity in a
% Three-Phase System. All equations are based on Hansen Matrix
% formulation: W.N.Hansen,J.Opt.Soc.Am, 58(3),380(1966).
% The required input are:
% wn: wavenumber over the entier calculated spectrum
% t0: angle of incidence (radian)

```

```

%n0: refractive index of IRE
%nkf: complex refractive index spectrum of the film
%h: thickness of the film (micrometer)
%nks: complex refractive index spectrum of the substrate
%
%cost1=sqrt(1-(sin(t0)*n0/nkf)^2);
%sint1=sin(t0)*n0/nkf;
%costs=sqrt(1-(n0*sin(t0)/nks)^2);
%sints=n0*sin(t0)/nks;
beta=2*pi*h.*(wn/10000).*sqrt(1-(sin(t0)*n0./nkf).^2).*nkf;
%s-polarized component
g0=n0*cos(t0);
g1=nkf.*sqrt(1-(sin(t0)*n0./nkf).^2);
gs=nks.*sqrt(1-(sin(t0)*n0./nks).^2);
r01=(g0-g1)/(g0+g1);
r0s=(g0-gs)/(g0+gs);
r1s=(g1-gs)/(g1+gs);
t01=2*g0/(g0+g1);
t0s=2*g0/(g0+gs);
t1s=2*g1/(g1+gs);
R01=(abs(r01)).^2;
R0s=(abs(r0s)).^2;
R1s=(abs(r1s)).^2;
rs=(r01+r1s.*exp(i*2*beta))/(1+r01.*r1s.*exp(i*2*beta));
ts=(t01.*t1s.*exp(i*beta))/(1+r01.*r1s.*exp(i*2*beta));
Rs=(abs(rs)).^2;
Ts=(real(gs)/g0).*(abs(ts)).^2;
%p-polarized component
g0=cos(t0)/n0;
g1=sqrt(1-(sin(t0)*n0./nkf).^2)/nkf;
gs=sqrt(1-(sin(t0)*n0./nks).^2)/nks;
r01=(g0-g1)/(g0+g1);
r0s=(g0-gs)/(g0+gs);
r1s=(g1-gs)/(g1+gs);
t01=2*g0/(g0+g1);
t0s=2*g0/(g0+gs);
t1s=2*g1/(g1+gs);
R01=(abs(r01)).^2;
R0s=(abs(r0s)).^2;
R1s=(abs(r1s)).^2;
rp=(r01+r1s.*exp(i*2*beta))/(1+r01.*r1s.*exp(i*2*beta));
tp=(t01.*t1s.*exp(i*beta))/(1+r01.*r1s.*exp(i*2*beta));
Rp=(abs(rp)).^2;
Tp=((real(gs))/g0).*(abs(tp)).^2;

```

**APPENDIX E**

**PROGRAM FOR SIMULATING ATR SPECTRA**

**OF MEDIUM 2 WITH MADIUM 1**

**1. SpectSim\_3P\_data.m**

```
% This is the data file for spectral simulation in Three-Phase System
% The detail description for all parameters can be found in Hansen's Papers.
% W.N.Hansen,J.Opt.Soc.Am, 58(3),380(1966).
%
% ***** THE INPUT INFORMATION *****
% file_out: filename (with dot '.') for output file
% n0: refractive index of the incident medium
% file_film: filename for complex refractive index spectrum of absorbing medium (with
% dot '.')
% film_thick: film thickness in micrometer
% file_subs: filename for complex refractive index spectrum of substrate medium (with
% dot '.')
% polarize: degree_of_polarization; -1=s, 0=non, 1=p
% t0: angle of incidence (degree)
%
file_out = char('h0_5liquidfilmsolid.');
```

สถาบันวิทยบริการ  
วิทยาลัยการปกครองส่วนท้องถิ่น

**2. SpectSim\_3P\_main.m**

```
% This is the program file for spectral simulation in Three-Phase System (incident
medium/absorbing medium)
% The detail description for all parameters can be found in Hansen's Papers.
% W.N.Hansen,J.Opt.Soc.Am, 58(3),380(1966).
%
clear;
SpectSim_3P_data;
%Load n and k spectra of film
temp = load(strrep(file_film, '.', '.n'));
```



```

wnf = temp(:,1); nf = temp(:,2);
temp = load(strrep(file_film,',';'.k'));
kf = temp(:,2);
%Load n and k spectra of substrate
temp = load(strrep(file_subs,',';'.n'));
wns = temp(:,1); ns = temp(:,2);
temp = load(strrep(file_subs,',';'.k'));
ks = temp(:,2);
resolution_compatibility(wnf,wns);
%Perform calculation based on Optical Theory
disp('CALCULATION STARTED');
angle = angle*pi/180;
nkf = complex(nf,kf);
nks = complex(ns,ks);
Dp = PenetrnDepth(wnf,n0,nf,angle);
[Rp,Rs, Tp, Ts] = Hansen_3Phase(wnf,angle,n0,nkf,film_thick,nks);
Rps = ((1+polarize)*Rp+(1-polarize)*Rs)/2; %reflectance
Aps = 1 - Rps; % Absorptance
Abs = -log10(Rps); % Absorbance
disp('CALCULATION ENDED');

file_name=strrep(file_out,',';'.Abs'); %export Absorbance
data_out=[wnf Abs];
dlmwrite(file_name,data_out,'\t');
file_name=strrep(file_out,',';'.Dp'); %export Absorbance
data_out=[wnf Dp];
dlmwrite(file_name,data_out,'\t');
disp('STOP WRITING ASCII FILES');

clf,
plot(wns,Abs)

```

### 3. PenetrnDepth.m

% This is program for calculating the penetration depth

```

function Dp = PenetrnDepth(wn,n0,nf,t0);
Dp=1./(2*pi*(wn/10000)*n0.*sqrt(sin(t0)^2-nf.^2/n0^2));

```

#### 4. Hansen\_3Phase.m

```

function [Rp,Rs, Tp,Ts] = Hansen_3Phase(wn,t0,n0,nkf,h,nks)
%
% This is a function for calculation spectral intensity in a
% Three-Phase System. All equations are based on Hansen Matrix
% formulation: W.N.Hansen,J.Opt.Soc.Am, 58(3),380(1966).
% The required input are:
% wn: wavenumber over the entire calculated spectrum
% t0: angle of incidence (radian)
% n0: refractive index of IRE
% nkf: complex refractive index spectrum of the film
% h: thickness of the film (micrometer)
% nks: complex refractive index spectrum of the substrate
%
% cost1=sqrt(1-(sin(t0)*n0/nkf)^2);
% sint1=sin(t0)*n0/nkf;
% costs=sqrt(1-(n0*sin(t0)/nks)^2);
% sints=n0*sin(t0)/nks;
beta=2*pi*h.*(wn/10000).*sqrt(1-(sin(t0)*n0./nkf).^2).*nkf;

% s-polarized component
g0=n0*cos(t0);
g1=nkf.*sqrt(1-(sin(t0)*n0./nkf).^2);
gs=nks.*sqrt(1-(sin(t0)*n0./nks).^2);
r01=(g0-g1)/(g0+g1);
r0s=(g0-gs)/(g0+gs);
r1s=(g1-gs)/(g1+gs);
t01=2*g0/(g0+g1);
t0s=2*g0/(g0+gs);
t1s=2*g1/(g1+gs);
R01=(abs(r01)).^2;
R0s=(abs(r0s)).^2;
R1s=(abs(r1s)).^2;
rs=(r01+r1s.*exp(i*2*beta))/(1+r01.*r1s.*exp(i*2*beta));
ts=(t01.*t1s.*exp(i*beta))/(1+r01.*r1s.*exp(i*2*beta));
Rs=(abs(rs)).^2;
Ts=(real(gs)/g0).*(abs(ts)).^2;

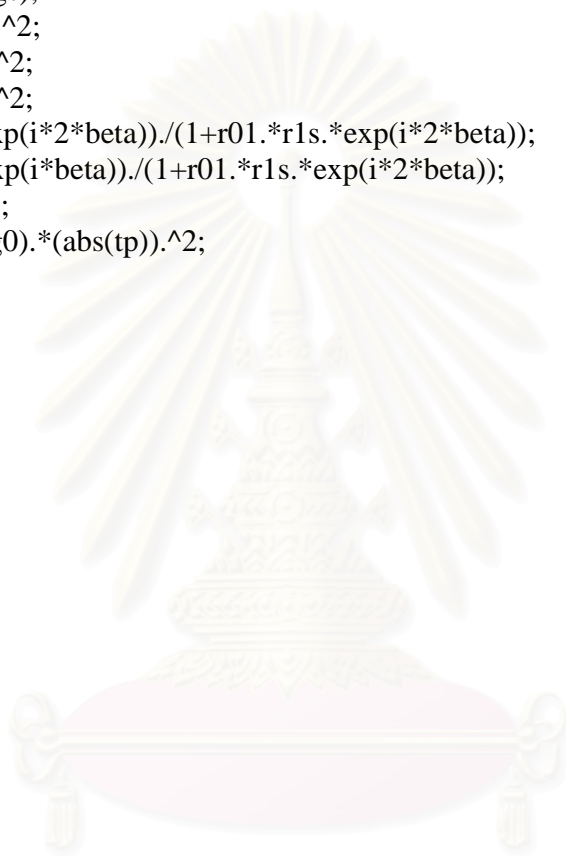
% p-polarized component
g0=cos(t0)/n0;
g1=sqrt(1-(sin(t0)*n0./nkf).^2)/nkf;
gs=sqrt(1-(sin(t0)*n0./nks).^2)/nks;
r01=(g0-g1)/(g0+g1);

```

```

r0s=(g0-gs)/(g0+gs);
r1s=(g1-gs)/(g1+gs);
t01=2*g0/(g0+g1);
t0s=2*g0/(g0+gs);
t1s=2*g1/(g1+gs);
R01=(abs(r01)).^2;
R0s=(abs(r0s)).^2;
R1s=(abs(r1s)).^2;
rp=(r01+r1s.*exp(i*2*beta))/(1+r01.*r1s.*exp(i*2*beta));
tp=(t01.*t1s.*exp(i*beta))/(1+r01.*r1s.*exp(i*2*beta));
Rp=(abs(rp)).^2;
Tp=((real(gs))/g0).*(abs(tp)).^2;

```



สถาบันวิทยบริการ  
จุฬาลงกรณ์มหาวิทยาลัย

## APPENDIX F

### PROGRAM FOR CALCULATING BULK SPECTRUM

#### 1. CalBulkSubs\_data.m

```

%This is the data file of calculating the bulk spectrum of solid sample;
%The detail description for all parameters can be found in Sanong's paper;
%S. Ekgasit, Appl. %Spectrosc, 52(3), 367(1998).

%file_out: filename (with dot '.') for output file
%file_3P: filename for ATR spectrum of Three-phase system(with %dot '.')
%file_film: filename for ATR spectrum of liquid film medium (with %dot '.')
%file_subs: filename for ATR spectrum of substrate medium (with %dot '.')
%h: liquid film thickness in micrometer
%n0: refractive index of the incident medium
%nf: refractive index of the absorbing medium
%polarize: degree_of_polarization; -1=s, 0=non, 1=p
%t0: angle of incidence (degree)

file_out = char('bulk_h0_5liquidfilmsolid');
file_3P = char('h0_5liquidfilmsolid');
file_film = char('2P_liquid');
file_subs = char('2P_solid');
h = 0.5;
n0 = 2.4;
nf = 1.5;
polarize = 0
t0 = 45*pi/180;

```

#### 2. CalBulkSubs\_main.m

```

%This program is for calculating the bulk spectrum of solid sample;
%The detail description for all parameters can be found in Sanong's paper;
%S. Ekgasit, Appl. %Spectrosc, 52(3), 367(1998).

CalBulkSubs_data;
temp = load(file_3P);
wn = temp(:,1);
A3p = temp(:,2);
temp = load(file_film);
Af = temp(:,2);
temp = load(file_subs);

```

```

As_2P = temp(:,2);
Dp = PenetrnDepth(wn,n0,nf,t0);

%start calculation
Factor = exp(-2*h./Dp);
As = (A3p-(1-Factor).*Af)./Factor;
disp('Calculation Finished')
%Plot the Results;
clf;
plot(wn,As,wn,As_2P);
%Writing ASCII Files;
disp('START WRITING ASCII FILES');
file_name = strrep(file_out,','.Abs');
data_out = [wn As];
dlmwrite(file_name,data_out,'\t');
disp('STOP WRITING ASCII FILES');

```

### 3. PenetrnDepth.m

% This is program for calculating the penetration depth

```

function Dp = PenetrnDepth(wn,n0,nf,t0);
Dp=1./(2*pi*(wn/10000)*n0.*sqrt(sin(t0)^2-nf.^2/n0^2));

```

สถาบันวิทยบริการ  
จุฬาลงกรณ์มหาวิทยาลัย

## APPENDIX G

### PROGRAM FOR CALCULATING THICKNESS OF LIQUID FILM IN THREE-PHASE SYSTEM

#### 1. CalThickFilm.data.m

```
% This is a data file for calculating the thickness of liquid film
% The detail description for all parameters can be found in Sanong's paper;
% S. Ekgasit, Appl. Spectrosc, 52(3), 367(1998).
```

```
%file_out: filename (with dot '.') for output file
%file_3P: filename for ATR spectrum of Three-phase system(with %dot '.')
%file_film: filename for ATR spectrum of liquid film medium (with %dot '.')
%file_subs: filename for ATR spectrum of substrate medium (with %dot '.')
%h: liquid film thickness in micrometer
%hs: increase of liquid film thickness per round of calculation in micrometer
%n0: refractive index of the incident medium
%nf: refractive index of the absorbing medium
%polarize: degree_of_polarization; -1=s, 0=non, 1=p
%t0: angle of incidence (degree)
```

```
file_out = char('bulk_ZnProPVC');
file_3P = char(' ZnProPVC');
file_film = char('Zn_Propanol');
file_subs = char('Zn_PVC');
h = 0.01;
hs = 0.001;
n0 = 2.4;
nf = 1.5;
polarize = 0
t0 = 45*pi/180;
```

#### 2. CalThickFilm.main.m

```
% This program is for calculating the thickness of liquid film;
% The detail description for all parameters can be found in Sanong's paper;
% S. Ekgasit, Appl. Spectrosc, 52(3), 367(1998).
```

```
CalThickFilm.data.m;
temp = load(file_3P);
wn = temp(:,1);
```



```

A3p = temp(:,2);
temp = load(file_film);
Af = temp(:,2);
%temp = load(file_thick);
%h = temp(:,2);
temp = load(file_subs);
As_2P = temp(:,2);
Dp = PenetrnDepth(wn,n0,nf,t0);

for k=1:20;
    Factor = exp(-2*h./Dp);
    As = (A3p-(1-Factor).*Af)./Factor;
    clf;
    plot(wn,As,wn,As_2P,wn,Af,wn,A3p);
    disp(h);
    pause;
    h=h+hs;
end

%disp('START WRITING ASCII FILES');
%file_name = strrep(file_out,','.As1');
%data_out = [wn As1];
%dlmwrite(file_name,data_out,'\t');
%file_name = strrep(file_out,','.As2');

data_out = [wn,As];
%dlmwrite(file_name,data_out,'\t');
%disp('STOP WRITING ASCII FILES');
disp('calculation finished')

```

### 3. PenetrnDepth.m

```

% This is program for calculating the penetration depth

function Dp = PenetrnDepth(wn,n0,nf,t0);
Dp=1./(2*pi*(wn/10000)*n0.*sqrt(sin(t0)^2-nf.^2/n0^2));

```

## APPENDIX H

### PROGRAM FOR CALCULATING BULK SPECTRUM

#### 1. CalBulkSubs\_data.m

%This is the data file of calculating the bulk spectrum of solid sample;  
 %The detail description for all parameters can be found in Sanong's paper;  
 %S. Ekgasit, Appl. %Spectrosc, 52(3), 367(1998).

%file\_out: filename (with dot '.') for output file  
 %file\_3P: filename for ATR spectrum of Three-phase system(with %dot '.')  
 %file\_film: filename for ATR spectrum of liquid film medium (with %dot '.')  
 %file\_subs: filename for ATR spectrum of substrate medium (with %dot '.')  
 %h: liquid film thickness in micrometer  
 %n0: refractive index of the incident medium  
 %nf: refractive index of the absorbing medium  
 %polarize: degree\_of\_polarization; -1=s, 0=non, 1=p  
 %t0: angle of incidence (degree)

```
file_out = char('bulk_ZnProPVC');
file_3P = char(' ZnProPVC');
file_film = char('Zn_Propanol');
file_subs = char('Zn_PVC');
h = 0.034;
n0 = 2.4;
nf = 1.5;
polarize = 0
t0 = 45*pi/180;
```

#### 2. CalBulkSubs\_main.m

%This program is for calculating the bulk spectrum of solid sample;  
 %The detail description for all parameters can be found in Sanong's paper;  
 %S. Ekgasit, Appl. %Spectrosc, 52(3), 367(1998).

```
CalBulkSubs_data;
temp = load(file_3P);
wn = temp(:,1);
A3p = temp(:,2);
temp = load(file_film);
Af = temp(:,2);
```

```

temp = load(file_subs);
As_2P = temp(:,2);
Dp = PenetrnDepth(wn,n0,nf,t0);

%start calculation
Factor = exp(-2*h./Dp);
As = (A3p-(1-Factor).*Af)./Factor;
disp('Calculation Finished')
%Plot the Results;
clf;
plot(wn,As,wn,As_2P);
%Writing ASCII Files;
disp('START WRITING ASCII FILES');
file_name = strep(file_out,','.Abs');
data_out = [wn As];
dlmwrite(file_name,data_out,'\t');
disp('STOP WRITING ASCII FILES');

```

### 3. PenetrnDepth.m

% This is program for calculating the penetration depth

```

function Dp = PenetrnDepth(wn,n0,nf,t0);
Dp=1./(2*pi*(wn/10000)*n0.*sqrt(sin(t0)^2-nf.^2/n0^2));

```

สถาบันวิทยบริการ  
จุฬาลงกรณ์มหาวิทยาลัย

## CURRICULUM VITAE

Miss Nutsima Deechalao was born on September 17, 1976 at Bangkok, Thailand. She got bachelor degree at Department of Chemistry, Faculty of Science from Chulalongkorn University, in 1998 and master degree at Department of Chemistry, Faculty of Science from Chulalongkorn University, in 2001.



สถาบันวิทยบริการ  
จุฬาลงกรณ์มหาวิทยาลัย